


Fall 12-15-2017

The Role of YES-Associated Protein 1 in Ovarian Physiology and Pathology

Xiangmin Lv
University of Nebraska Medical Center

Follow this and additional works at: <https://digitalcommons.unmc.edu/etd>

 Part of the [Cancer Biology Commons](#), [Cell Biology Commons](#), [Developmental Biology Commons](#), [Medical Cell Biology Commons](#), and the [Medical Molecular Biology Commons](#)

Recommended Citation

Lv, Xiangmin, "The Role of YES-Associated Protein 1 in Ovarian Physiology and Pathology" (2017). *Theses & Dissertations*. 225.

<https://digitalcommons.unmc.edu/etd/225>

This Dissertation is brought to you for free and open access by the Graduate Studies at DigitalCommons@UNMC. It has been accepted for inclusion in Theses & Dissertations by an authorized administrator of DigitalCommons@UNMC. For more information, please contact digitalcommons@unmc.edu.

THE ROLE OF YES-ASSOCIATED PROTEIN 1 IN OVARIAN PHYSIOLOGY AND PATHOLOGY

by

Xiangmin Lv

A DISSERTATION

Presented to the Faculty of
the University of Nebraska Graduate College
in Partial Fulfillment of the Requirements
for the Degree of Doctor of Philosophy

Medical Sciences Interdepartmental Area
Graduate Program
(Obstetrics & Gynecology)

Under the Supervision of Professor Cheng Wang

University of Nebraska Medical Center
Omaha, Nebraska

December, 2017

Supervisory Committee:

Jennifer D. Black, Ph.D.

John S. Davis, Ph.D.

Jixin Dong, Ph.D.

Steven W. Remmenga, M.D.

ACKNOWLEDGEMENTS

Funding support:

University of Nebraska Medical Center Graduate Studies Fellowship; National Cancer Institute (NCI/NIH); Eunice Kennedy Shriver National Institute of Child Health and Human Development (NICHD/NIH); The Olson Center for Women's Health, Department of Obstetrics and Gynecology, The Fred and Pamela Buffett Cancer Center, University of Nebraska Medical Center; The Colleen's Dream Foundation; The Marsha Rivkin Center for Cancer Research; The COBRE Grant from the Nebraska Center for Cell Signaling/National Institute of General Medical Sciences (NIGMS/NIH); and The VA Nebraska-Western Iowa Health Care System Department of Veterans Affairs.

Much more important than funding support, I would like to thank all the people who encouraged and supported me to move forward during my Ph.D. studies and complete this dissertation.

First and foremost, I want to express my sincere gratitude to my advisor Dr. Cheng Wang. He opened the door of science for me and guided me on the road of research, step by step, from running a western blot to writing manuscripts for publication, from sharing an idea to preparing proposals for funding support. He is always patient and helpful whenever we have problems. His door is always open for us to talk about our research projects. In addition, he leads our lab like a family. Everyone in the lab is so friendly, gratefully, and lovely.

I would like to thank my supervisory committee members: Dr. John S Davis, Dr. Jixin Dong, Dr. Jennifer D Black, and Dr. Steven W. Remmenga. I deeply appreciate for their scientific guidance, constructive comments, and invaluable thoughts to support my research career development. I also want to thank Dr. Adam Karpf and Dr. David Klinkebiel for their strong support and collaboration in my research projects.

Many Thanks to my lab members: Chunbo He, Cong Huang, Guohua Hua, Jin Zhou, Zhengfeng Wang, David Fu, Jingfeng Jiang and members in Dr. Davis lab. They are so supportive and friendly to work with and make the lab full of fun.

Thank all my friends from both China and the US. They make life so colorful.

Last but by no mean the least, I must thank my family. Thank my dad, mom, and sisters for their endless love and cares. Thank my parents-in-law who gave me the best gift for my life: my wife, who pushes me every day to be a reliable husband, a good scientist, and a better man.

ABSTRACT

THE ROLE OF YES-ASSOCIATED PROTEIN 1 IN OVARIAN PHYSIOLOGY AND PATHOLOGY

Xiangmin Lv, Ph.D.

University of Nebraska, 2017

Supervisor: Cheng Wang, Ph.D.

Ovarian granulosa cells are the major somatic components of the ovarian follicle. Proper proliferation and differentiation of ovarian granulosa cells are essential for successful follicle development. Accumulating evidence indicates that the Hippo-YAP signaling pathway plays critical roles in both development and tumorigenesis of several organs. The present study aims to investigate the role of Yes-associated protein 1 (YAP) in ovarian granulosa cell proliferation, differentiation, and malignant transformation. At first, we found that nuclear YAP (active) was highly expressed in proliferative granulosa cells, whereas cytoplasmic YAP (inactive) was detected mainly in terminally-differentiated luteal cells. Further studies suggested that endogenous YAP activity is essential for granulosa cell proliferation and survival to support follicle growth. However, overactive YAP impaired differentiation and stimulated malignant transformation of granulosa cells, indicating that YAP overactivation may play a role in the development of granulosa cell tumors which come from failure of terminal differentiation of granulosa cells to luteal cells. This idea was further supported by the overexpression of YAP detected in the human granulosa cell tumor tissues and the critical role of YAP in the progression of granulosa cell tumor.

High-grade serous ovarian cancer (HGSOC) is the most common and lethal type of ovarian cancer. A novel mesenchymal subtype of HGSOC has been recently identified by

both The Cancer Genome Atlas and Australian Ovarian Cancer Study studies and the origin of this subtype has yet to be defined. Here, my studies show that YAP can induce high-grade ovarian cancers with mesenchymal features from poorly differentiated granulosa cells. In xenograft mouse models, overactive YAP elicits malignant ovarian cancer development in the peritoneum of host mice from poorly differentiated human granulosa cells. These tumors presented in mouse peritoneum as typical human HGSOC morphologically, histologically, and genetically. However, these tumors overexpressed N-cadherin and vimentin but had low expression of CA125 and E-cadherin, features reminiscent of the recently identified mesenchymal HGSOC. These studies suggest that granulosa cells may be a cell-of-origin for the mesenchymal type of HGSOC.

TABLE OF CONTENTS

ACKNOWLEDGEMENTS.....	I
ABSTRACT.....	III
TABLE OF CONTENTS	V
LIST OF FIGURES.....	X
LIST OF TABLES.....	XII
LIST OF ABBREVIATIONS	XIII
CHAPTER 1:YAP REGULATES PHYSIOLOGY OF GRANULOSA CELLS	1
ABSTRACT	2
1.1. INTRODUCTION.....	3
1.1.1. Ovarian granulosa cells	3
1.1.2. The Hippo-YAP pathway.....	3
1.1.3. Yes-associated protein 1 (YAP).....	4
1.1.4. Previous research and present study.....	4
1.2. MATERIALS AND METHODS	6
1.2.1. Chemicals.....	6
1.2.2. Immunohistochemistry and immunocytochemistry	6
1.2.3. Cell collection and culture	7
1.2.4. YAP protein knockdown and overexpression	8
1.2.5. Three-dimensional hanging drop cell culture.....	9
1.2.6. Cell proliferation analysis	9
1.2.7. Apoptosis assays.....	10
1.2.8. Enzyme-linked immunosorbent assay (ELISA)	10
1.2.9. Western blots.....	10

1.2.10. Reverse transcriptase-polymerase chain reaction (RT-PCR)	11
1.2.11. BODIPY staining	11
1.2.12. Colony formation assays	12
1.2.13. In vitro ovary culture	12
1.2.14. In vivo YAP inhibition	13
1.2.15. Statistical analysis	13
1.3. RESULTS	14
1.3.1. Expression of YAP in human and mouse ovaries.....	14
1.3.2. YAP promotes proliferation and survival of human granulosa cells	15
1.3.3. YAP overexpression impairs steroidogenesis and cell differentiation	16
1.3.4. Overactive YAP induces dedifferentiation of granulosa cells.....	17
1.3.5. HBEGF stimulates YAP activity and granulosa cell proliferation	18
1.3.6. Gonadotropin inhibits YAP activity and induces hormone production....	18
1.3.7. YAP overactivation promotes granulosa cell growth in soft agar	19
1.3.8. YAP inhibition results in defects of mouse follicle development	20
1.4. DISCUSSION.....	21
1.4.1. Overview.....	21
1.4.2. YAP promotes granulosa cell proliferation and follicle growth	21
1.4.3. YAP impairs GC differentiation	22
1.4.4. Hippo-YAP signaling in follicle development	23
1.4.5. Conclusion.....	24
CHAPTER 2:YAP PROMOTES GRANULOSA CELL TUMOR PROGRESSION.....	42
ABSTRACT	43
2.1. INTRODUCTION.....	44
2.1.1. The Hippo-YAP pathway in organ size control and tumorigenesis	44

2.1.2.	Etiology of granulosa cell tumor	45
2.1.3.	The present study	46
2.2.	MATERIALS AND METHODS	47
2.2.1.	Chemicals.....	47
2.2.2.	Cell lines and human GCT tissue slides.....	47
2.2.3.	Immunohistochemistry analysis of YAP expression in ovarian tissues ..	48
2.2.4.	Localization of YAP protein in KGN cells.....	49
2.2.5.	YAP mRNA expression.....	49
2.2.6.	Western blot analysis.....	50
2.2.7.	Establishment of wild-type and mutant YAP overexpressed cell lines ...	50
2.2.8.	Cell proliferation assay.....	51
2.2.9.	Cell migration assay	51
2.2.10.	Statistical analysis	52
2.3.	RESULTS	53
2.3.1.	Expression of YAP protein in GCT	53
2.3.2.	Expression of YAP in ovarian GCT tumor cell lines.....	53
2.3.3.	Knockdown of YAP expression in KGN cells inhibits cell proliferation ...	54
2.3.4.	Overexpression of YAP promotes KGN cell proliferation and migration	55
2.4.	DISCUSSION.....	56
2.4.1.	Overview of previous studies and the present study on GCT	56
2.4.2.	YAP expression in GCT and ovarian epithelial cancer	57
2.4.3.	YAP promotes GCT progression.....	58
2.4.4.	Conclusion.....	59

CHAPTER 3:YAP INDUCES HIGH-GRADE OVARIAN CANCER WITH MESENCHYMAL FEATURE FROM POORLY DIFFERENTIATED GRANULOSA CELLS	70
ABSTRACT	71
3.1. INTRODUCTION.....	72
3.1.1. High-grade serous ovarian cancer	72
3.1.2. Origin of HGSOC.....	72
3.1.3. Novel mesenchymal subtype of HGSOC	73
3.1.4. Ovarian granulosa cells	73
3.1.5. Hippo-YAP signaling.....	74
3.1.6. Present study.....	74
3.2. MATERIALS AND METHODS	75
3.2.1. Cell culture.....	75
3.2.2. Retrovirus system for overexpression	75
3.2.3. CRISPR Cas9 system to knockout BRCA1	76
3.2.4. Cell proliferation analyses.....	76
3.2.5. Western blot	76
3.2.6. Three-dimensional hanging drop cell culture.....	76
3.2.7. Colony formation assays.....	76
3.2.8. Immunohistochemistry and immunocytochemistry	77
3.2.9. Hematoxylin and eosin stain for histology analyses	77
3.2.10. Alcian blue pH 2.5-periodic acid–Schiff stain	77
3.2.11. Xenograft mouse model.....	77
3.2.12. Array Comparative Genomic Hybridization (aCGH).	78
3.2.13. Statistical analysis	78

3.3.	RESULTS	79
3.3.1.	Overactive YAP induces malignant tumors from poorly differentiated human granulosa cells	79
3.3.2.	YAP overactivation induces malignant ovarian cancers like high-grade serous ovarian cancer from granulosa cells	80
3.3.3.	YAP induces high-grade ovarian cancers with mesenchymal features from granulosa cells	83
3.4.	DISCUSSION.....	84
3.4.1.	YAP induces high-grade ovarian cancers from poorly differentiated granulosa cells	84
3.4.2.	YAP elicits mesenchymal subtype of HGSOE from poorly differentiated granulosa cells	85
3.4.3.	The genomic instability of HGSOE.....	86
3.4.4.	Clinical significance	87
	BIBLIOGRAPHY.....	104

LIST OF FIGURES

Figure 1-1. Expression of YAP and LATS1/2 in various stages of mouse ovarian follicles.	25
Figure 1-2. The expression of YAP with the development of ovarian follicles in human.	27
Figure 1-3. YAP promotes proliferation and supports survival of human granulosa cells.	29
Figure 1-4. YAP overactivation compromises cell steroidogenesis and impedes cell differentiation	32
Figure 1-5. YAP hyperactivation induces dedifferentiation of granulosa cells.....	34
Figure 1-6. HBEGF and Gonadotropins regulate YAP activity and granulosa cell proliferation and steroidogenesis.....	36
Figure 1-7. YAP promotes granulosa cell growth in soft agar.	38
Figure 1-8. Inhibition of YAP disrupts ovarian follicle development in vitro and in vivo. ...	40
Figure 2-1. YAP is expressed in human granulosa cell tumors (GCT).	60
Figure 2-2. YAP is expressed in human ovarian GCT cell lines and epithelial ovarian cancer cell lines.	62
Figure 2-3. YAP is required for KGN cell proliferation.	64
Figure 2-4. Overexpression of YAP stimulates KGN cell proliferation.	66
Figure 2-5. YAP regulation of KGN cell migration.	68
Figure 3-1. YAP induces non-granulosa cell tumors from poorly differentiated granulosa cells.	89
Figure 3-2. YAP induces malignant ovarian cancers from poorly differentiated granulosa cells.	92
Figure 3-3. YAP elicits HGSOc-like tumors from poorly differentiated granulosa cells. .	94

Figure 3-4. YAP induces HGSOc-like tumors with mesenchymal features from poorly differentiated granulosa cells.....	96
Figure 3-5. Tumors derived from poorly differentiated granulosa cells genetically resemble HGSOc.....	98

LIST OF TABLES

Table 1. Primers for PCR.....	100
Table 2. Antibodies.....	102

LIST OF ABBREVIATIONS

<i>3βHSD/HSD3B1</i>	3 beta-hydroxysteroid dehydrogenase/delta 5-->4-isomerase type I
aCGH	array comparative genomic hybridization
AOCS	Australian ovarian cancer study
AKT	AKT serine/threonine kinase
ANOVA	analysis of variance
AREG	amphiregulin
<i>CYP19A1</i>	cytochrome p450 family 19 subfamily a member 1
BRCA1	breast and ovarian cancer susceptibility protein 1
BSA	bovine serum albumin
CA125	mucin 16, cell surface associated
CDH1	Cadherin 1/E-Cadherin
CDH2	Cadherin 2/N-Cadherin
cGC	cumulus granulosa cells
CREB	cAMP responsive element binding protein 1
CTGF	connective tissue growth factor
DAPI	4',6-diamidino-2'-phenylindole dihydrochloride
DMEM/F-12	Dulbecco's modified eagle medium/nutrient mixture F-12
DMSO	dimethylsulfoxide
DNA	deoxyribonucleic acid

EGFR	epidermal growth factor receptor
ERBB	Erb-b2 receptor tyrosine kinase
ERK	extracellular signal-regulated kinase
FBS	fetal bovine serum
FSH	follicle stimulating hormone
FSHR	follicle stimulating hormone receptor
FSK	forskolin
GADPH	glyceraldehyde-3-phosphate dehydrogenase
GC	granulosa cell
GCT	granulosa cell tumor
H & E	hematoxylin and eosin
HBEGF	heparin binding EGF like growth factor
HGSOC	high-grade serous ovarian carcinoma
INHA	inhibin alpha subunit
INHBA	inhibin beta a subunit
INHBB	inhibin beta b subunit
JASP	jasplakinolide
Ki67	marker of proliferation Ki-67
KRT20	keratin 20
KRT7	keratin 7
LATS1	large tumor suppressor kinase 1
LATS2	large tumor suppressor kinase 2

LC	luteal cell
LH	luteinizing hormone
LHCGR	luteinizing hormone/chorionic gonadotropin receptor
mGC	mural granulosa cell
MOB1	MOB kinase activator 1
mRNA	messenger ribonucleic acid
MST1	mammalian ste20-like protein kinase 1
MST2	mammalian ste20-like protein kinase 2
Myc	proto-oncogene c-myc
P450scc/CYP11A1	cholesterol side-chain cleavage enzyme,
p53	tumor protein p53
PAX2	paired box 2
PAX8	paired box 8
PBS	phosphate-buffered saline
PCR	polymerase chain reaction
PKA	protein kinase a
PLIN2	perilipin 2
PVDF	polyvinylidene difluoride
qPCR	quantitative real-time polymerase chain reaction
RT-PCR	reverse transcriptase polymerase chain reaction
SAV1	salvador homolog 1
S1P	sphingosine-1-phosphate

SNP	single-nucleotide polymorphism
TAZ	WW domain containing transcription regulator 1
TCGA	the cancer genome atlas
TEAD	TEA domain transcription factor
TERT	telomerase reverse transcriptase
UNMC	University of Nebraska Medical Center
WT1	Wilms tumor 1
YAP	Yes-associated protein 1

CHAPTER 1: YAP REGULATES PHYSIOLOGY OF GRANULOSA CELLS*

* The material presented in this chapter was submitted as a manuscript: Lv *et al.* 2017.

ABSTRACT

Ovarian granulosa cells are the major somatic components of the ovarian follicle, and proper granulosa cell proliferation and differentiation are critical for normal follicle development. Recent studies suggest that the Hippo-YAP pathway controls the development of several organs; however, its role in ovarian follicle development remains largely unknown. The present study investigates the role of YAP in ovarian granulosa cell physiology. Immunohistochemical analyses showed that nuclear YAP was highly expressed in proliferative granulosa cells, whereas cytoplasmic YAP was mainly detected in terminally differentiated luteal cells, indicating that YAP activity may be involved in the regulation of proliferation and differentiation of ovarian granulosa cells. YAP inhibition by siRNA or pharmacological antagonist in human granulosa cells suppressed cell proliferation, and overexpression of wild-type or constitutively active YAP impaired gonadotropin-induced differentiation and stimulated rapid proliferation and malignant transformation of granulosa cells. Cell signaling studies suggested that HBEGF, which upregulated by YAP, activated YAP and promoted proliferation of granulosa cells. Conversely, gonadotropin-activated PKA signaling inhibited YAP activity and stimulated differentiation. Ovary *in vitro* culture experiments demonstrated that YAP inhibition blocked growth of pre-antral ovarian follicles to antral follicles by suppressing granulosa cell proliferation. Further, injection of Verteporfin (a selective antagonist of YAP) into female CD1 mice inhibited disrupted mouse ovarian follicle development *in vivo*. Our studies demonstrate that dynamic regulation of YAP activity is essential for granulosa cell proliferation and differentiation to support ovarian follicle development.

1.1. INTRODUCTION

1.1.1. Ovarian granulosa cells

The ovary is a complex organ essential for producing oocytes and secreting steroid hormones to achieve reproduction and maintain women's health. The follicle is the basic functional unit of the ovary. Ovarian granulosa cells, which contribute to most of the somatic components of the ovarian follicle, can produce sex hormones and growth factors for follicle development (1). After a fast-growth phase in undifferentiated status, granulosa cells undergo differentiation under induction of the follicle stimulating hormone (FSH). Transgenic mouse models demonstrated that FSH-deficient females became infertile due to failure of antral follicle development, indicating the significance of gonadotropin-induced granulosa cell differentiation during follicle development (2). Under the stimulation of luteinizing hormone (LH), ovulation occurs, and granulosa cells exit the cell cycle and terminally differentiate to luteal cells for progesterone production (3). Therefore, it is essential that granulosa cells are coordinately regulated to proliferate and differentiate for follicle growth and maturation to maintain normal ovarian function.

1.1.2. The Hippo-YAP pathway

Recent studies suggest that the Hippo-YAP pathway controls organ development (4-7). The Hippo-YAP pathway was first discovered in *Drosophila* and later found to be conserved in mammals. The core components of the Hippo-YAP pathway in mammals consist of the serine/threonine kinases Mammalian STE20-like protein kinase 1/2 (MST1/2) and Large Tumor Suppressor kinase 1/2 (LATS1/2), the scaffold proteins Salvador homolog 1 (Sav1) and MOB kinase activator 1 (MOB1), and the downstream transcriptional coactivators Yes associated protein 1 (YAP) and WW Domain Containing Transcription Regulator 1 (WWTR1 or TAZ). Activation of upstream kinases by

phosphorylation leads to subsequent phosphorylation of YAP and TAZ proteins, which retains them in the cytoplasm and inhibits their transcriptional activity (4, 7, 8). Without inhibition from upstream kinases, non-phosphorylated YAP and TAZ translocate into the nucleus to bind with transcriptional factors such as TEA Domain Transcription Factor (TEAD) to activate targeting gene expression to promote cell proliferation, survival, and stem cell function.

1.1.3. Yes-associated protein 1 (YAP)

Extensive studies have recently indicated that YAP is a proto-oncogene that plays important roles in organ growth and tumorigenesis by regulating cell proliferation and apoptosis (6, 9-12). It has also been shown that YAP activity is involved in the regulation of cell fate in the liver, lung, intestine and skin (13-21). For example, Hippo pathway activation regulates maintenance of the differentiated hepatocyte state, whereas increased YAP activity defines hepatic progenitor identity, driving liver overgrowth and tumorigenesis (22). Furthermore, our previous report showed that YAP expression is elevated in the granulosa cell tumor (GCT) compared with normal ovaries and that YAP can promote GCT cell proliferation and migration (23).

1.1.4. Previous research and present study

Although many reports have focused on the Hippo pathway in the last decade, its role in the development of mammalian ovarian follicle remains unclear. Studies from Kawamura et.al. showed that fragmentation of ovaries stimulates follicle growth through disruption of the Hippo-YAP pathway (24). Cheng et.al. recently showed that Jasplakinolide (JASP) and sphingosine-1-phosphate (S1P) can stimulate follicle growth by activating YAP protein (25). However, the cell types involved in these processes and the underlying molecular mechanisms are not known. A recent study indicated that YAP

is dispensable for oocyte survival, growth, and maturation in mouse model (26). Thus, the present study focuses on the roles of YAP in regulation of granulosa cell physiology. Our results indicate that the dynamic regulation of YAP activity is vital for granulosa cell proliferation and differentiation to support ovarian follicle development for female fertility.

1.2. MATERIALS AND METHODS

1.2.1. Chemicals

DMEM/F12 and other cell culture media were purchased from Sigma-Aldrich (St. Louis, MO); fetal bovine serum (FBS) was from Atlanta Biologicals, Inc. (Lawrenceville, GA); Alexa-conjugated secondary antibodies were from Life Technologies (Grand Island, NY); YAP siRNA#1 and siRNA#2 were from Dharmacon/Thermo Scientific (Pittsburgh, PA); RNeasy Mini Kit was from QIAGEN Inc. (Valencia, CA); PCR reagents were from Invitrogen (Carlsbad, CA), QIAGEN (Carlsbad, CA) or Bio-Rad (Hercules, CA); Peroxidase-conjugated secondary antibodies for Western blotting were from Jackson ImmunoResearch Laboratories Inc. (West Grove, PA); the SuperSignal West Femto Chemiluminescent Substrate Kit was from Pierce/Thermo Scientific (Rockford, IL); and the Optitran® Nitrocellular transfer membrane was from Schleicher&Schuell Bioscience (Dassel, Germany).

1.2.2. Immunohistochemistry and immunocytochemistry

Fluorescent immunohistochemistry was used to detect expression of YAP, Ki67, 3 β -HSD, and cleaved caspase-3 protein in the mouse ovary or the spheroids of 3D culture system. Briefly, tissues were frozen in Tissue-Tek optimal cutting temperature (O.C.T.) compound (Sakura Finetek Europe B.V., Flemingweg, AJ Alphen aan den Rijn, The Netherlands). The blocks were sectioned at 6 μ m thickness using a Leica CM3050S instrument and attached to silane-coated slides. The frozen sections were fixed in freshly prepared 4% paraformaldehyde and stained using antibodies for YAP, Ki67, 3 β -HSD, and cleaved caspase 3 protein overnight. Sections were then incubated with the appropriate fluorescein-labeled (red or green) secondary antibody at room temperature for 30 min in a humidified chamber. F-actin was stained with Rhodamine Phalloidin and nuclei were

labeled with DAPI. Slides were mounted with Fluoromount-G (Southern Biotech, Birmingham, AL) and coverslips. Images were captured using a Zeiss 710 Meta Confocal Laser Scanning Microscope and analyzed using Zeiss Zen 2010 software (Carl Zeiss Microscopy, LLC, Thornwood, NY).

YAP, LATS1, and LATS2 expression in paraffin-embedded human ovarian tissues was detected using a peroxidase-based immunohistochemistry assay (VECTASTAIN Elite ABC HRP kit, Vector Laboratories) and immunosignals were visualized with a DAB kit (ImmPACT DAB Peroxidas HRP Substrate, Vector Laboratories). Stained sections were counterstained with hematoxylin and covered with coverslips using Sakura Automated Slide Stainer and Coverslipper. In negative controls, the primary antibody was replaced by a blocking buffer containing the same amount of IgG from non-immune rabbit serum. The sections were scanned with an iSCAN Coreo Slide Scanner (Ventana Medical Systems, Inc., Oro Valley, AZ). Paraffin-embedded normal human ovarian tissue slides were obtained from the Department of Pathology, Tianjin Medical University Cancer Hospital and University of Nebraska Medical Center (UNMC). These human tissue slides were used according to protocols approved by the UNMC Institutional Review Board and Tianjin Medical University Institutional Review Board.

Fluorescent immunocytochemistry was used to localize YAP protein in KGN cells. Briefly, cells were cultured on the coverslips. After treatments, cells were fixed in freshly prepared 4% paraformaldehyde and stained for YAP protein as fluorescent immunohistochemistry.

1.2.3. Cell collection and culture

Primary human granulosa cells were collected from follicular aspirates of reproductive-age patients during oocyte retrieval for *in vitro* fertilization (IVF) at the Heartland Center

for Reproductive Medicine (Omaha, NE). Patients were treated with recombinant human follicle stimulating hormone (FSH), followed by administration of hCG to induce follicle development. After hCG treatment for 35 h, oocyte and follicular fluid were retrieved under guidance by ultrasound. The oocyte and cumulus cells were collected for IVF. The remaining follicular aspirates were held on ice and sent to the laboratory for studies. The aspirates donated from a single patient were pooled and centrifuged at 500 g for 5 min. Cells were resuspended in DMEM/F12 (Fisher Scientific Inc. Pittsburgh, PA) containing 2% penicillin-streptomycin. The cell suspension was then carefully layered onto 50% Percoll, and centrifuged at 800 × g for 15 min. Granulosa cells were harvested from the interphase of the medium and Percoll. After being washed 3 times with DMEM/F12, granulosa cells were seeded into 10 cm dishes with DMEM/F12 containing 1% Ultrosor G serum substitute (Pall Corporation, Saint-Germain-en-Laye Cedex, France) and 1% penicillin-streptomycin. The following day, granulosa cells were trypsinized and plated into 6-well plate for siRNA transfection or virus infection.

The HGrC1 and KGN cell lines were purchased from the Riken Biosource Center (Riken Cell Bank, Tsukuba, Japan) and has been validated by short tandem repeat polymorphism analysis. Cells were cultured in DMEM/F12 with the addition of 1% Ultrosor G serum substitute and 1% penicillin-streptomycin. Cells were incubated at 37 °C, 5% CO₂, and 95% air.

1.2.4. YAP protein knockdown and overexpression

YAP protein knockdown was performed with YAP targeting siRNA#1 and siRNA#2 (GE Dharmacon, Lafayette, CO). Lipofactamine® RNAiMAX Transfection Reagent (Grand Island, NY) was used to deliver siRNA into cells according to manufacturer instructions.

Using retrovirus-based YAP overexpression constructs given by Dr. Jixin Dong (University of Nebraska Medical Center), hGC-YAP, and hGC-YAP^{S127A} cells were established with overexpression of wild-type YAP and constitutively active mutant YAP in primary human granulosa cells (hGC), respectively. hGC-MX cells were established as control with transfection of empty vector. Mutated YAP protein (S to A at residue 127) prevents YAP from being phosphorylated at residue 127, resulting in constitutive activation. Primary human granulosa cells were plated and cultured at 30 – 40% confluence in 6-well plates, retrovirus with MX, YAP, and YAP^{S127A} vectors were incubated with cells overnight. After 72 h infection, positive cells were selected with G-418 (400 µg/ml) for 7 days.

1.2.5. Three-dimensional hanging drop cell culture

A three-dimensional (3D) hanging drop culture system was employed to mimic granulosa cell growth *in vivo*. Briefly, an equal number (0.5×10^6) of hGC-MX, hGC-YAP, and hGC-YAP^{S127A} cells was loaded onto a GravityPLUS™ 3D Cell Culture plate (InSphero, Schlieren, Switzerland) according to manufacturer instructions. Culture medium was replaced everyday and the spheroids were cultured at 37 °C, 5% CO₂, and 95% air for 7 days. Spheroids were imaged by an Olympus inverted microscopy (Olympus America, Inc. Center Valley, PA). The volume of spheroids ((shortest diameter)² × (longest diameter) × 3.14 /6) were calculated as indication of cell growth. The spheroids were then embeded in OCT for preparation of frozen sections.

1.2.6. Cell proliferation analysis

Cell numbers were monitored with an Invitrogen Countess automated cell counter after YAP knocked down or YAP/YAP^{S127A} overexpressed for indicated time with proper controls. Trypan blue was used to identify and quantify viable cells.

1.2.7. Apoptosis assays

Cell apoptosis was monitored by an Annexin V-FITC Apoptosis Detection Kit (BioVision Inc., San Francisco, CA) following manufacturer instructions. Briefly, after indicated treatments, cells were trypsinized and incubated with Annexin V-FITC and propidium iodide for 5 min. Flow cytometry was performed by the Flow Cytometry Research Facility at the University of Nebraska Medical Center to monitor apoptosis.

1.2.8. Enzyme-linked immunosorbent assay (ELISA)

Estradiol and progesterone levels in cell culture media and mouse serum were detected using ELISA assays. Medium estradiol levels were monitored using 17 β -Estradiol Enzyme Immunoassay Kit (Arbor Assays, Ann Arbor, Michigan). Progesterone production was detected by using Progesteron(e) ELISA kit (DRG International Inc., Springfield, NJ).

1.2.9. Western blots

Cells were harvested on ice with ice-cold cell lysis buffer (10 mM Tris pH (7.4), 100 mM NaCl, 1 mM EDTA, 1 mM EGTA, 1 mM NaF, 20 mM Na₄P₂O₇, 1% Triton x-100, 10% glycerol, 0.1% SDS, and 0.5% deoxycholate, plus protease and phosphatase inhibitor cocktails (Pierce/Thermo Scientific, Rockford, IL)). Each lysate was then sonicated for 3 s. Lysates were centrifuged at 18,350 x g for 15 min at 4 °C and supernatants were collected for SDS-PAGE analysis. Protein concentration was determined by Bradford assay (Bio-Rad 500-0006). Protein samples (30 μ g) were loaded with protein-loading buffer (50 mM Tris pH 6.8, 300 mM glycerol, 25 mM SDS, 45 mM DTT, 260 mM 2-mercaptoethanol, and bromophenol) on 10% SDS-PAGE gel and separated by electrophoresis. Separated proteins were then transferred to nitrocellulose membranes,

which were blocked with 5% BSA in TBST (10 mM Tris-HCl, 150 mM NaCl, 0.1% Tween 20; pH 7.5) for 1 h at room temperature. Primary antibodies diluted in TBST with 5% BSA were incubated with blocked membranes overnight at 4 °C or for 2 h at room temperature. After washing 3 times with TBST for 5 min, membranes were further probed with anti-rabbit or anti-mouse HRP-conjugated IgG diluted in TBST with 5% BSA (1: 2,000) for 1 h at room temperature. After washing 3 times with TBST for 5 min, protein bands were detected with Thermo Scientific SuperSignal West Femto Chemiluminescent Substrate Kit. Images were captured and analyzed with a UVP gel documentation system (UVP, Upland, CA).

1.2.10. Reverse transcriptase-polymerase chain reaction (RT-PCR)

Total RNA was isolated from indicated cell cultures using the RNeasy mini kit (Qiagen, Inc.) according to manufacturer instructions. First-strand cDNA was synthesized from 1 µg total RNA using iScript Reverse Transcription Supermix for RT-qPCR kit (Bio-Rad). Quantitative RT-PCR was performed with gene-specific primers and iTaq Universal SYBR green supermix by using CFX96 Real-Time System (Bio-Rad). GAPDH was used as normalized control. RT-PCR was performed with GoTaq Flexi DNA Polymerase (Bio-Rad). Products were loaded onto an agarose gel and separated by electrophoresis. Images were captured by UVP gel documentation system.

1.2.11. BODIPY staining

Fluorescent neutral lipid dye 4,4-difluoro-1,3,5,7,8-pentamethyl-4-bora-3a,4a-diaza-s-indacene (BODIPY 493/503, green) was used to stain lipid droplets. Cells or frozen tissues on slides were fixed with 4% paraformaldehyde and washed with PBS for 3 x 5 min. BODIPY, Rhodamine Phalloidin, and DAPI diluted in normal donkey serum were incubated with tissues/cells for 30 min. After three 5 min washes, slides were mounted

with Fluoromount-G and coverslips. Pictures were captured by Zeiss 710 Meta Confocal laser scanning microscopy.

1.2.12. Colony formation assays

The role of YAP in transformation was determined using a Cytoselect 96-Well Cell Transformation assay kit (Cell Biolabs, Inc., San Diego, CA) according to manufacturer instructions. Briefly, equal numbers of cells from diverse groups were plated in 0.6% soft agar condition and cultured with treatments for 10 days. MTT (3-(4,5-dimethylthiazol-2-yl)-2,5-diphenyltetrazolium bromide) was used to stain colonies, which were then imaged and counted.

1.2.13. *In vitro* ovary culture

Mouse ovaries were collected at day 12 after birth. Ovaries were excised from the ovarian bursa and transferred with a drop of medium onto Costar Transwell membrane (non-tissue culture treated, Nucleopore polycarbonate membrane, 3.0- μ m pore size, 24-well insert). About one half ml of medium (Waymouth medium MB752/1 supplement with 0.23 mM pyruvic acid, 3 mg/ml BSA, 10% FBS, and 1% penicillin and streptomycin, 5 ng/ml FSH (Recombinant human FSH was obtained from National Institute of Diabetes and Digestive and Kidney Diseases (Bethesda, MD)) was also added to support follicle development) had been added in the well below the membrane insert. When the drop of medium was add onto the membrane, the ovary was covered by only a thin film of medium. The medium was changed every 2 days by adding 0.5 ml of medium to the chamber below the membrane and then withdrawing the same volume. Cultures were incubated at 37 °C, 5% CO₂, and 95% air for 7 d. Verteporfin or vehicle was added to medium for treatments. At the end of experiments, ovaries were photographed and fixed. Histology and immunohistochemistry were performed to exam the ovarian follicle development.

1.2.14. *In vivo* YAP inhibition

Verteporfin (VP, 50 mg/kg) or vehicle (10% DMSO in PBS, 100 μ l) was injected into adult female CD-1 mice daily for 5 d. Ovaries and serum were collected for RNA, protein, IHC, and TUNEL analyses according to approved ICAUC protocols.

1.2.15. Statistical analysis

All experiments were performed at least three times unless otherwise noted. The data are presented as representative experiments or as the means \pm SEM of the averages from multiple experiments. Statistical analysis was conducted using GraphPad Prism software (GraphPad Software, Inc. La Jolla, CA). Statistical comparisons between two groups were analyzed for significance by two-tailed Student's t-test. Multiple group comparisons were assessed by one-way analysis of variance with Tukey's post-Hoc test. $P \leq 0.05$ was considered statistically significant.

1.3. RESULTS

1.3.1. Expression of YAP in human and mouse ovaries

The spatio-temporal expression of YAP during ovarian follicle development in mammals has not been thoroughly investigated. We monitored the expression level and location of YAP in both mouse and human ovaries using immunohistochemistry. Fluorescent immunohistochemistry analyses showed that the expression of YAP was mainly located in the granulosa and luteal cells of the mouse ovary (Fig. 1-1 A¹, B¹, C¹ & C⁰). In early granulosa cells of primary (P1) and secondary (P2) follicles, YAP was moderately expressed in the nuclei (Fig. 1-1 A¹). In the growing follicle, granulosa cells are proliferative, as indicated by high expression of proliferation marker Ki67 (Fig. 1-1 A², B² & C²). In granulosa cells of growing follicles, YAP protein was highly expressed in the nuclei (Fig. 1-1 A¹, B¹, C¹ & C⁰). However, when granulosa cells terminally differentiated into luteal cells, which highly expressed 3 β HSD enzyme (Fig. 1-1 A³, B³ & C³), YAP was largely located to the cytoplasm (Fig. 1-1 A¹, B¹, C¹ & C⁰), indicating inhibited YAP activity (9). The expression of YAP decreased dramatically in the late phase of luteal cells (ILC) which express less 3 β HSD enzyme and undergo regression (Fig. 1-1 B¹ & B³). In addition, LATS1 and LATS2, the upstream suppressors of YAP in the Hippo pathway, were detected with elevated expression in luteal cells compared with their expression in granulosa cells, respectively (Fig. 1-1 D¹ & D²).

A similar expression pattern was observed in human ovaries. YAP was mainly expressed in the nuclei of granulosa cells of early stage follicles (Fig. 1-2). In the differentiating granulosa cells of antral follicle, YAP expression was detected in both cytoplasm and nuclei (Fig. 1-2). Consistently, YAP was mainly located in the cytoplasm of luteal cells (Fig. 1-2). Interestingly, YAP expression was focused in the nuclei of cumulus

granulosa cells (cGC), though YAP tends to disperse much more in the cytoplasm of mural granulosa cells (mGC) (Fig. 1-2). Previous study suggested that cGC were enriched in transcripts for cell proliferation and mGC were enriched in transcripts associated with cell differentiation and steroidogenesis (27). Together, these results suggest that proliferative granulosa cells express active YAP protein, whereas YAP activity is gradually suppressed during the differentiation of granulosa cells to luteal cells. Thus, YAP may be critical in the regulation of proliferation and differentiation of granulosa cells.

1.3.2. YAP promotes proliferation and survival of human granulosa cells

The co-localization of active YAP and Ki67 staining in granulosa cells (Fig. 1-1) suggests that YAP may be critical for granulosa cell proliferation. Using YAP-targeting siRNA#1 and siRNA#2, YAP expression was efficiently knocked down in primary human granulosa cells (hGC) (Fig. 1-3 A), and cell proliferation was suppressed significantly after knockdown for 5 d (Fig. 1-3 B). YAP inhibition with siRNA#1 and siRNA#2 dramatically increased cell apoptosis (Fig. 1-3 C), indicating essential role of YAP to support granulosa cell survival. Employing a retrovirus-based system, hGC were expressed with empty vector (hGC-MX), wild-type YAP (hGC-YAP), or constitutively active YAP (hGC-YAP^{S127A}, Serine 127 site was mutated to Alanine to avoid inhibition by LATS1/2 phosphorylation (4, 10)) to investigate the effects of YAP overactivation in human granulosa cells. Western blots showed that both hGC-YAP and hGC-YAP^{S127A} cells expressed high level of YAP (Fig. 1-3 D), indicating high efficiency of overexpression. Compared with high levels of phosphorylated YAP (S127) in hGC-YAP, hGC-YAP^{S127A} cells had much less phosphorylated YAP (S127) expression, which is similar with that of control (Fig. 1-3 D). These results demonstrated that in hGC-YAP cells, the Hippo pathway actively suppressed, in some extent, overexpressed wild-type YAP, whereas hGC-YAP^{S127A} cells successfully expressed constitutively active YAP^{S127A} protein avoiding phosphorylation

and inhibition. Overexpression of both wild-type and constitutively active YAP significantly increased the proliferation of hGC, with hGC-YAP^{S127A} cells have the most cell number (Fig. 1-3 E).

To mimic the growth of granulosa cells *in vivo*, we established a three-dimensional (3D) hanging drop culture system in which cells form natural cell contacts to grow as spheroid structure (1, 28). YAP overexpression significantly stimulated human granulosa cell growth in 3D culture, indicated by the increased volume of the spheroids formed by hGC-YAP and hGC-YAP^{S127A} cells compared with control (Fig. 1-3 F). Further fluorescent immunocytochemistry analyses showed that YAP overexpression increased Ki67 and decreased cleaved Caspase 3 expression (Fig. 1-3 G & H). A pharmacological inhibitor Verteporfin (VP), which specifically blocks YAP activity (29), reduced Ki67 and increased cleaved Caspase 3 expression (Fig. 1-3 G & H). Taken together, YAP stimulates proliferation and supports survival of human granulosa cells.

1.3.3. YAP overexpression impairs steroidogenesis and cell differentiation

The distinct expression pattern of YAP in granulosa cells and luteal cells suggests that YAP activity may negatively regulate the differentiation of granulosa cells. Gonadotropins-induced PKA pathway activation regulates the differentiation of granulosa cells (30, 31). We utilized FSH and forskolin (FSK, an adenylate cyclase activator (32)) to induce hormone production of hGC and KGN cells with different YAP activity (hGC-MX, hGC-YAP, hGC-YAP^{S127A}, KGN-MX, KGN-YAP, and KGN-YAP^{S127A}). FSK or FSH treatments induced hormone production in control cells as expected (Fig. 1-4 A & C). Overexpression of YAP or YAP^{S127A} decreased both the basal and FSK or FSH induced production of estradiol and progesterone (Fig. 1-4 A & C). Interestingly, YAP or YAP^{S127A} overexpression almost eliminated FSH induced hormone production (Fig. 1-4 C). Quantitative PCR results

demonstrated that YAP overexpression reduced mRNA of steroidogenic enzymes aromatase (*CYP19A1*) and cholesterol side-chain cleavage enzyme (*P450scc/CYP11A1*) in granulosa cells with or without FSK treatment (Fig. 1-4 B). Western blot results further demonstrated that overexpression of YAP or YAP^{S127A} dramatically decreased FSH- and FSK- induced expression of aromatase and P450scc (Fig. 1-4 D). These results indicate that overactivation of YAP compromised steroidogenesis of human granulosa cells by down-regulation of key enzymes.

Lipid droplet formation is a marker of granulosa cell differentiation (33, 34), BODIPY staining showed numerous lipid droplets in the differentiated luteal cells but few in granulosa cells (Fig. 1-4 E). FSK treatment induced mass production of lipid droplets in control cells, indicating cell differentiation induced by FSK (Fig. 1-4 E). However, overexpression of YAP or YAP^{S127A} reduced the formation of lipid droplets under FSK induction, suggesting that differentiation was impaired by YAP overactivation (Fig. 1-4 E).

1.3.4. Overactive YAP induces dedifferentiation of granulosa cells

To further investigate the role of YAP in cell differentiation, key molecules related to granulosa cell differentiation were detected by Quantitative PCR. On the one hand, YAP or YAP^{S127A} overexpression significantly increased mRNA expression of *Myc*, and *TERT* (Fig. 1-5 A), which are important molecules for retaining stemness and are enriched in early granulosa cells and tumor cells (35, 36). On the other hand, overexpression of YAP significantly decreased mRNA expression of *FSHR*, *CYP19A1*, *CYP11A1*, *INHA*, *INHBA*, *INHBB*, and *PLIN2*, all of which are differentiation markers of granulosa cells (Fig. 1-5 A). Together these results suggest that YAP hyperactivity induces dedifferentiation of granulosa cells.

Previous studies showed that YAP can promote epithelial cells to undergo epithelial–mesenchymal transition (EMT) (37-39). However, our results showed hyperactive YAP promotes mesenchymal–epithelial transition (MET) of granulosa cells by decreasing mesenchymal proteins including vimentin, Snail, Slug, and by elevating epithelial markers Claudin 1 and ZO-1 (Fig. 1-5 B). Recent studies suggested that MET is vital for cell reprogramming (40, 41), support our idea that YAP reprograms granulosa cells to a dedifferentiation status.

1.3.5. HBEGF stimulates YAP activity and granulosa cell proliferation

The epidermal growth factor (EGF) family plays significant role in granulosa cell proliferation and differentiation during follicle development (42). A previous study showed that HBEGF, a member of EGF family ligands, is expressed in the granulosa cells of early-stage follicle (43). We found that YAP upregulated HBEGF expression in granulosa cells (Fig. 1-6 A). HBEGF stimulated granulosa cell proliferation, but suppressed production of both estradiol and progesterone (Fig. 1-6 B). In turn, we found that HBEGF can activate YAP in granulosa cells. Western blot results showed that HBEGF can dephosphorylate YAP at S127 site following dephosphorylation of upstream LATS1 kinase (Fig. 1-6 C). The phosphorylation of ERK and AKT were induced by HBEGF in 10 minutes, which occurred before the dephosphorylation of YAP and LATS1. These results suggest that HBEGF stimulates YAP activity and granulosa cell proliferation.

1.3.6. Gonadotropin inhibits YAP activity and induces hormone production

Then we ask how gonadotropin-induced differentiation signaling affects YAP activity. Both FSH and FSK were able to induce cultured granulosa cell differentiation to produce estradiol and progesterone (Fig. 1-6 D), whereas cell proliferation was suppressed (Fig. 1-6 D). Interestingly, we found that FSH and FSK increased YAP phosphorylation at S127

site following elevated LATS1 phosphorylation (Fig. 1-6 E). The phosphorylation of CREB indicated that differentiation PKA signaling pathway was activated by FSH and FSK as expected (Fig. 1-6 E). Fluorescent immunocytochemistry results showed that the cytoplasmic retention of YAP was increased under FSK treatment (Fig. 1-6 F). Further, FSK can down regulated mRNA expression of HBEGF, which was upregulated by YAP (Fig. 1-6 G). These results suggest that gonadotropin-induced PKA pathway activation inhibits YAP activity and induces hormone production of granulosa cells.

1.3.7. YAP overactivation promotes granulosa cell growth in soft agar

Impairment of granulosa cell differentiation may result in uncontrolled proliferation and thus malignant cell transformation (44). To examine the role of YAP in the transformation of granulosa cells, *in vitro* soft agar assays were performed. Empty vector transfected hGC-MX cells formed few or no large colonies in the soft agar culture after seeding for 10 d, whereas both wild-type (hGC-YAP) and constitutively active YAP (hGC-YAP^{S127A}) overexpressing granulosa cells formed many large colonies (Fig. 1-7 A & B). hGC-YAP^{S127A} cells formed the most colonies (Fig. 1-7 A & B). Pharmacological inhibition of YAP by Verteporfin resulted in failure of colony formation in YAP or YAP^{S127A} overexpressing cells (Fig. 1-7 A & B), indicating that YAP may promote the transformation of granulosa cells. To avoid potential subjective results from manual colony number counting, fluorescence-based cell transformation assays were used to analyze cell growth in the anchorage-independent culture. The results further demonstrated that YAP or YAP^{S127A} overexpression stimulated human granulosa cell growth in soft agar, whereas inhibition of YAP activity reversed the anchorage-free growth induced by YAP overactivation (Fig. 1-7 A & B).

1.3.8. YAP inhibition results in defects of mouse follicle development

In vitro ovary culture system was used to examine the role of YAP for ovarian follicle development. Mouse ovaries were collected at day 12 after birth and cultured on membrane with or without addition of Verteporfin (VP). After culture *in vitro* for 7 d, ovaries of control (CTL) group developed growth follicles which can be observed under microscopy, whereas Verteporfin treated ovaries did not show follicle growth (Fig. 1-8 A). Histological analyses showed antral follicles were formed in control ovaries, indicating that *in vitro*-cultured ovaries keep the same pace of follicle development with *in vivo* condition (Fig. 1-8 B). However, there is no antral follicle found in the Verteporfin treated group (Fig. 1-8 B). Further IHC analyses demonstrated that YAP inhibition blocked granulosa cell proliferation and induced cell apoptosis, resulting in arrested follicle growth (Fig. 1-8 C & D).

To further investigate inhibition of YAP effects on mouse follicle development *in vivo*, intraperitoneal injection of Verteporfin (50 mg/kg, daily) or vehicle was conducted for 5 d. Downstream YAP targeting genes *Ctgf*, *Areg*, *Hbegf*, *Myc*, and *ErbB3* were downregulated after Verteporfin treatment (Fig. 1-8 E), suggesting YAP activity was successfully blocked by Verteporfin. TUNEL assay results evidenced increased apoptotic follicles in ovaries after Verteporfin treatment (Fig. 1-8 F). Meanwhile, 3 β HSD staining showed that the number of corpus luteum were reduced with Verteporfin injection (Fig. 1-8 G), which was also supported by decreased mRNA of *Hsd3b* (Fig. 1-8 H), a key enzyme expressed in corpus luteum. Progesterone, secreted by the corpus luteum, was decreased in the blood of Verteporfin treated mice compared with control group (Fig. 1-8 I). These results further suggest that inhibition of YAP activity leads to defects of ovarian follicle development *in vivo*.

1.4. DISCUSSION

1.4.1. Overview

Ovarian follicle development is vital for women's fertility and health. Ovarian granulosa cells are the major components of the follicle, contributing significantly to follicle growth and oocyte maturation (1). In this study, we demonstrate that YAP, the key downstream effector of the Hippo pathway, regulates granulosa cell proliferation and survival to support follicle growth. However, overactivation of YAP impairs differentiation of granulosa cells, leading to malignant transformation. Thus, our studies suggest that the orchestrated regulation of YAP activity is critical for granulosa cell proliferation and differentiation to support normal ovarian follicle development.

1.4.2. YAP promotes granulosa cell proliferation and follicle growth

Both fluorescent and chromogenic immunohistochemical analyses clearly showed that a high level of nuclear-localized YAP was expressed in the rapid-proliferating granulosa cells of mouse and human ovaries. These results suggest that YAP may play a key role in promoting granulosa cell growth, thereby stimulating overall ovarian follicle growth. Then we demonstrated that YAP is vital for granulosa cell proliferation and survival *in vitro* using both traditional 2D culture and a novel 3D culture system. Utilizing Verteporfin to block YAP activity, our *in vitro* ovary culture and *in vivo* mouse experiments further support the vital role of YAP in granulosa cell proliferation to support follicle growth.

Previous studies showed that epidermal growth factor (EGF) family regulate granulosa cell proliferation and differentiation during follicle development (42, 45). Our previous study showed that TGF α promotes proliferation and migration of granulosa cell tumor cells via EGFR signaling (46), which has been shown to interact with YAP to regulate cell

proliferation (47-49). A previous study showed that HBEGF was expressed in early stage granulosa cells (43). Here, our results showed that nuclear YAP was highly expressed in proliferative granulosa cells. Overexpression of YAP upregulated HBEGF expression and HBEGF stimulates granulosa cell proliferation. In turn, HBEGF can activate YAP via inhibition of Hippo signaling component LATS1. Our previous studies suggested that YAP interacts with ERBB signaling and FGFR signaling to promote ovarian cancer progression (50, 51). ERBB signaling and FGFR signaling are also implicated in the development of ovarian follicles (42, 52-55). Here our data indicate that Hippo-YAP signaling may interact with HBEGF signaling to regulate granulosa cell proliferation and differentiation.

1.4.3. YAP impairs GC differentiation

In differentiated luteal cells, however, YAP was found largely in the cytoplasm, in which its transcriptional activity was presumably suppressed (9, 10), indicating that inactivation of YAP activity may be necessary for granulosa cell luteinization. In addition, LATS1 and LATS2 expression were elevated in luteal cells compared with granulosa cells, supporting that YAP activity may be suppressed by upstream Hippo signaling kinases during the differentiation of granulosa cells to luteal cells. Our studies demonstrated that overexpression of YAP impedes differentiation and induces dedifferentiation and anchorage-free growth of granulosa cells, suggesting malignant cell transformation. During ovarian follicle development, differentiation of granulosa cells was elicited by FSH, while terminal differentiation of granulosa cells into non-dividing luteal cells is triggered after ovulation by high levels of LH, where exit from the cell cycle is required to stop division (3, 56). Protein Kinase A (PKA) mediates gonadotropin signals to induce granulosa cell differentiation (57). Our results demonstrate that gonadotropin-induced differentiation signals inactivate YAP by phosphorylation, resulting in proliferation arrest and increase of hormone production. On the other hand, HBEGF, which activates YAP,

stimulates proliferation and decreased hormone production of granulosa cells. The presence of lower levels or lack of LH receptor in GCTs suggests that loss of LH stimulation may lead to failure of granulosa cell luteinization, contributing to GCT formation (44, 58). Our results showed that overactive YAP can suppress expression of differentiation genes, resulting in failure of granulosa cell differentiation and uncontrolled proliferation. However, the mechanism of suppressive effects of YAP on the expression of differentiation genes need further studies.

1.4.4. Hippo-YAP signaling in follicle development

It is becoming clear that the Hippo signaling pathway constrains ovarian follicle growth (1, 24). Previous studies showed that LATS1-null female mice presented a primary ovarian insufficiency (POI) phenotype and developed ovarian tumors (59, 60), and LATS1 regulates the transcriptional activity of FOXL2, which is mutated in most of granulosa cell tumor patients and some POI patients (61). In addition, Genome-wide association study (GWAS) of polycystic ovary syndrome (PCOS) implicated YAP as a susceptibility gene for PCOS (62). More importantly, recent studies in Dr. Hsueh's lab shed lights on novel therapy for PCOS by showing that temporary activation of YAP with physical fragmentation or chemical treatments using JASP or S1P can promote ovarian follicle growth (24, 25). The authors proposed that YAP activation in the whole ovary can stimulate follicle development, however, the exact cell types involved in these process is unclear. Our results demonstrate that YAP is vital for promoting growth and survival of granulosa cells to support follicle growth, which provides the underlying mechanism of why activation of YAP can stimulate follicle growth. Importantly, our study indicates that granulosa cells may be the target cells for treating patients with defects of ovarian follicle development. Recently, Yu *et al* demonstrated that YAP is dispensable for the survival, growth and maturation of mouse oocytes (26), which further support our idea that

granulosa cells are the targets of Hippo-YAP signaling regulation for follicle development. However, hyperactivation of YAP impairs steroidogenesis and differentiation of granulosa cells, leading to malignant transformation of granulosa cells. Taken together, our study suggests that YAP activity should be dynamically regulated for granulosa cell proliferation and differentiation to support follicle development and reminds us to be cautious and meticulous when treating patients with ovarian failure by activation of YAP.

1.4.5. Conclusion

In conclusion, our data show that YAP is mainly expressed in the proliferative granulosa cell nuclei and the cytoplasm of luteal cells. The YAP activity promotes granulosa cell proliferation but prevents cell differentiation. HBEGF signaling activates YAP and stimulate proliferation. On the other hand, gonadotropin-induced PKA activation inhibits YAP activity and stimulate granulosa cell differentiation. YAP inhibition blocks granulosa cell proliferation, resulting in arrested follicle growth and increased apoptotic follicles. However, overactive YAP compromises cell differentiation and promotes malignant transformation of granulosa cells. Therefore, the orchestrated regulation of YAP activities is vital for granulosa cell physiology to support follicle development and ovarian function.

Figure 1-1. Expression of YAP and LATS1/2 in various stages of mouse ovarian follicles.

The fluorescent immunohistochemistry shows YAP expression (**A¹, B¹, C¹, C⁰**) in mouse ovaries. Ki67 staining (**A², B², C²**) shows location of proliferative granulosa cells, while 3 β -HSD staining (**A³, B³, C³**) represents differentiated luteal cells. (**A¹, A², A³**), (**B¹, B², B³**), and (**C¹, C², C³**) are serial frozen sections respectively. **C⁰** showing the single green color of YAP stain in **C¹** image. Actin was stained as rhodamine phalloidin (red) and nuclei were stain by DAPI (blue). The chromogenic immunohistochemistry shows expression of LATS1 (**D¹**) and LATS2 (**D²**) in the granulosa cells and luteal cells. (**D¹, D²**) are serial paraffin sections. GC: granulosa cells; LC: luteal cells; ILC: late luteal cells; P1: primary follicle; P2: secondary follicle. Bar: 50 μ m.

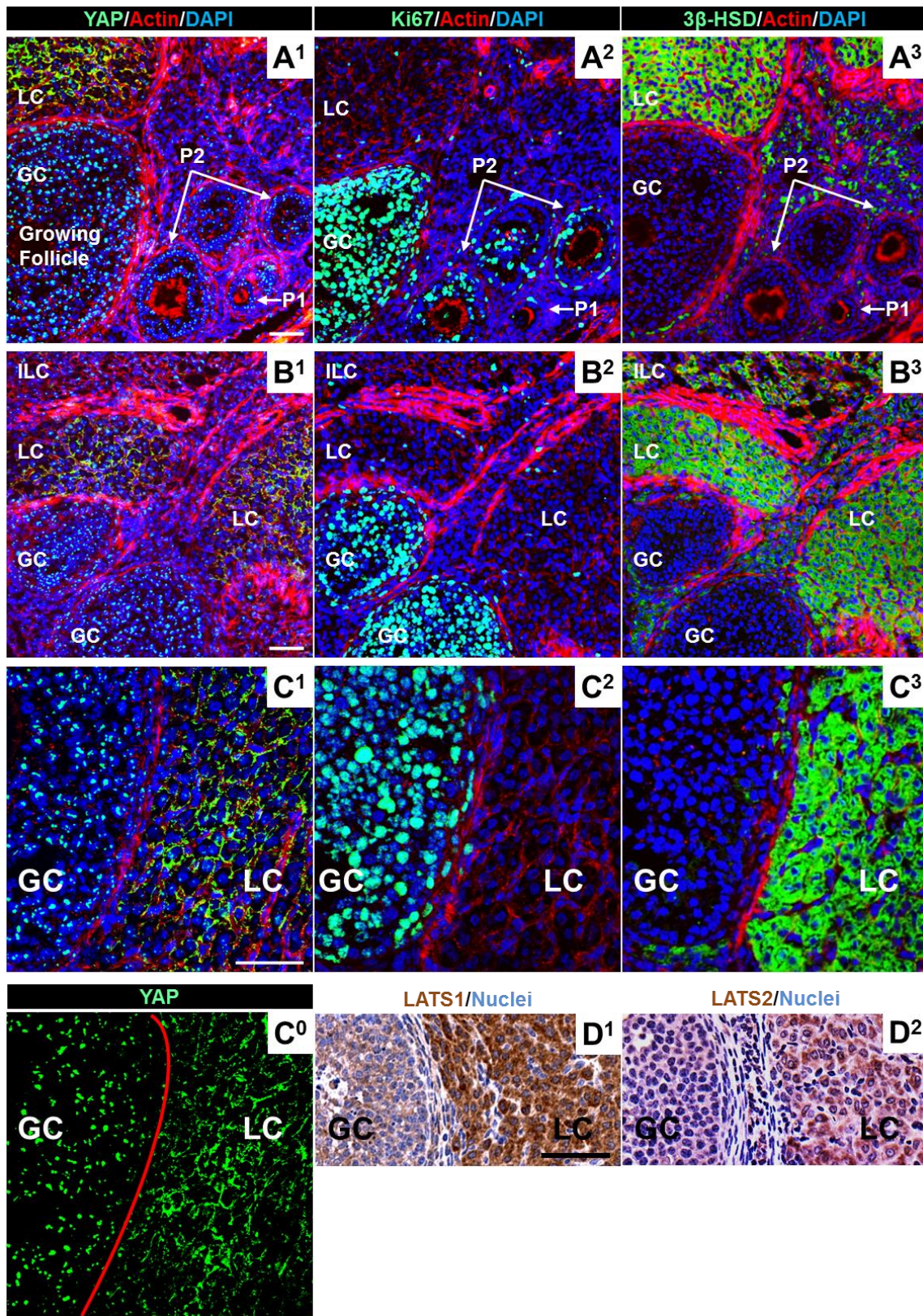


Figure 1-2. The expression of YAP with the development of ovarian follicles in human.

The chromogenic immunohistochemistry shows YAP expression in human ovaries. P0: primordial follicle; P1: primary follicle; P2: secondary follicle; GC: granulosa cells; cGC: cumulus granulosa cells; mGC; mural granulosa cells; LC: luteal cells; SC: stromal cells; TC: theca cells; O: oocyte; CTL: negative staining control. Bar: 100 μ m.

YAP/Nuclei

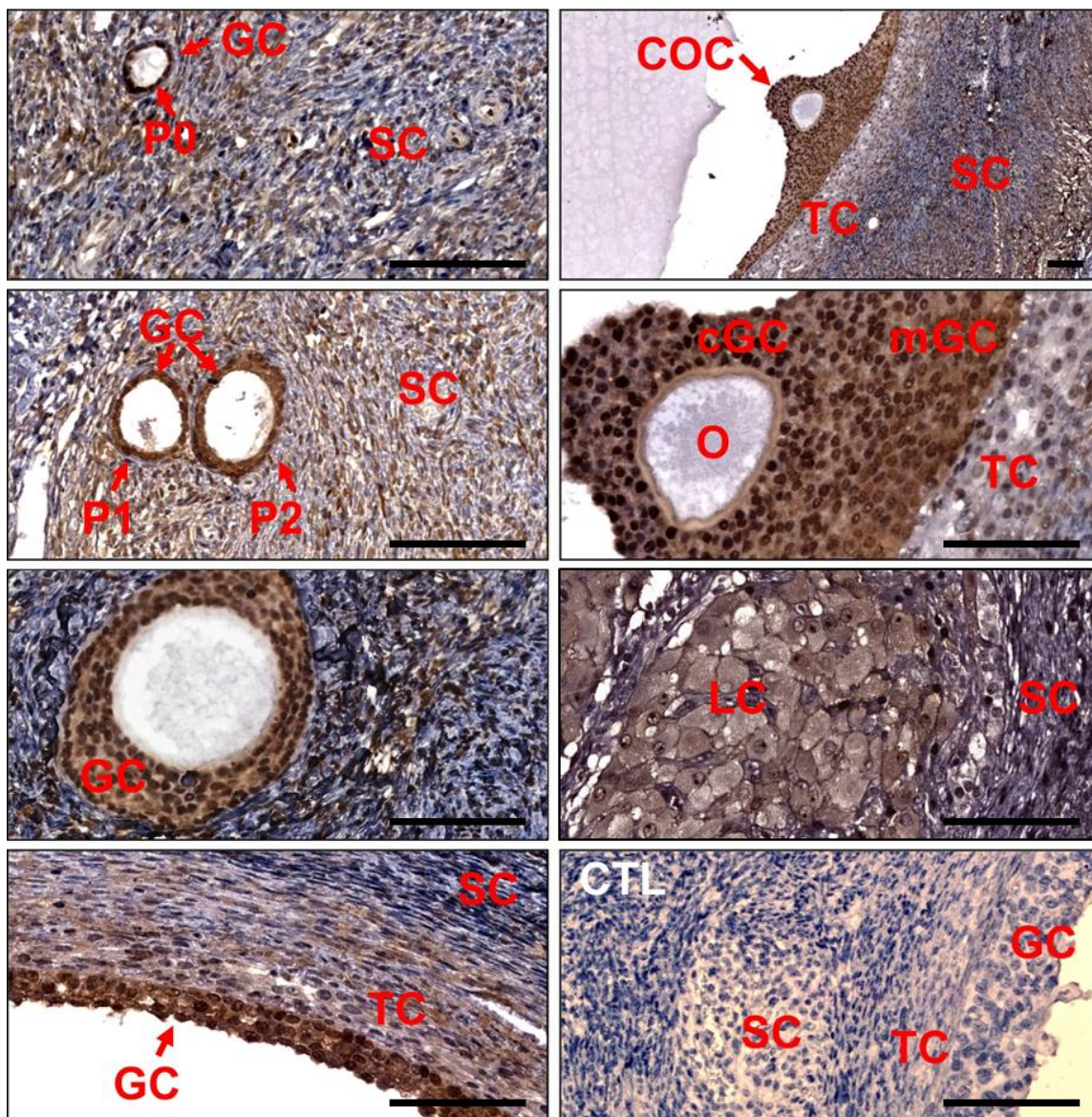


Figure 1-3. YAP promotes proliferation and supports survival of human granulosa cells.

A) Western blots showing YAP protein knockdown with YAP-targeting siRNA#1 and siRNA#2 for 5 d. β -Actin was used as loading control.

B) Representative pictures show growth suppression of hGC under YAP targeting siRNA incubation for 5 d; the bar graph showing cell number counted 5 d after hGC cells were transfected with control or YAP-targeting siRNA; scale bar: 200 μ m.

C) YAP knockdown induces apoptosis of human granulosa cells: representative images show Annexin V-FITC/propidium iodide double staining of hGC 5 d after transfection with control or YAP siRNA; the bar graph showing quantitative data for the ratio of Annexin V positive cells.

D) Western blots show YAP and phosphor-YAP (S127) expression in hGC-MX, hGC-YAP, and hGC-YAP^{S127A} cells, using β -Actin as loading control.

E) Representative images showing multilayer-growth of hGC after YAP overexpression; bar graph showing cell number counting after plating for 5 d; scale bar: 200 μ m.

F) Overexpression of YAP promotes human granulosa cell growth in a 3D culture system: representative images showing the spheroids from hGC-MX, hGC-YAP, and hGC-YAP^{S127A} cells for 5 d; the bar graph showing quantitative data for the volume of spheroids; scale bar: 500 μ m.

G) Representative images showing Ki67 staining in spheroids formed by hGC-MX, and hGC-YAP^{S127A} cells with vehicle (DMSO, 0.1%) or Verteporfin (VP, 5 μ M) treatment for 5 d; the bar graph showing quantitative data for the Ki67 ratio; scale bar: 20 μ m.

H) Representative images showing cleaved caspase 3 (C-Cas 3) staining in spheroids formed by hGC-MX, and hGC-YAP^{S127A} cells with vehicle (DMSO, 0.1%) or Verteporfin (VP, 5 μ M) treatment for 5 d; the bar graph showing quantitative data for the cleaved caspase 3 ratio; scale bar: 20 μ m.

Each bar represents the mean \pm SEM ($n \geq 4$). Bars with different letters are significantly different from each other ($P < 0.05$).

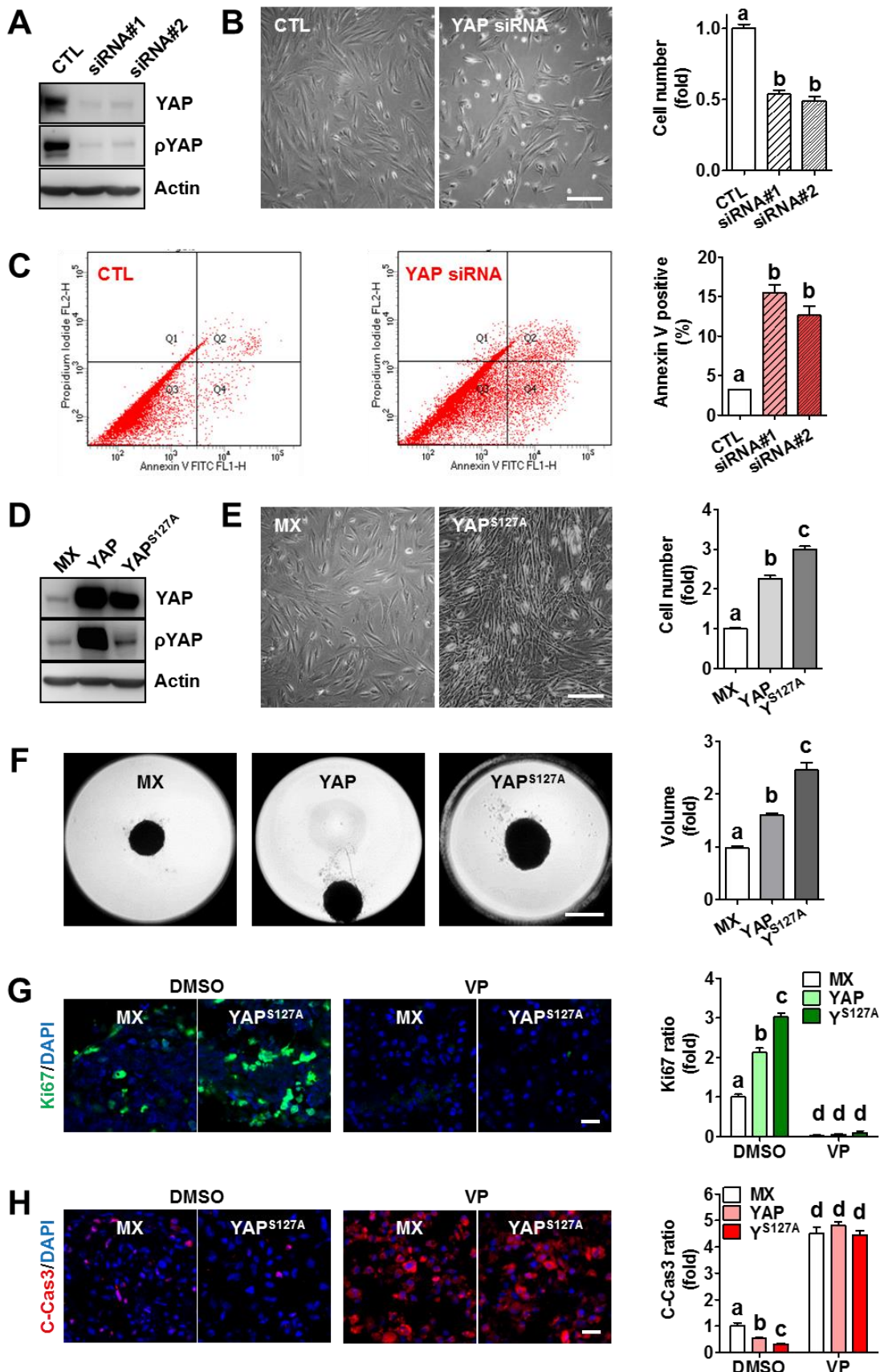


Figure 1-4. YAP overactivation compromises cell steroidogenesis and impedes cell differentiation

A) Overexpression of YAP or YAP^{S127A} decreased base (CTL) and forskolin (FSK) induced production of estrogen and progesterone in primary human granulosa cells.

B) Quantitative RT-PCR results show mRNA expression of *CYP19A1* and *CYP11A1* in primary human granulosa cells with different YAP activity.

C) Overexpression of YAP or YAP^{S127A} reduced base and FSH or FSK induced production of estradiol and progesterone in KGN cells.

D) Western blot results show expression of key enzymes for steroidogenesis of KGN cells with different YAP activity.

E) BODIPY staining showing lipid droplets distribution; upper panel: BODIPY staining (green) showing the distribution of lipid droplets in mouse ovaries; lower panel: BODIPY staining shows that YAP overexpression retarded FSK-induced lipid droplet formation; scale bar = 50 μ m.

Each bar represents the mean \pm SEM ($n \geq 4$). When compared with control, *: $P < 0.05$, **: $P < 0.01$, ***: $P < 0.001$.

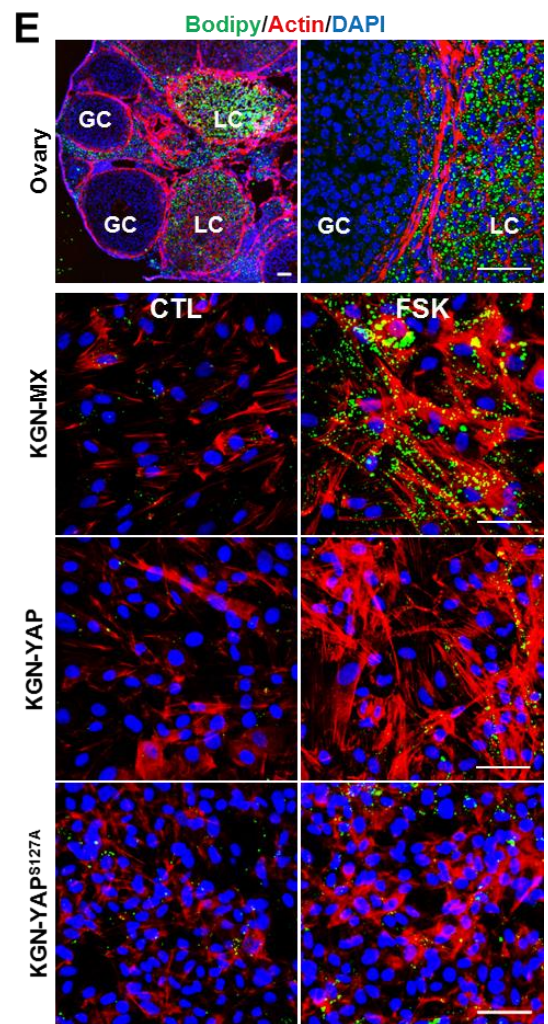
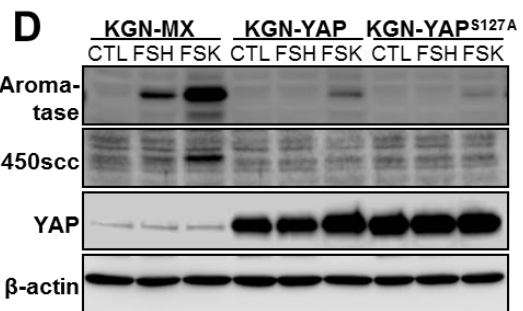
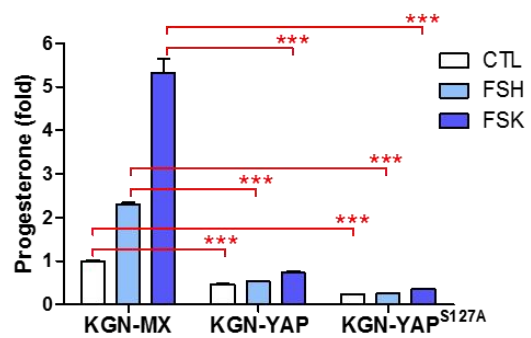
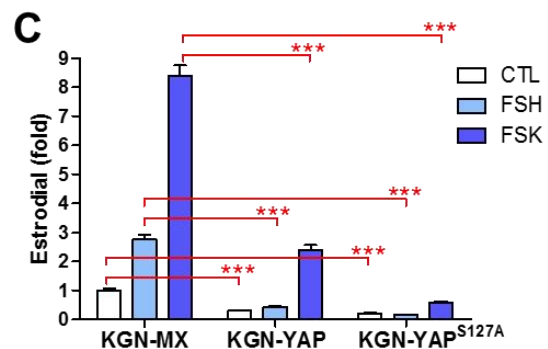
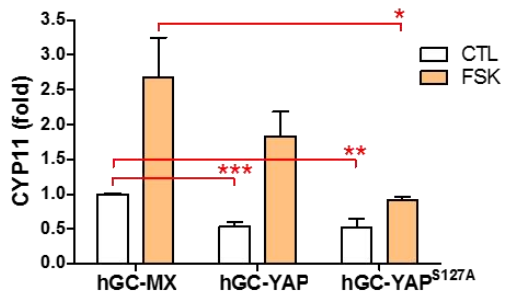
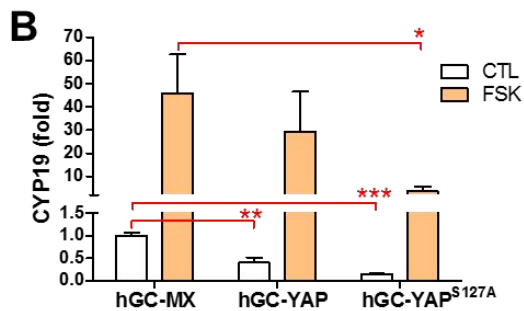
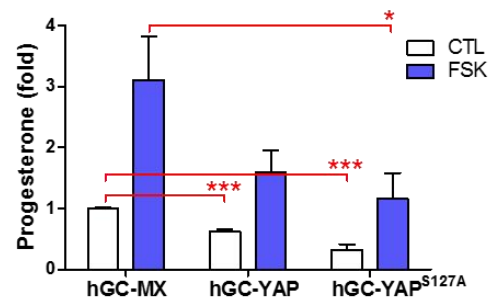
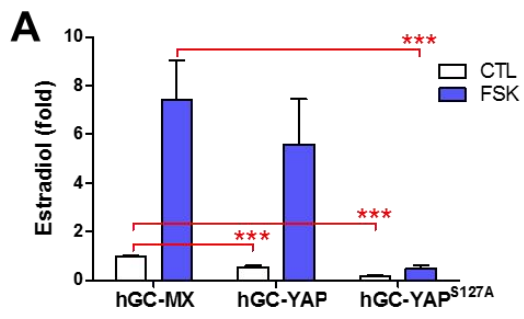


Figure 1-5. YAP hyperactivation induces dedifferentiation of granulosa cells.

A) mRNA expression of key molecules of differentiation in KGN cells with YAP or YAP^{S127A} overexpression; each bar represents the mean \pm SEM ($n \geq 3$); when compared with control, *: $P < 0.05$, **: $P < 0.01$, ***: $P < 0.001$.

B) Western blots showing the expression of proteins related to mesenchymal–epithelial transition (MET) after YAP or YAP^{S127A} overexpression in KGN cells; β -Actin as loading control.

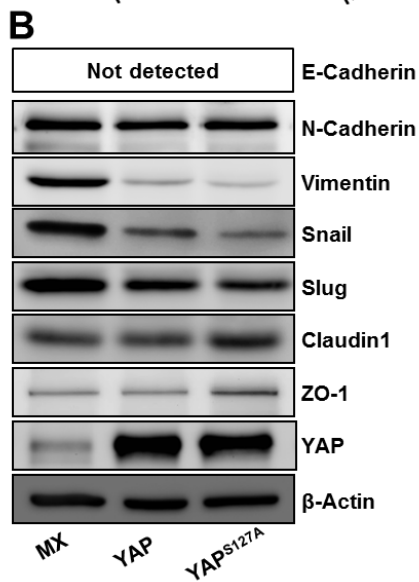
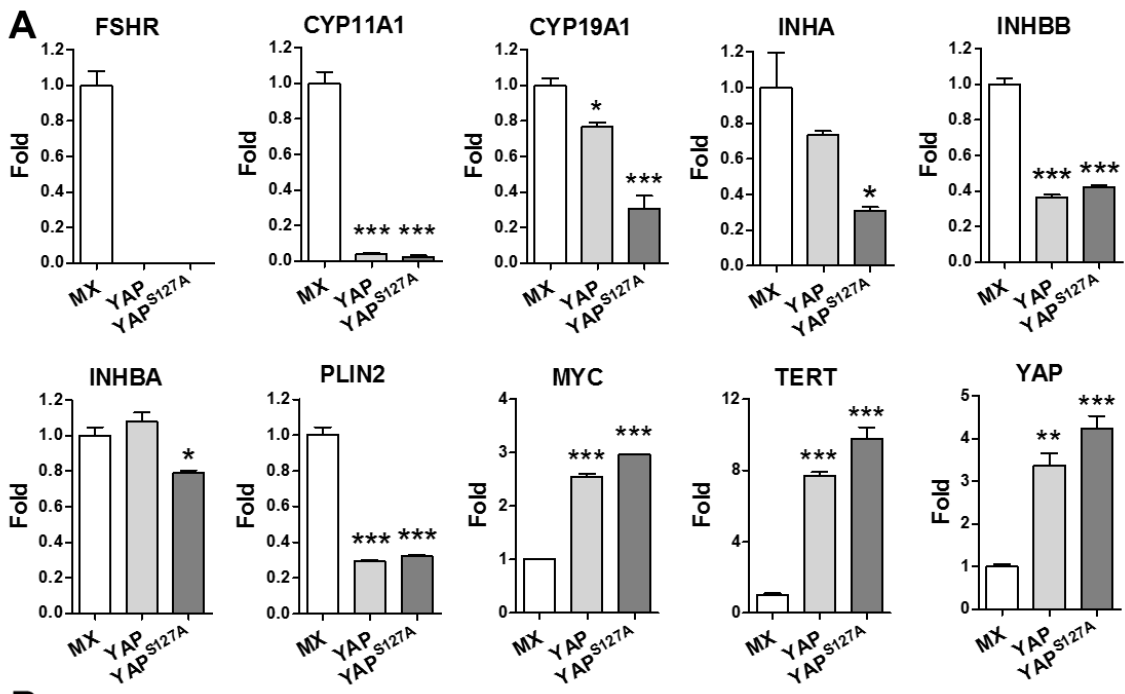


Figure 1-6. HBEGF and Gonadotropins regulate YAP activity and granulosa cell proliferation and steroidogenesis.

A) Overexpression of YAP upregulated HBEGF mRNA expression in hGC, HGrC1, and KGN cells.

B) HBEGF treatment (50 ng/ml, 3 d) stimulated cell proliferation and suppressed production of estradiol and progesterone.

C) Western blots showed that HBEGF (50 ng/ml) dephosphorylated YAP at S127 site following LATS1 (S909) dephosphorylation; p-ERK and p-AKT were increased before dephosphorylation of LATS1; β -Actin was used as loading control.

D) Bar graphs show the effects of FSH (50 ng/ml, 3 d) and forskolin (FSK, 10 μ M, 3 d) on the estrogen and progesterone production and cell proliferation.

E) Western blots showed that FSH (50 ng/ml) and FSK (10 μ M) stimulate YAP phosphorylation of S127 site following LATS1 (S909) phosphorylation; p-CREB was used to show activation of PKA and β -Actin was used as loading control.

F) Forskolin (FSK) treatment (10 μ M, 60') increased YAP retention in the cytoplasm. Scale bar = 20 μ m.

G) Forskolin (FSK) treatment (10 μ M, 3 d) decreased HBEGF mRNA expression.

Each bar represents the mean \pm SEM ($n \geq 3$). When compared with control (CTL), * means $P < 0.05$; ** means $P < 0.01$; *** means $P < 0.001$.

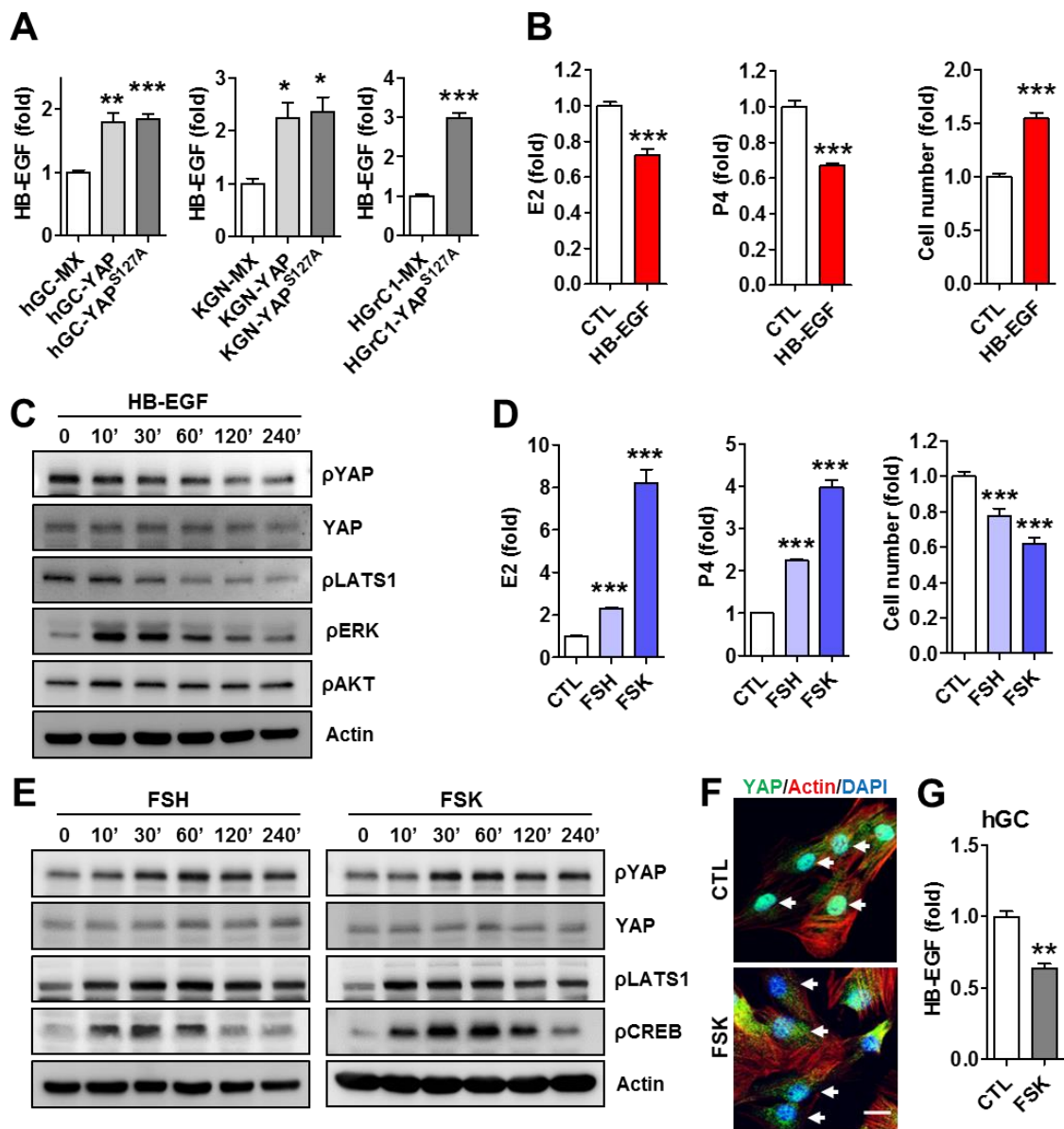


Figure 1-7. YAP promotes granulosa cell growth in soft agar.

A) Representative pictures showing colony formation in soft agar of hGC-MX, hGC-YAP, and hGC-YAP^{S127A} cells with or without Verteporfin (VP) incubation; scale bar: 500 μ m.

B) Bar graphs showing colony number counting and relative fluorescent unit (RFU) to reflect viable cells in soft agar culture; each bar represents the mean \pm SEM ($n \geq 4$); when compared with control, *: $P < 0.05$, **: $P < 0.01$, ***: $P < 0.001$.

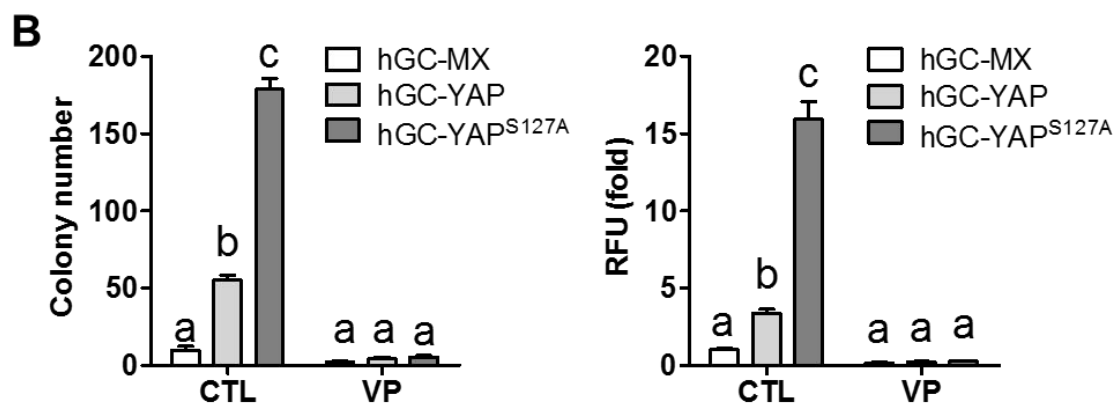
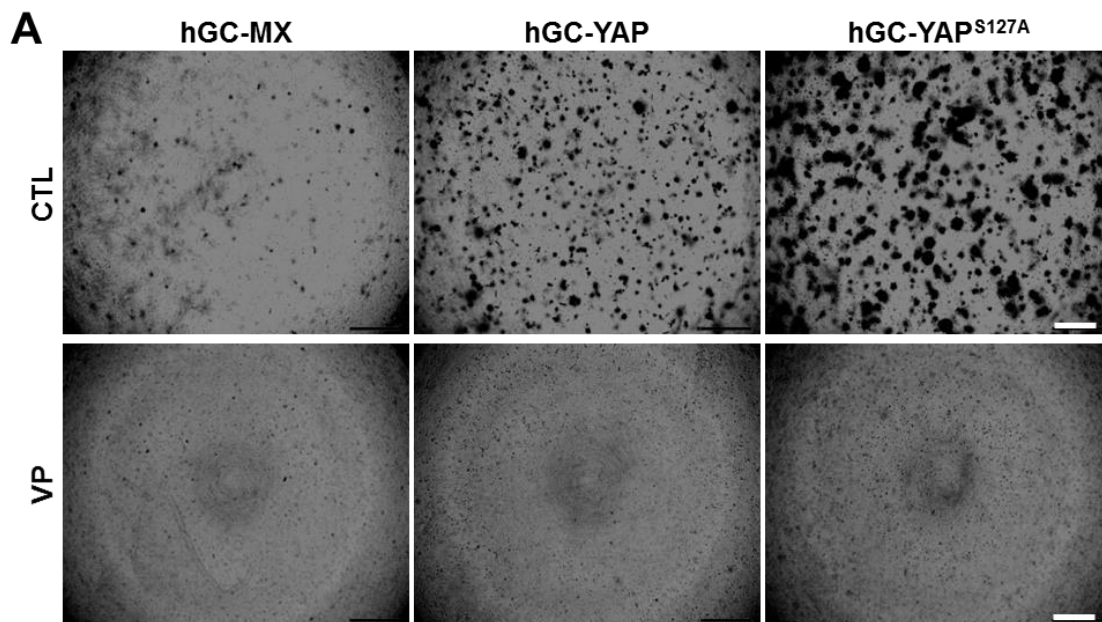


Figure 1-8. Inhibition of YAP disrupts ovarian follicle development *in vitro* and *in vivo*.

A) Representative images showing morphology of d 12 mouse ovaries cultured for 7 d *in vitro* with Verteporfin (VP) or not (CTL); scale bar: 500 μm .

B, C, D) Representative images showing H & E, Ki67, and cleaved Caspase 3 staining of cultured mouse ovaries respectively; yellow arrows and cycles indicating antral follicles in control group; scale bar: 50 μm .

E) *Yap* and targeting gene expression in the control and Verteporfin injected mouse ovaries were detected with RT-PCR and western blots.

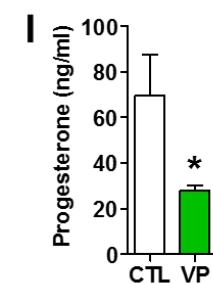
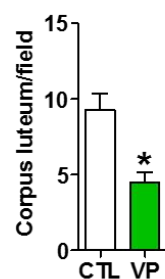
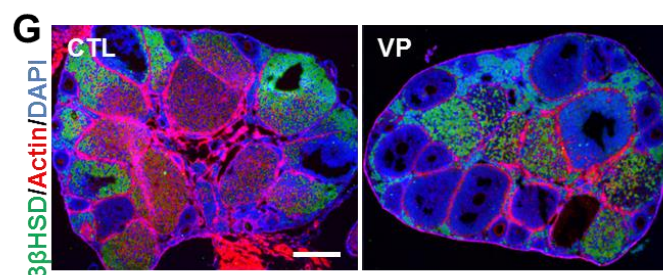
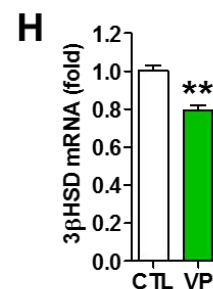
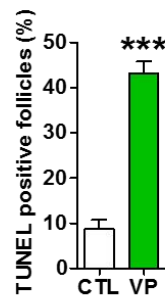
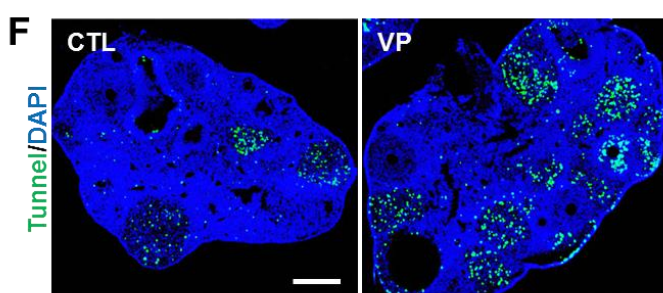
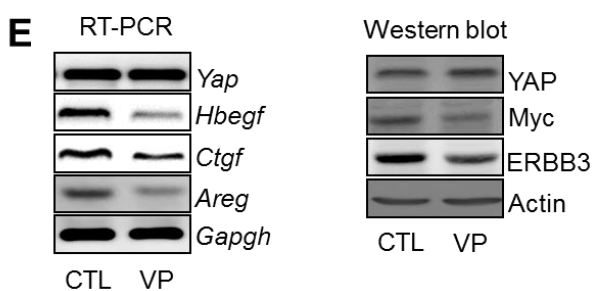
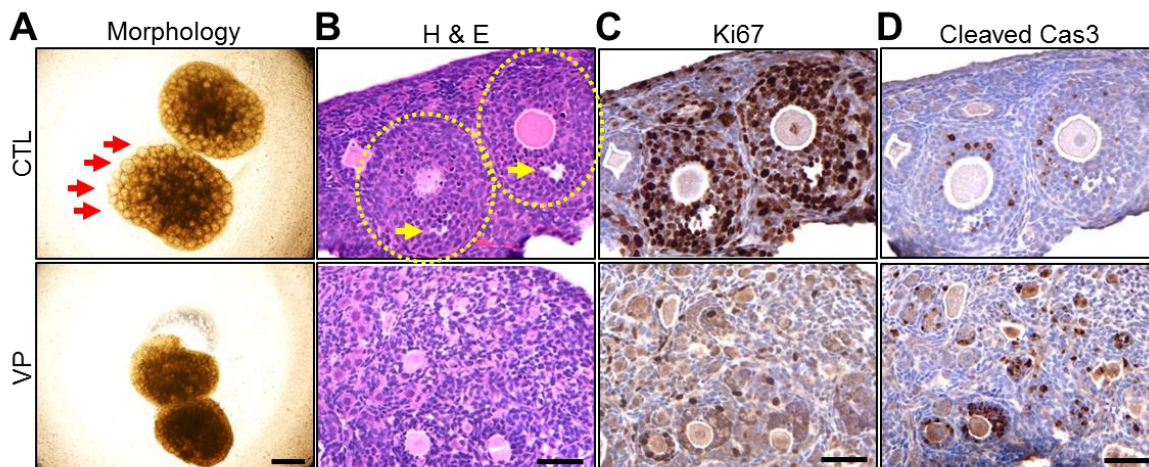
F) TUNEL assays show YAP inhibition increases the number of apoptotic follicles; scale bar: 500 μm .

G) YAP inhibition decreases corpus luteum number; $3\beta\text{HSD}$ staining represent corpus luteum location.

H) Bar graph showing the RNA expression of $3\beta\text{HSD}$ in control (CTL) and Verteporfin (VP) injected mouse ovaries; scale bar: 500 μm .

I) YAP inhibition by Verteporfin (VP) decreases progesterone level of mouse serum.

Each bar represents the mean \pm SEM ($n \geq 3$). When compared with control (CTL), * means $P < 0.05$; ** means $P < 0.01$; *** means $P < 0.001$.



**CHAPTER 2: YAP PROMOTES GRANULOSA CELL TUMOR
PROGRESSION†**

† The material presented in this chapter was previously published: Fu & Lv *et al. Endocrine-Related Cancer* 2014; 21(2):297-310.

ABSTRACT

The Hippo signaling pathway has been implicated as a conserved regulator of organ size in both drosophila and mammals. Yes-associated protein (YAP), the central component of the Hippo signaling cascade, functions as an oncogene in several malignancies. Ovarian granulosa cell tumors (GCT) are characterized by enlargement of the ovary, excess production of estrogen, a high frequency of recurrence, and the potential for malignancy and metastasis. Whether the Hippo pathway plays a role in the pathogenesis of GCT is unknown. This study was conducted to examine the expression of YAP in human adult GCT and to determine the role of YAP in the progression of GCT cells. Compared with age-matched normal human ovaries, GCT tissues exhibited higher levels of YAP expression. YAP protein was predominantly expressed in the nucleus of tumor cells, whereas the non-tumor ovarian stromal cells expressed very low levels of YAP. YAP was also expressed in cultured primary human granulosa cells and in KGN and COV434 GCT cell lines. siRNA-mediated knockdown of YAP in KGN cells resulted in a significant reduction in cell proliferation ($P < 0.001$). Conversely, overexpression of wild type YAP or a constitutively active YAP (YAP^{S127A}) mutant resulted in a significant increase in KGN cell proliferation and migration. These results demonstrate that YAP plays an important role in the regulation of GCT cell proliferation and migration. Targeting the Hippo/YAP pathway may provide a novel therapeutic approach for GCT.

2.1. INTRODUCTION

2.1.1. The Hippo-YAP pathway in organ size control and tumorigenesis

The balance between cell growth and death plays a vital role in the maintenance of tissue homeostasis, organ size, and normal biological functions of the human body. Under physiological conditions, cell growth and apoptosis are tightly controlled. Aged or damaged cells commit to programmed cell death, whereas adult stem cells may divide and differentiate to replace those dysfunctional cells to maintain tissue homeostasis and organ size. Under pathological conditions, however, uncontrolled cell proliferation and decreased cell death and/or differentiation can lead to hyperplasia or even tumorigenesis. The mechanisms underlying the control of organ size are still largely unknown. Studies have shown that the Hippo signaling pathway (Salvador/Warts/ Hippo pathway) plays a critical role in controlling organ size by regulating both cell proliferation and apoptosis in both *Drosophila* and mammals (8, 9, 63)

Yes-associated protein 1 (YAP1, also known as YAP) is the major downstream effector of the Hippo pathway (64). The expression and role of YAP in cancer are cell-type- and/or cellular-context-dependent (64, 65). Amplification of the YAP gene locus at 11q22 is found in hepatocellular carcinoma, breast cancer, oral squamous cell carcinomas, medulloblastomas, and esophageal squamous cell carcinomas (37, 66-69). In addition, overexpression and nuclear localization of YAP protein are found in colon, liver, lung, ovarian, and prostate cancers (8, 10, 67, 70). Moreover, overexpression of YAP leads to oncogenic transformation of an immortalized epithelial cell line MCF10A (37). However, YAP enhances p73-dependent cell death during cisplatin-induced DNA damage (65, 71), indicating that YAP may interact with other pathways to optimize a tumor suppressor response. In a subset of breast cancers, the expression of YAP protein was significantly

decreased due to loss of heterozygosity, and short hairpin RNA (shRNA) knockdown of YAP increased migration and invasiveness, and enhanced tumor growth (72). Therefore, the expression and function of YAP in specific cancers requires further investigation.

2.1.2. Etiology of granulosa cell tumor

Granulosa cell tumors of ovary (GCT), accounting for 70% of malignant sex-cord stromal tumors and 5–8% of all ovarian malignancies, are poorly understood ovarian neoplasms (73). Patients with GCT have a high overall survival rate, which is mainly attributed to diagnosis of GCT at an early stage. The prognosis is significantly poorer for patients with advanced tumors. The 10-year survival rates in stage III and IV are lower than 20% (74). Clinically, GCT have a propensity for late recurrence (75, 76). Approximately, 80% of patients with advanced stage or recurrent tumors succumb to their disease due to the limited treatment options for advanced and recurrent disease (73, 77). These tumors also have malignant potential and metastatic ability. Indeed, metastases from GCT have been reported in the lung, liver, brain, bone, diaphragm, abdominal wall, pancreas, and adrenal gland (78).

Some factors and pathways have been shown to affect the development of GCT (73). Importantly, recent studies have shown that a somatic mutation in FOXL2 (C402G) is a potential driver in the pathogenesis of adult-type GCT (79-84). However, the exact mechanisms underlying GCT progression, recurrence, and metastasis are largely unknown. Oftentimes, GCT are hemorrhagic and manifest as painful abdominal masses, with an average diameter more than 10 cm (74, 85-87). Occasionally, the diameter of the GCT tumor can be over 30 cm (86, 88-90). This volume is several hundred-fold larger than the regular human ovary, which is around 5 cm³. The significant increase in the volume of the ovary indicates that the system controlling organ size in the patients with GCT is

disrupted. As GCT are derived from ovarian granulosa cells, the proliferation of granulosa cells in the patient's ovary may be deregulated. However, the molecular pathology underlying this remarkable increase in tissue size is unknown.

2.1.3. The present study

In this study, we compared YAP expression in normal human ovarian tissues and GCT tissues using immunohistochemistry. YAP was also consistently detected in ovarian GCT cell lines. We also examined the role of YAP in the regulation of GCT cell proliferation and migration using the KGN human GCT cell line as a cellular model. Our results indicate that the Hippo/YAP signaling pathway plays a critical role in the regulation of GCT progression.

2.2. MATERIALS AND METHODS

2.2.1. Chemicals

Human FSH was from NHPP/NIDDK (Torrance, CA, USA). DMEM/F12 and other cell culture medium were from Invitrogen. FBS was from Atlanta Biologicals, Inc. (Lawrenceville, GA, USA). The Ribogreen RNA quantification kit and Alexa-conjugated secondary antibodies were from Life Technologies Corp.; YAP small interfering RNA (siRNA) was from Dharmacon/Thermo Scientific (Pittsburgh, PA, USA). Secondary antibodies for western blotting chemiluminescence were from Jackson ImmunoResearch Laboratories, Inc. (West Grove, PA, USA); PCR reagents were from Invitrogen, Qiagen or Bio-Rad. All other molecular-grade chemicals were purchased from Sigma, Fisher (Pittsburgh, PA, USA), or United States Biochemical (Cleveland, OH, USA).

2.2.2. Cell lines and human GCT tissue slides

The KGN cell line, an adult GCT cell line expressing a mutated FOXL2 (C402G) gene, was obtained from the Riken BioSource Center (Riken Cell Bank, Ibaraki, Japan). The COV434 cell line, a juvenile GCT cell line expressing wildtype FOXL2 gene, was received from Dr. C E van der Minne (University Hospital, Leiden, The Netherlands). The SKOV-3 ovarian cancer cell line was purchased from the American Type Culture Collection (ATCC, Manassas, VA, USA). The IGROV-1 ovarian cancer cell was received from Dr. Bo Reuda (Massachusetts General Hospital, MA, USA). Human ovarian granulosa cells isolated from two medium-sized follicles (5–10 mm in diameter) were obtained from a 33-year-old patient who received oophorectomy for causes other than an ovarian disorder. The collection of this tissue was permitted by a protocol approved by the University of Nebraska Medical Center Institutional Review Board. The cells were isolated manually with a needle and cultured in DMEM/F12 supplemented with 5% FBS. All cell lines used

in this study were passaged fewer than ten times in our laboratories and were validated for their authenticity by short tandem repeat (STR) analysis. Formalin-fixed, paraffin-embedded normal human ovarian tissues (n = 10) and human GCT (n = 12) slides were obtained from the Department of Pathology, Tianjin Medical University Cancer Hospital and UNMC. The retrospective use of these human tissue slides was permitted by protocols approved by the UNMC Institutional Review Board and Tianjin Medical University Institutional Review Board.

The KGN GCT cells were derived from a patient with recurrent, metastasized GCT in the pelvic region (91). These cells maintain many features of ovarian granulosa cells such as expression of the FSH receptor and induction of aromatase (CYP19A1) and production of estrogen in response to FSH. To date, to our knowledge, the KGN cell line is the only appropriate cellular model for studying the growth and metastasis of the adult GCT (80, 92). In this study, we examined the role of YAP in the proliferation and migration of KGN cells. The KGN cells used in these experiments were from passages 6 to 10. The cell line was validated by STR polymorphism analysis performed by both the Riken BioSource Center (Riken Cell Bank) and the Genetica DNA Laboratories (Burlington, NC, USA).

2.2.3. Immunohistochemistry analysis of YAP expression in ovarian tissues

The expression of YAP protein in paraffin-embedded human ovarian tissues was detected using a previously described peroxidase-based immunohistochemistry protocol (46). Immunosignals were visualized with a 3,3'-diaminobenzidine (DAB) kit (Invitrogen). The sections were counterstained with Mayer's hematoxylin. In case of negative controls, the primary antibody was replaced by blocking buffer containing the same amount of IgG from non-immune rabbit serum. The sections were scanned with an iSCAN Coreo Slide Scanner (Ventana Medical Systems, Inc., Oro Valley, AZ, USA). The positivity (i.e., the

number of positively stained cells relative to the total number of cells in the tissue section) and the intensity of the positive immunosignals were quantified with Aperio ImageScope software (Vista, CA, USA).

2.2.4. Localization of YAP protein in KGN cells

KGN cells were seeded onto glass coverslips and incubated in a growth medium (DMEM/F12 supplemented with 5% FBS) for 36 h before fixation in ice-cold 4% paraformaldehyde for 10 min. Staining was performed using methods described previously (46). The fixed cells were incubated with YAP antibody (1:100) overnight at 4 °C in a humidified chamber. Antigens were visualized by applying Alexa-488-conjugated donkey anti-rabbit secondary antibodies. Actin filaments were stained with rhodamine-conjugated phalloidin and the nuclei were stained with 4',6-diamidino-2-phenylindole (DAPI). The images were captured and analyzed with an LSM 710 confocal microscope (Thornwood, NY, USA). The exposure time of the camera was set for subtracting background fluorescence that was present in the sections incubated with the nonimmune IgG of the host species. YAP-specific fluorescence signals (immunosignal) were merged with the nuclear and actin signals to determine the sub-cellular site of protein expression.

2.2.5. YAP mRNA expression

YAP mRNA expression in GCT cell lines was detected with RT-PCR as described previously (46). Total RNA was isolated from primary cultures of normal human granulosa cells, cultured GCT cell lines (KGN cells and COV434 cells), and epithelial ovarian cancer (EOC) cells (SKOV-3, CAOV-3, and IGROV-1 cells) using the RNeasy mini kit (Qiagen, Inc.) according to the manufacturer's instructions. The first-strand cDNA was synthesized from 1 µg total RNA using iScript cDNA synthesis kit (Bio-Rad). PCR products were loaded onto an agarose gel and separated by electrophoresis. The images were captured by a

UVP gel documentation system (UVP, Upland, CA, USA). The PCR products were validated by sequence analysis.

2.2.6. Western blot analysis

Western blot was performed as described previously. Briefly, normal cell lines or treated KGN cells were harvested on ice with ice-cold cell lysis buffer containing 10 mM Tris (pH 7.4), 100 mM NaCl, 1 mM EDTA, 1 mM EGTA, 1 mM NaF, 20 mM Na₄P₂O₇, 1% Triton X-100, 10% glycerol, 0.1% SDS, 0.5% deoxycholate and protease and phosphatase inhibitor cocktails. Proteins (30 µg) were loaded onto a 10% SDS-PAGE gel, separated by electrophoresis, and transferred onto nitrocellulose membranes. The membranes were blocked with 5% BSA and probed with appropriate primary and HRP-conjugated secondary antibodies. The immunosignal was detected with a Thermo Scientific SuperSignal West Femto Chemiluminescent Substrate Kit. The images were captured and analyzed with a UVP gel documentation system.

2.2.7. Establishment of wild-type and mutant YAP overexpressed cell lines

KGN cells were cultured to 40% confluence and then transfected with retrovirus-based human YAP expression constructs. The characteristics and use of these vectors have been reported previously (9). Two days following transfection, cells were selected with G-418 (400 µg/ml) for 7 days. Three stable cell lines were established: i) the KGN-MXIV control cell line was transfected with the control vector MXIV and expresses endogenous YAP; ii) the KGN-YAP cell line overexpresses wild-type YAP protein; and iii) the KGN-YAP^{S127A} cell line expresses a constitutively activated YAP mutant. Mutation of YAP protein (serine to alanine at residue 127) prevents YAP phosphorylation, leading to its nuclear localization and constitutive activation.

2.2.8. Cell proliferation assay

To determine the effect of YAP on GCT cell proliferation, KGN cells were plated in 60 mm cell culture dishes and incubated in a growth medium supplemented with 5% FBS until 60% confluent. The cells were then transfected with siGLO (a cy5-labeled non-targeting siRNA as control) or YAP siRNA for 6 h using METAFECTENE (Biontexas-USA, San Diego, CA, USA) according to the manufacturer's instructions. The cells were harvested 72 h after siRNA transfection for determination of protein levels or cell numbers. YAP protein expression was determined by western blot analysis and the cell numbers were quantified with an Invitrogen Countess automated cell counter. The effect of YAP on GCT cell proliferation was also determined in KGN cell lines that overexpressed the WT or mutant YAP proteins. Each cell line was cultured in the growth medium containing 10% FBS for up to 3 days. Cell number and cell size for each cell line were determined daily with an Invitrogen Countess Automated cell counter.

2.2.9. Cell migration assay

A chemotaxis assay was used to determine the effect of YAP on KGN cell migration. KGN cells (4×10^5) in 250 μ l of serum-free DMEM were placed in a Transwell insert (8 μ m pore size, Corning-Costar, Lowell, MA, USA). The inserts were then placed in the wells of a 24-well-plate containing 750 μ l of DMEM-FBS (5%) and incubated at 37 °C for 6 h. After incubation, the cells on the top of the membrane were removed with a cotton swab. The cells which had migrated to the underside of the membrane were fixed and stained with 0.04% crystal violet in methanol for 30 min. The cells were then photographed (100 \times magnification) and ten pictures per group were quantified under a microscope.

The wound-healing assay was also used to determine whether YAP regulates KGN cell motility. KGN cells were cultured in six-well cell plates until confluent. Wounds were

made by scratching the cell layer with a 100 μ l pipette tip. After washing away the cell debris, pictures were taken for each 'wound' with an Olympus inverted microscope equipped with a DP71 digital camera (Olympus America, Inc., Center Valley, PA, USA). The cells were incubated in serum-free medium for 20 h and then another picture was taken for each 'wound'.

2.2.10. Statistical analysis

All experiments were repeated at least three times unless otherwise noted. Data were analyzed for significance by student T-test or one-way ANOVA with Tukey's post-test. A value of $P < 0.05$ was considered to be significant. Statistical analysis was conducted using GraphPad Prism software (GraphPad Software, Inc., La Jolla, CA, USA).

2.3. RESULTS

2.3.1. Expression of YAP protein in GCT

Adult GCT are commonly identified in women during the perimenopausal period (73). The expression of YAP in the normal human ovary and GCT was detected by immunohistochemistry. In control perimenopausal ovarian sections, the main cellular component and the stroma, exhibited very little or no staining for YAP (Fig. 2-1 A, C, and E). In control ovarian sections, few small follicles or luteinized structures were observed. When follicles were present, YAP immunosignals were detected in granulosa cells and were distributed in both nucleus and cytoplasm (too few follicles, data not shown). When luteinized cells were present, YAP was predominantly localized to the cytoplasm (Fig. 2-1 C and E). Compared with the control ovarian tissues, YAP immunosignals were significantly increased ($P < 0.001$) in the GCT tumor tissues and the protein was predominantly located in the nucleus of tumor cells (Fig. 2-1 B, D, and F). Nontumor stromal cells had low levels of YAP expression. Immunostaining controls revealed no non-specific staining in GCT tissues (Fig. 2-1 G). The intensities of YAP immunostaining signals were quantified with Aperio imagescope software (Aperio). The data showed that both YAP signal intensity and YAP positivity (percentage of the YAP positive cells relative to the total number of cells per section) in the ovarian GCT tissues were significantly higher than the signals in the normal ovarian tissues (Fig. 2-1 H, $P < 0.001$).

2.3.2. Expression of YAP in ovarian GCT tumor cell lines

As mentioned earlier, the KGN cell is a suitable cellular model for the GCT research. Fluorescent immunocytochemistry showed that YAP is expressed in KGN cells (Fig. 2-2 A). Most of the immunosignal was localized to the nucleus. Interestingly, the YAP immunosignal was also localized to punctate regions in the periphery of the cells that co-

localized with β -actin (Fig. 2-2 A). It is very possible that YAP may interact with the focal adhesion proteins. Antibody controls using the same amount of IgG to replace the primary YAP antibody were not stained (Fig. 2-2 A, lower panel).

RT-PCR and western blot analysis showed that YAP mRNA and YAP protein were expressed in primary cultures of human granulosa cells, KGN and COV434 GCT cell lines (Fig. 2-2 B and C). YAP RNA and YAP protein were also expressed in three ovarian epithelial cancer cell lines (Fig. 2-2 B and C). IGROV-1 cells had lower expression of YAP compared with SKOV-3 and CAOV-3 cells. It is well known that YAP protein activity is highly regulated by phosphorylation. Western blot analysis revealed that phospho-YAP(S127) was present in each of the cell lines. Our results also showed that compared with the KGN cells YAP was less phosphorylated in COV434 cells (Fig. 2-2 B and C), a juvenile GCT cell line (73, 80).

2.3.3. Knockdown of YAP expression in KGN cells inhibits cell proliferation

To explore the role of YAP in GCT cell proliferation, we transiently transfected KGN cells with two YAP siRNAs to knock down YAP expression. Cy5-labeled scrambled siRNA (siGLO) was used as a control. Results showed that the transfection efficiency was very high in the KGN cells, with more than 95% of cells being siGLO positive (Fig. 2-3 A). Western blot analysis revealed that both YAP siRNA1 and siRNA 2 significantly ($P < 0.001$) reduced YAP protein in KGN cells (Fig. 2-3 B). The YAP knockdown KGN cells were only 50–60% confluent compared with siGLO-treated cells, which were nearly 100% confluent (Fig. 2-3 C). Quantification of cell numbers showed that compared with the normal KGN cells or the KGN cells treated with siGLO, the cell numbers in the YAP knockdown KGN cells was significantly reduced (~55%; $P < 0.001$; Fig. 2-3 D). Knockdown of YAP not only suppressed cell proliferation but also affected cell

morphology. As shown in Fig. 2-3 C, YAP-knockdown KGN cells were more spindle-shaped compared with control KGN cells, indicating that YAP may regulate the actin cytoskeleton of the KGN cells.

2.3.4. Overexpression of YAP promotes KGN cell proliferation and migration

To further explore the role of YAP in GCT cell proliferation, we established cell lines which express the wildtype YAP protein (KGN-YAP) or the constitutively active YAP protein (KGN-YAP^{S127A}). The empty vector (MX) was also transfected into KGN cells and served as a control cell line (KGN-MX). Results showed that compared with the control cell line (KGN-MX), both KGN-YAP and the KGN-YAP^{S127A} cells expressed more YAP protein (Fig. 2-4 A). Morphologically, KGN-YAP^{S127A} cells were smaller and much more elongated compared with control cells (Fig. 2-4 B). Compared with the control group, cell numbers almost tripled in KGN-YAP^{S127A} cells and almost doubled in KGN-YAP cells within 24 h of plating (Fig. 2-4 C). After 3 days of culture, the number of KGN-YAP^{S127A} cells increased more than ten-fold, the number of KGN-YAP cells increased more than six-fold, while the number of control cells (KGN-MX) increased only 2.5-fold (Fig. 2-4 C). We also found that in comparison to the KGN-MX control cells, the diameter of KGN-YAP and KGN-YAP^{S127A} cells was reduced.

Transwell migration assays showed that cells in KGN-YAP group migrated faster than cells in KGN-MX group, while cells in the KGN-YAP^{S127A} group migrated faster than cells in the KGN-YAP group (Fig. 2-5 A and B). This result was further confirmed by the wound-healing assay (Fig. 2-5 C). The morphology of the migrated cells further demonstrated that the KGN-YAP^{S127A} cells were smaller than the corresponding control KGN-MX cells (Fig. 2-5 A).

2.4. DISCUSSION

2.4.1. Overview of previous studies and the present study on GCT

More than one and half centuries have passed since the first report of GCT in women (93). The etiology and mechanisms underlying the progression and metastasis of GCT are largely unknown. GCT are derived from granulosa cells, which are highly regulated by reproductive hormones and growth factors in an endocrine, paracrine, and autocrine manner (94, 95). Therefore, hormones, growth factors, and signaling pathways involved in the regulation of normal ovarian granulosa cell functions may also affect the initiation and/or progression of GCT. Indeed, several hormones and growth factors have been implicated in the development of GCT. Inhibin- α has been suggested to be a critical GCT tumor suppressor in rodents because the targeted deletion of the inhibin- α subunit in mice resulted in ovarian granulosa-stromal tumors with very high penetrance (96). However, human GCT are generally associated with high levels of circulating inhibins (97). Therefore, the function of inhibin in the development of GCT in humans requires further evaluation. Transgenic mice with constitutively activated WNT/b-catenin signaling in their granulosa cells developed GCT (98), indicating that the WNT/b-catenin signaling pathway maybe involved in the rodent GCT initiation and progression. However, it remains unclear if the molecular mechanisms of tumorigenesis in this mouse model are related to those involved in GCT development in women. A more recent whole transcriptome sequencing study with human samples has demonstrated that a somatic mutation in FOXL2 (C402G; Cys134TrP) was present in almost all morphologically identified adult-type GCT and indicated that mutant FOXL2 is a potential driver in the pathogenesis of adult-type GCT (79, 80). More recently, Rosario et al. found that patients with homozygous FOXL2 mutations had a significantly higher relapse rate ($P < 0.04$). However, they did not find a significant correlation between FOXL2 mutation status or FOXL2 expression and any

other clinical variables. The author's indicated that due to the limitation of the sample size, the prognostic significance of this gene mutation still needs to be confirmed (99). Therefore, although nearly all adult GCT express the mutant FOXL2 gene, the mechanisms underlying the progression, recurrence, and metastasis of ovarian GCT remain unknown. In this study, our data clearly show that YAP, a central component of the Hippo pathway, is highly expressed in human GCT tissues and that overexpression of YAP protein significantly stimulates the proliferation and migration of the KGN GCT cell line, demonstrating that the Hippo pathway may be involved in the progression of GCT.

2.4.2. YAP expression in GCT and ovarian epithelial cancer

YAP is the major downstream effector of the Hippo pathway. Activation of the Hippo pathway suppresses YAP activity by phosphorylating YAP and subsequently retaining it in the cytoplasm. In this study, we found that YAP immunostaining was significantly higher in human GCT tumor tissues compared with normal ovarian tissues. Moreover, YAP was mainly localized in the nucleus of tumor cells. In comparison, little YAP protein was found in age-matched normal ovarian tissues. When luteinized cells were present in age-matched normal ovarian tissues, YAP was mainly localized to the cytoplasm. Consistent with our results, elevated YAP expression and nuclear localization have been observed in multiple types of human cancers, including liver cancers, colon cancers, EOC, lung cancers, and prostate cancers (9, 10, 67, 70). In hepatocellular carcinoma, YAP was determined to be an independent prognostic marker for overall survival and disease-free survival (100). In EOC, very recent data indicated that subcellular levels of YAP showed an exceptionally strong association with poor patient survival (101). The authors suggested that high levels of nuclear YAP, or low levels of cytoplasmic phosphorylated YAP, were associated with poor survival in patients with EOC. Patients with both high-nuclear YAP and low-phosphorylated YAP had about 50% lower 5-year survival, and this

combination serves as an independent prognostic marker for survival (101). In another study, levels of active nuclear YAP were reported to be expressed at high levels in around 14% of a cohort of 284 human ovarian cancer samples. Segregation by histotype showed that the correlation between nuclear YAP and poor survival is predominantly associated with clear cell tumors, independent of stage (102). As patient survival data are not available for the samples used in this study, we cannot correlate YAP expression data with survival of GCT patients. However, the high level of expression and nuclear location of YAP protein in samples from GCT patients indicate that YAP may play important role in regulation of GCT progression.

2.4.3. YAP promotes GCT progression

Control of ovarian cell proliferation is critical for the normal function of the ovary. Uncontrolled granulosa cell proliferation and decreased cell death and/or differentiation can lead to hyperplasia of the granulosa layer and the formation of GCT. Our results indicate that dysregulation of the Hippo/YAP signaling pathway may contribute to uncontrolled granulosa cell proliferation and development of GCT which expands the size of the ovary. We used the KGN cell line as a model to determine the role of YAP in GCT cell proliferation. Consistent with the results from the patient samples, immunohistochemical and molecular studies showed that KGN cells express YAP. Knockdown of YAP protein in KGN cells with YAP-targeting siRNA significantly suppressed cell proliferation without reducing cell viability, indicating that YAP is critical for the proliferation of KGN cells. Furthermore, overexpression of YAP or its constitutively active mutant (YAP^{S127A}) in KGN cells stimulated KGN cell proliferation and migration, indicating that the Hippo/YAP pathway may play a very important role in the regulation of GCT cell growth and potentially GCT cell metastasis. Taken together, our results indicate that YAP protein is required for the proliferation of KGN cells and the Hippo/YAP pathway

might be one of the major pathways that are involved in the regulation of GCT progression. To our knowledge, this is the first direct evidence showing the function of the Hippo/YAP pathway in the progression of GCT.

The mechanism by which YAP regulates GCT cell proliferation is unclear. Granulosa cells are highly regulated by gonadotropins, steroid hormones, and growth factors. Abnormal activities in the pathways activated by any of these factors may induce transformation of follicular granulosa cells and may promote GCT tumor growth, recurrence, or metastasis. As a major effector of the Hippo pathway, YAP was reported to interact with many important factors associated with GCT development. For example, YAP has been reported to regulate the Wnt/b-catenin pathway in colorectal cancer. β -catenin has been reported to be a potential initiator of GCT (98, 103). YAP was also reported to interact with the TGF β signaling pathway (104), which is a critical regulator of granulosa cell proliferation (105). We have recently found that TGF α , via EGFR signaling pathways, plays an important role in the proliferation of GCT cells (46). Interestingly, YAP was reported to interact with EGFR to regulate cell proliferation (48, 106, 107). Future studies on the interaction between the Hippo pathway and these critical regulators of ovarian function may reveal novel mechanisms by which YAP promotes the initiation and/or progression of GCT.

2.4.4. Conclusion

In conclusion, our data show that YAP is highly expressed in human GCT tissues and is a critical regulator of proliferation and migration in the KGN human GCT cell line. We propose that the Hippo-YAP signaling pathway may be involved in the regulation of GCT growth and progression. YAP may be a potential novel biomarker for GCT diagnosis and a promising target for the development of drugs for GCT therapy.

Figure 2-1. YAP is expressed in human granulosa cell tumors (GCT).

Immunohistochemistry was used to examine the expression of YAP in normal ovarian tissues (A, C, and E) and human GCT tissues (B, D, and F). YAP staining is indicated in brown. The counter stain is hematoxylin, shown in blue. **A)** Whole-tissue section scan of a representative normal ovary stained with YAP antibody; **B)** Scanned image of partial ovarian GCT tissue stained with YAP. Amplified representative images of normal ovarian tissues (**C)** and GCT tissues (**D)** stained with YAP antibody to show cell-type-specific YAP expression. Representative high-resolution images were also presented to show the subcellular localization of YAP in the normal ovarian tissues (**E)** and GCT tissues (**F**). Tissue sections probed with the same amount of non-immunized rabbit IgG were used as antibody control (**G**). (**H**) Quantitative results of DAB intensity were also presented to show the difference of positivity (percentage of the number of DAB positive cells relative to number of total cells in each tissue section) and relative intensity of YAP immunosignal between normal human ovarian tissues (CTRL) and tumor tissues (GCT). Each bar represents the mean \pm S.E.M. *: $P < 0.001$ when compared with the control (CTRL) groups. Scale bars = 2 mm in A and B; scale bars = 100 μ m in C and D; scale bars = 50 μ m in E and F; SC, stromal cells; CL, corpus luteum; TC, tumor cells.

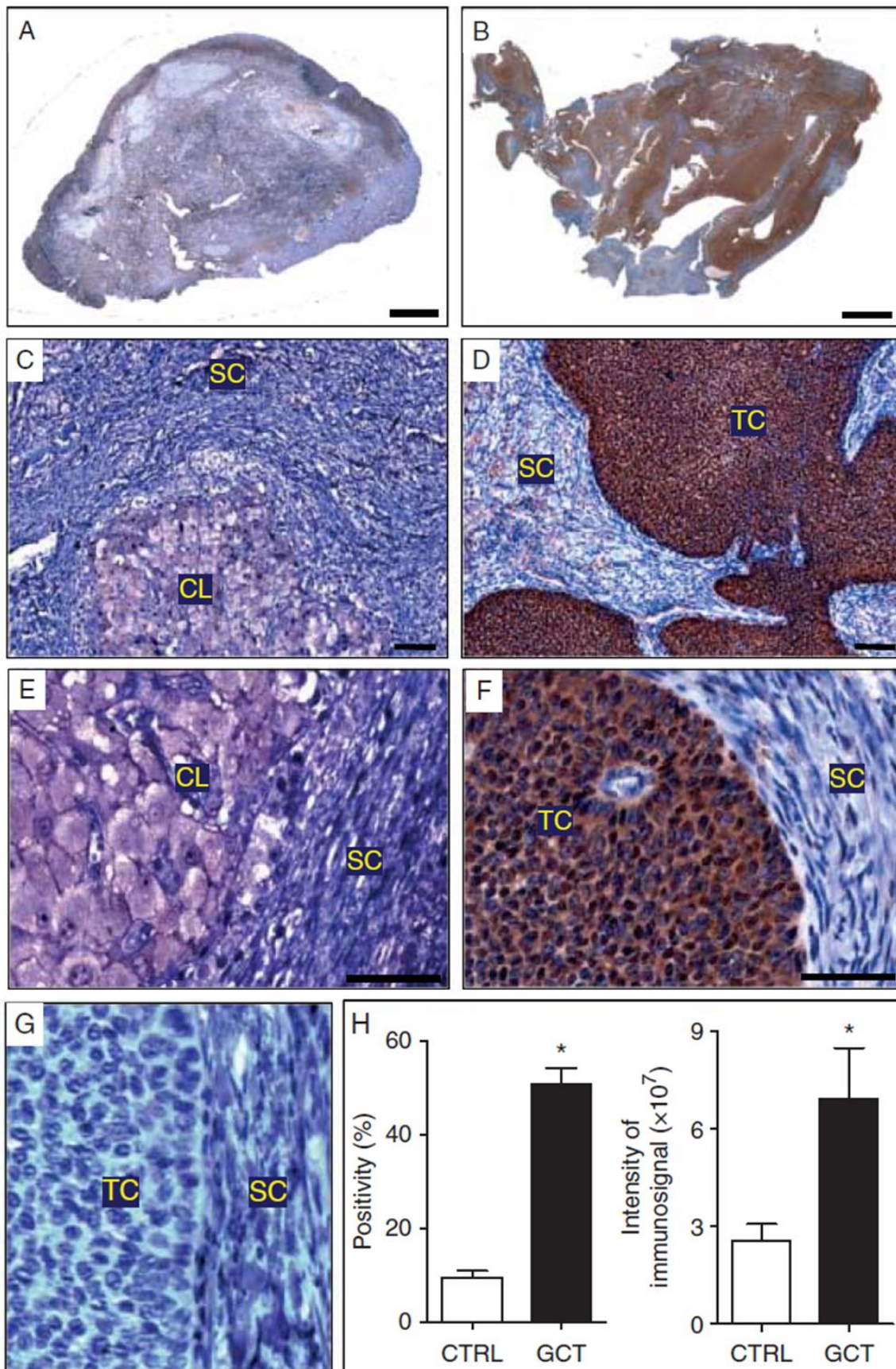


Figure 2-2. YAP is expressed in human ovarian GCT cell lines and epithelial ovarian cancer cell lines.

A) Localization of YAP protein in KGN cells using fluorescent immunocytochemistry. (A1) Total YAP (green); (A2) YAP protein (green) merged with actin filaments (red, stained with Rhodamine-phalloidin). The nucleus was stained with DAPI (blue). (A3) KGN cells stained with same amount of rabbit IgG (antibody control) and Rhodamine-phalloidin. Scale bars = 25 μ m.

B) RT-PCR detection of YAP mRNA expression in cultured human granulosa cells (human-GC), GCT cell lines (KGN and COV434) and ovarian cancer cell lines (IGROV-1, SKOV-3, and CAOV-3). GAPDH was used as mRNA loading control.

C) Western blot detection of YAP protein expression in the same cell lines. β -tubulin was used as protein loading control.

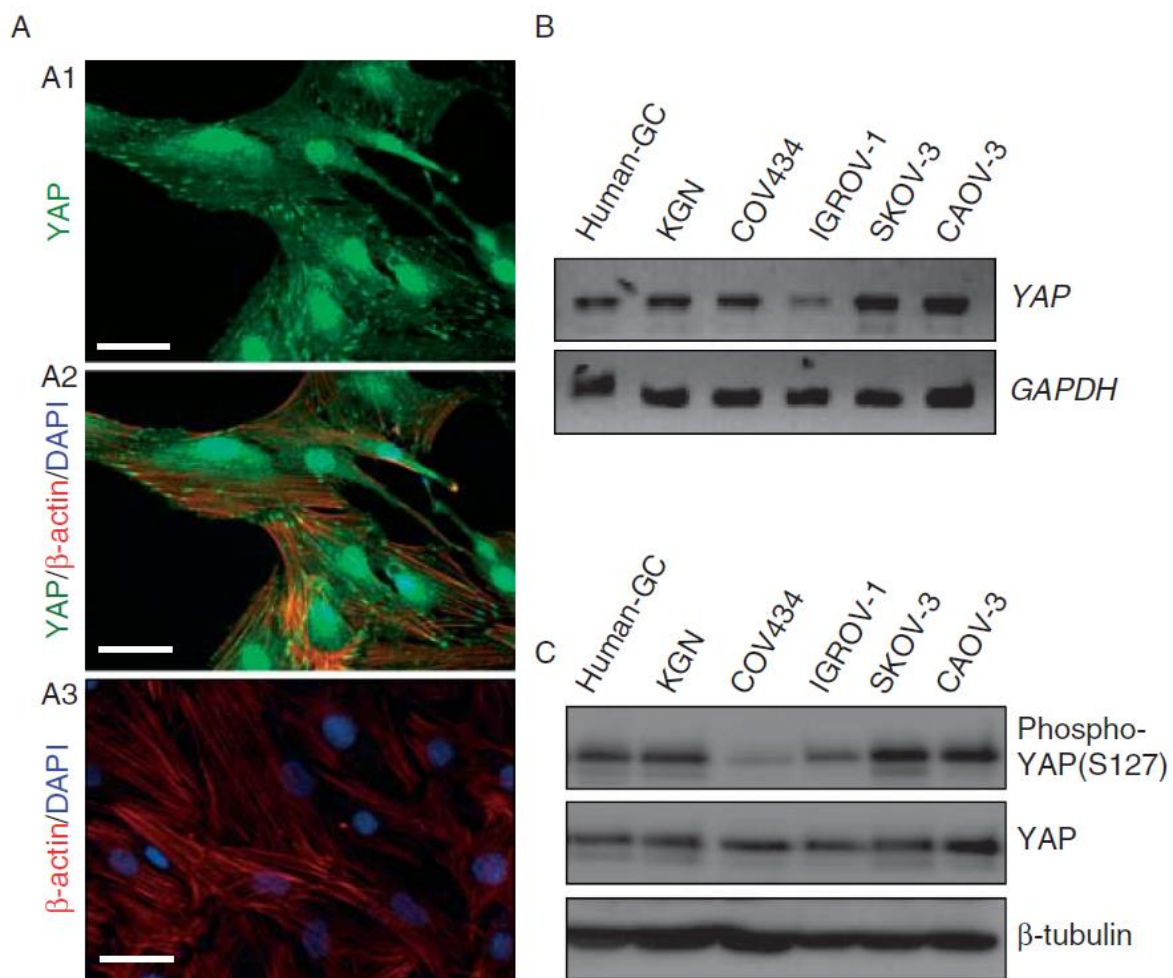


Figure 2-3. YAP is required for KGN cell proliferation.

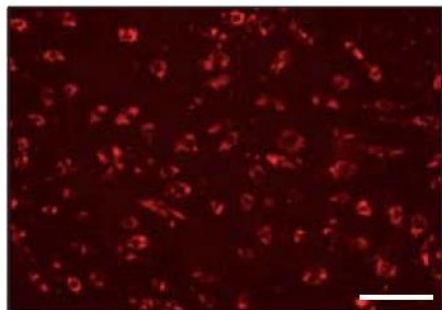
A) Fluorescence-labeled scramble siRNA (siGLO) indicates siRNA transfection efficiency in KGN cells.

B) Western blot shows the downregulation of YAP protein after YAP siRNA treatments. β -tubulin was used as a protein loading control. The lower panel shows the quantitative results for the western blot. Bars represent means \pm S.E.M. ($n = 3$).

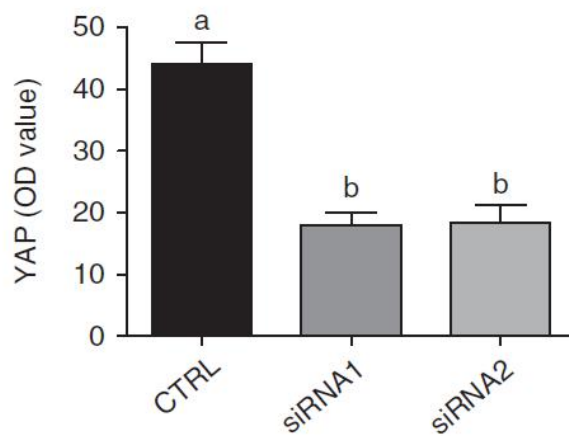
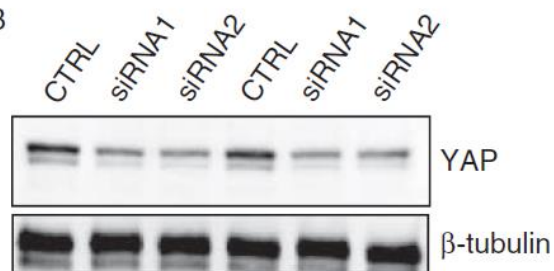
C) Morphology of siGLO-transfected and YAP siRNA-transfected KGN cells. Scale bars = 100 μ m.

D) KGN cells were transfected with YAP siRNAs for 6 h and then cultured for another 72 h. Cell numbers in each group were determined with an INVITROGEN Countess automatic cell counter. Each bar represents the mean \pm S.E.M. ($n = 5$). Bars with the different letter are significantly ($P < 0.05$) different from each other.

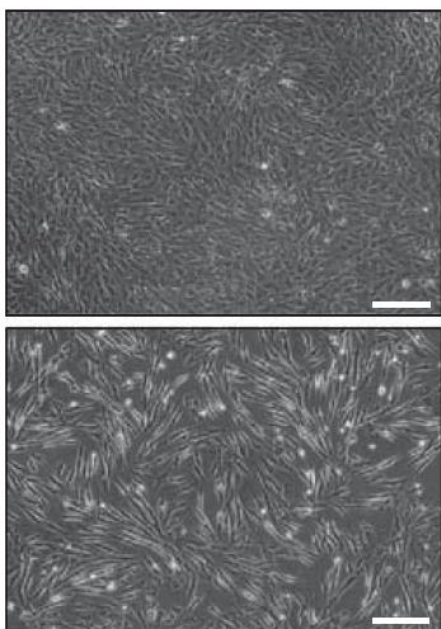
A



B



C



D

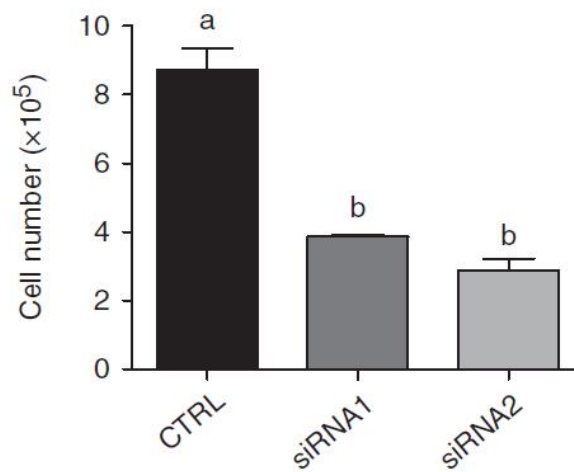


Figure 2-4. Overexpression of YAP stimulates KGN cell proliferation.

A) Empty plasmid-transfected KGN cells (KGN-MX), wildtype YAP overexpression cells (KGN-YAP), and mutant YAP-transfected KGN cells (KGN-YAP^{S127A}) were plated in six-well plates and the levels of YAP and phosphorylated YAP in these established stable cell lines were examined by western blot. β -tubulin was used as a protein loading control.

B) Upper panel: morphological difference between mutant YAP-transfected KGN cells (KGN-YAP^{S127A}) and Empty plasmid-transfected KGN cells (KGN-MX). Scale bars = 100 μ m. Lower panel: actin filaments stained with Rhodamine-phalloidin to demonstrate the morphological change between the two established cell lines. Nuclei were stained with DAPI. Scale bars = 25 μ m.

C) Effect of YAP overexpression on KGN cell proliferation. Control KGN cells (KGN-MX), KGN-YAP cells, and KGN-YAP^{S127A} cells were incubated for 24, 48, and 72 h, respectively, and the cell number was counted with an INVITROGEN Countess automatic cell counter. Each bar represents the mean \pm S.E.M., n = 5. Bars with the same letter are not significantly ($P < 0.05$) different from each other.

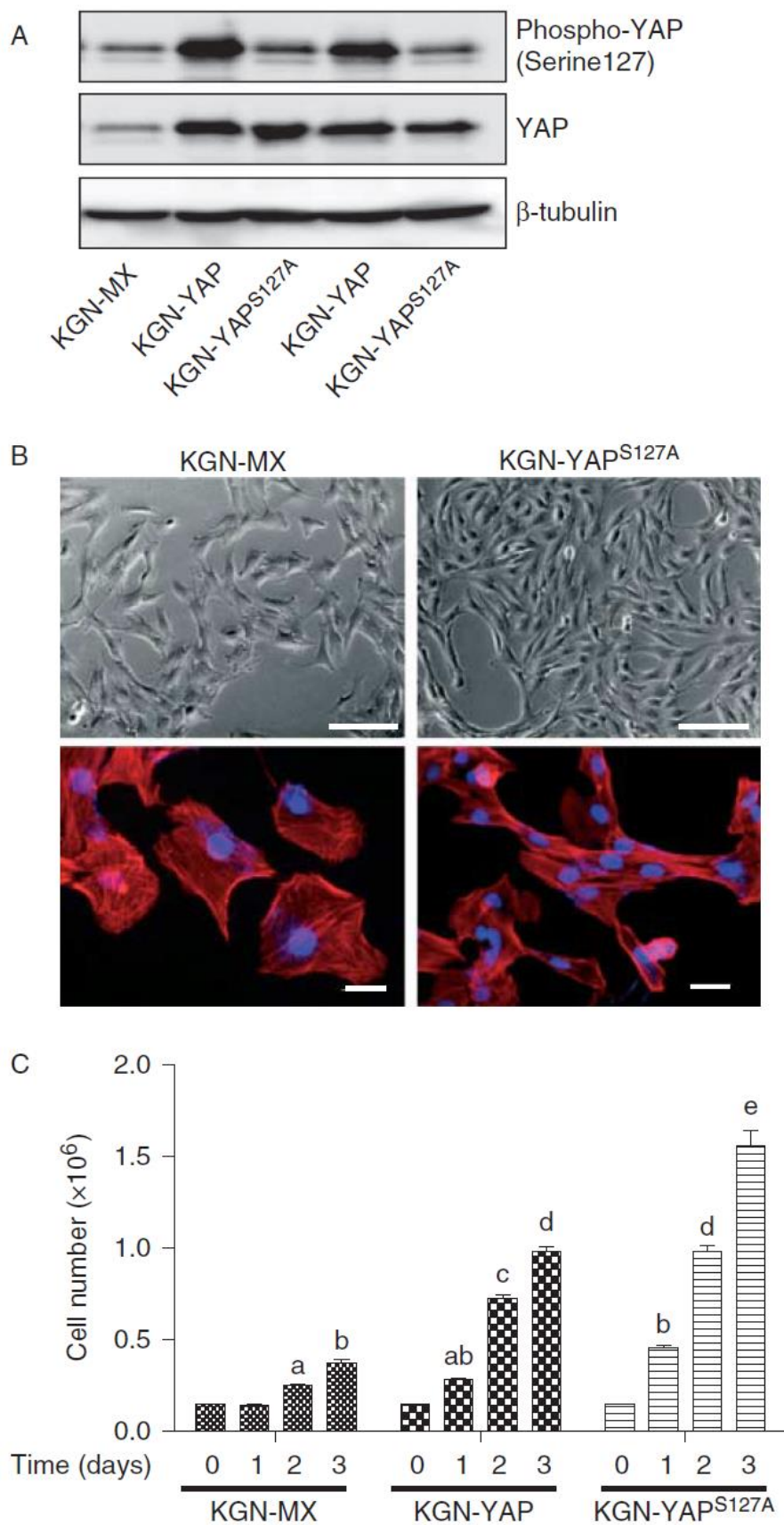
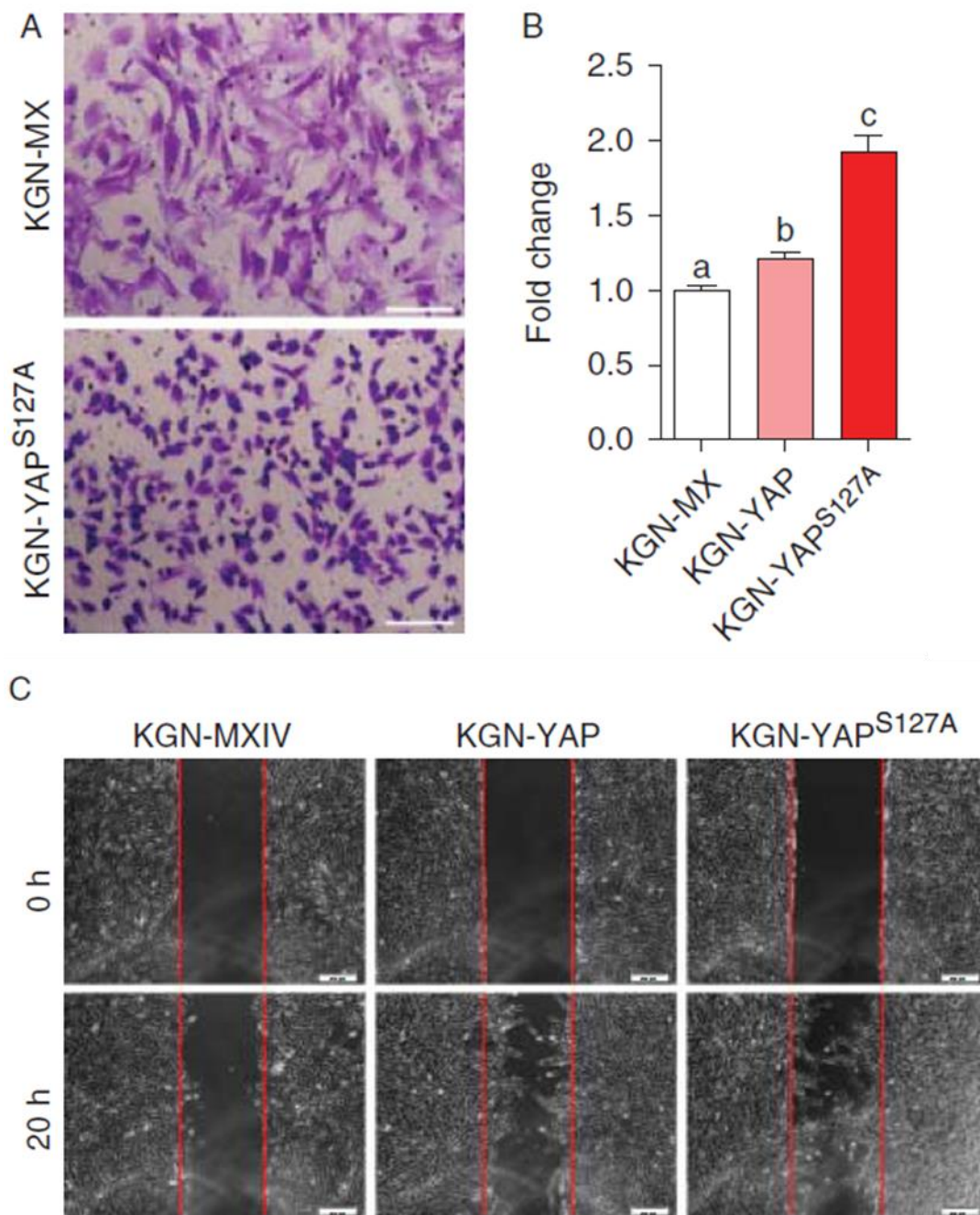


Figure 2-5. YAP regulation of KGN cell migration.

A) KGN-MX cells, KGN-YAP cells, and KGN-YAP^{S127A} cells were loaded to a Transwell migration assay chamber and the migration assay was performed as described in the materials and methods section. Top panel, representative image of the migrated KGN-MX cells. Lower panel, representative image of the migrated KGN-YAP^{S127A} cells. Scale bars = 100 μ m.

B) Migrated cells in each group were counted and the fold change (relative to the KGN-MX control group) of the migrated cells was determined. Each bar represents the mean \pm S.E.M. (n = 12). Bars with the same letter are not significantly ($P < 0.05$) different from each other.

C) Evaluation of the cell migration ability with the wound-healing assay. Representative images from triplicate experiments were presented. Scale bars = 100 μ m.



**CHAPTER 3: YAP INDUCES HIGH-GRADE OVARIAN CANCER WITH
MESENCHYMAL FEATURE FROM POORLY DIFFERENTIATED
GRANULOSA CELLS[‡]**

[‡] The material presented in this chapter was submitted as a manuscript: Lv *et al.* 2017.

ABSTRACT

Understanding the cell-of-origin of high-grade serous ovarian cancer (HGSOC) is the prerequisite for efficient prevention and early diagnosis of this most lethal gynecological cancer. However, the cell-of-origin of HGSOC is under debate. Recently, a novel mesenchymal subtype of HGSOC with poor prognosis was identified by both The Cancer Genome Atlas (TCGA) and Australian Ovarian Cancer Study (AOCS) studies. But the cell-of-origin of this subtype of HGSOC has not been defined. Our previous studies demonstrated the critical role of Yes-associated protein 1 (YAP) in the development of ovarian cancer. In the present study, we show that YAP can induce high-grade ovarian cancer from poorly differentiated granulosa cells. Employing xenograft mouse models, overactive YAP elicited malignant ovarian cancer development in the peritoneal cavity of host mice from granulosa cells. Histologically and genetically, tumors developed in our mouse models resembled women's HGSOC. Intriguingly, these tumors overexpressed N-cadherin and vimentin but had low expression of CA125 and E-cadherin, reminiscent of the recently identified mesenchymal subtype of HGSOC. Our studies suggest the granulosa cells as a previously unprecedented cell-of-origin for the mesenchymal type of HGSOC.

3.1. INTRODUCTION

3.1.1. High-grade serous ovarian cancer

Ovarian cancer is the most lethal gynecological cancer, ranking the fifth leading cancer-related death in women. In worldwide, 238,700 women are estimated to be diagnosed with ovarian cancer annually, with 151,900 ovarian cancer associated deaths (108). Ovarian cancers are collective tumors with distinguished features and origins. High-grade serous ovarian cancer (HGSOC), which accounts for 70-80% ovarian cancer death, is the most common and lethal ovarian cancer (109, 110). HGSOC patients almost always are diagnosed at advanced clinical stages. The aggressive nature of this disease makes the patients have a very poor overall survival. The obstacles for the early diagnosis and better treatments for HGSOC are the controversial cell of origin and the unclear molecular etiology of this disease.

3.1.2. Origin of HGSOC

More often than not by the time the disease has been detected the cancer cells are already widespread to other tissues or organs, making it challenging to assess origin of HGSOC (111). Supported by studies from epidemiology, pathology, genetics, and animal model, fallopian tube secretory epithelial cells (FTSECs) are recognized as the cell origin of a substantial proportion of HGSOC, although it is called ovarian cancer (110). Increasing evidence indicated that HGSOCs originate as serous tubal intraepithelial carcinomas (STICs) located on distal oviductal fimbriae, however, the development of some HGSOCs seem to come from somewhere other than the fallopian tube since only about 60% of HGSOCs have been found accompanied by STICs (112, 113). An alternative origin is the lining epithelial of cortical inclusion cysts in the ovary, which are considered to be derived from the invaginations of ovarian surface epithelium (OSE) (114,

115). Mesothelial OSE cells are believed to retain stem-cell characteristics including pluripotency and thus can undergo serous metaplasia to further develop HGSOC (116).

3.1.3. Novel mesenchymal subtype of HGSOC

Next generation sequencing technology made it possible to classify HGSOC based on their genomic signature. By mining The Cancer Genome Atlas (TCGA) database and analyzing the gene expression profile of ovarian high-grade serous cancer patients, the TCGA group described 4 subtypes of ovarian HGSOC, termed “differentiated”, “immunoreactive”, “proliferative”, and “mesenchymal” subtypes (117). Consistently, an earlier study by the Australian Ovarian Cancer Study (AOCS) Group identified subtypes of HGSOC consistent with this classification (118). Importantly, both studies identified the mesenchymal type of HGSOC with poor prognosis (117, 118). This subtype of HGSOC has a mesenchymal or dedifferentiated phenotype, with overexpression of N-cadherin and vimentin but low expression of conventional ovarian cancer marker CA125 and E-cadherin. The cell-of-origin of the newly identified mesenchymal type of HGSOC is yet to be identified.

3.1.4. Ovarian granulosa cells

Ovarian granulosa cells contribute to most of the somatic component of ovarian follicle. The proliferation and differentiation of granulosa cells are critically regulated to support follicle growth and oocyte maturation. The granulosa cell tumor (GCT) is thought to originate from differentiated granulosa cells of the late preovulatory follicle, maintaining many features of these cells including hormone production and response to gonadotropins (73). Expressing stem/tumor cell markers like MYC, KLF4, and TERT, poorly differentiated granulosa cells at early-stage follicles possess properties of stem/ tumor cells, including multipotential, indefinite self-renewal, loss of cellular contact inhibition, and anchorage-

free growth (35, 119-121). With mesenchymal features, granulosa cells have been demonstrated to transdifferentiate to neuron-like cells, osteoblasts, and chondrogenic lineages (120, 122).

3.1.5. Hippo-YAP signaling

First discovered in *Drosophila*, the Hippo-YAP pathway is highly conserved among species. The Hippo-YAP pathway has attracted growing interest in the research field due to its fundamental role in organ size control, stem cell function, and tumorigenesis (4, 7, 123). The transcriptional co-activator Yes-associated protein 1 (YAP) is the pivotal effector of the Hippo-YAP pathway. The Hippo pathway can phosphorylate YAP and subsequently exclude it from the nucleus to inhibit transcriptional activity of this oncoprotein (4, 5). Extensive studies have shown that YAP is overexpressed in a broad range of human cancer and promotes tumorigenesis (4, 64). YAP is also highly expressed in stem/progenitor cells in intestine, skin, liver, nerve, lung, heart, and muscle tissues, which is critical for stem/progenitor cell function (124, 125). Our previous reports demonstrated that YAP is overexpressed in ovarian cancers including HGSOC and YAP plays a significant role in the initiation and progression of ovarian cancers by interaction with ERBB and FGFR signaling pathways (23, 50, 51).

3.1.6. Present study

In the present study, unexpectedly, we found that overactive YAP elicited development of high-grade ovarian cancer with characteristics of mesenchymal type from poorly differentiated ovarian granulosa cells in xenograft mouse models, reminiscent of the mesenchymal subtype of HGSOC identified recently in women patients (117, 118). Our research unveiled a novel potential cell-of-origin of the mesenchymal type of HGSOC.

3.2. MATERIALS AND METHODS

3.2.1. Cell culture

HGrC1 cell lines was obtained from the Riken Biosource Center (Riken Cell Bank, Ibaraki, Japan). Cell lines were validated using short tandem repeat (STR) polymorphism analysis performed by Genetica DNA Laboratories (Burlinton, NC, USA). Cells were cultured in DMEM/F12 with supplement of Ultrosor G serum substitute and antibiotics at 37 °C, 5% CO₂, and 95% air condition.

3.2.2. Retrovirus system for overexpression

HGrC1 cells were overexpressed with YAP or YAP^{S127A} vectors (given by Dr. Jixin Dong at University of Nebraska Medical Center) and p53^{R175H} vector (a gift from Dr. Jeffrey N Myers at MD Anderson Cancer Center). Empty vector transfected HGrC1 cells were used as control. Recombinant retrovirus was generated as following: after co-transfecting HEK293GP cells with equal amounts of VSVG packaging vector and one of the following retroviral expression vectors: pMX-neo-YAP, pMX-neo-YAP^{S127A}, pBABE-puro-p53^{R175H} using Lipofactamine@ 3000 Transfection Reagent (Grand Island, NY), medium was replaced overnight. Viral supernatants were harvested at 48 h and 72 h post transfection by passing through a 0.45-µm filter. Then these viruses can be stored at -80 °C or directly used to infect target cells with 8 µg/mL polybrene overnight, followed by fresh medium change. After 72 h post infection, appropriate selective antibiotics were added to the culture medium to select positive cells (HGrC1-YAP, HGrC1-YAP^{S127A}, HGrC1-p53^{R175H}, HGrC1-YAP^{S127A}p53^{R175H}). The selection period lasted more than 1 week until no cells survival in the uninfected wells.

3.2.3. CRISPR Cas9 system to knockout BRCA1

The lentivirus containing CRISPR Cas9 system vectors to knockout BRCA1 gene were purchased from Applied Biological Materials Inc. (Richmond, BC, CANADA). Target cells were infected with lentivirus overnight and selected with puromycin after 72 h infection similarly as retrovirus infection procedure.

3.2.4. Cell proliferation analyses

Cell numbers were monitored with an Invitrogen Countess automated cell counter as described in chapter 1.

3.2.5. Western blot

Cell lysis was harvested and protein was analyzed by western blot as above description in chapter 1.

3.2.6. Three-dimensional hanging drop cell culture

A three-dimensional (3D) culture system, GravityPLUS™ 3D Cell Culture plate (InSphero, Schlieren, Switzerland), was employed to mimic cell growth *in vivo* as described in chapter 1.

3.2.7. Colony formation assays

Cell transformation *in vitro* was determined using a Cytoselect 96-Well Cell Transformation assay kit (Cell Biolabs, Inc., San Diego, CA) according to the manufacturer's instructions. Briefly, equal numbers of cells in different group as indication were plated in 0.6% soft agar condition and cultured with treatments or not for 10 days.

MTT (3-(4,5-dimethylthiazol-2-yl)-2,5-diphenyltetrazolium bromide) was used to stain colonies, which were then imaged and counted.

3.2.8. Immunohistochemistry and immunocytochemistry

Immunohistochemistry and immunocytochemistry analyses were performed using indicated antibodies as description in chapter 1.

3.2.9. Hematoxylin and eosin stain for histology analyses

Mouse xenografts were harvested and fixed with formalin. After paraffin-embedding and section, Hematoxylin and eosin (H & E) stain was performed for xenograft tissue slides. Histology analyses was conducted by the pathologist Dr. Yun-An Tseng at University of Nebraska Medical Center.

3.2.10. Alcian blue pH 2.5-periodic acid–Schiff stain

To determine the production of sulfated and carboxylated acid mucopolysaccharides and sialomucins in the tumor tissues, Alcian blue pH 2.5-periodic acid–Schiff (PAS) stain was performed. The colorectal epithelium tissues were used as a positive control for PAS stain. The sections were counter-stained with hematoxylin.

3.2.11. Xenograft mouse model

Cells (2×10^7) were trypsinized and collected by centrifugation. Cells in the pellet were suspended in 250 μ l of DMEM/F12 with 250 μ l of Matrigel (BD Biosciences Inc.) on ice. This mixture was injected subcutaneously or intraperitoneally into 5-week-old female Nude (Nu/J, Envigo) or NSG (NOD.Cg-*Prkdc*^{scid} *Il2rg*^{tm1Wjl}/SzJ, The Jackson Laboratory # 005557) mice. Mice were closely monitored after cell implantation. For intraperitoneal injection, after mice became very sick with distention in abdomen and weight loss, mice

were euthanized and solid tumors were collected for preparation of protein, RNA and paraffin tissue sections. The ascites was harvested and ascites cells were separated by centrifuge for culture. All animal experiments were approved by the Institutional Animal Care and Use Committee (IACUC) at University of Nebraska Medical Center.

3.2.12. Array Comparative Genomic Hybridization (aCGH).

Genomic DNA extracted from xenografts, cultured ascites cells, and control HGrC1 cells was hybridized with normal reference DNA to the Cancer Microarray (Agilent 180K CGH+SNP Array, CCMC design, GRCh37) to perform aCGH profiling. This array targets genes associated with cancer at 5-10 kb copy number resolution and provides 25 kb whole genome copy number coverage for precise breakpoint delineation. Copy number changes > 500 kb in size will be reported as well as copy-neutral loss of heterozygosity (LOH).

3.2.13. Statistical analysis

All experiments were performed at least three times unless otherwise noted. The data are presented as representative experiments or as the means \pm SEM of the averages from multiple experiments. Statistical analysis was conducted using GraphPad Prism software (GraphPad Software, Inc. La Jolla, CA). Statistical comparisons between two groups were analyzed for significance by two-tailed Student's t-test. Multiple group comparisons were assessed by one-way analysis of variance with Tukey's post-Hoc test. $P \leq 0.05$ was considered statistically significant.

3.3. RESULTS

3.3.1. Overactive YAP induces malignant tumors from poorly differentiated human granulosa cells

To explore the role of YAP in the malignant transformation of early-stage granulosa cells, we used HGrC1 as cellular model, which is an immortalized human granulosa cell line derived from poorly differentiated granulosa cells in the early stage of ovarian follicle development (126). As described above, we established HGrC1-MX (control), HGrC1-YAP (expressing wild-type of YAP), and HGrC1-YAP^{S127A} (expressing constitutively active YAP) three cell lines (Fig. 3-1 A). Overexpression of both wild-type and constitutively active YAP dramatically accelerated granulosa cell growth compared with control, while HGrC1-YAP^{S127A} grew most rapidly (Fig. 3-1 B). In the 3D culture system, overexpression of wild type or constitutively active YAP significantly increased the volume of spheroids, with HGrC1-YAP^{S127A} group forming the largest spheroids (Fig. 3-1 C). These results demonstrate that YAP overactivation promotes granulosa cell overgrowth.

To examine the role of YAP in the malignant transformation of undifferentiated granulosa cells *in vitro*, we performed soft agar assays. As immortalized non-transformed HGrC1 cells, control HGrC1-MX cells formed few or no colonies in the soft agar culture (Fig. 3-1 D). In contrast, HGrC1-YAP and HGrC1-YAP^{S127A} cells formed many colonies, and HGrC1-YAP^{S127A} cells formed more colonies than HGrC1-YAP (Fig. 3-1 D). These results suggested that YAP induces malignant transformation of poorly differentiated HGrC1 granulosa cells.

Consistent with *in vitro* experiments, HGrC1-YAP and HGrC1-YAP^{S127A} cells, but not HGrC1-MX cells, formed tumors after subcutaneous injection of these cells into the nude mice (Fig. 3-1 E). Tumors derived from HGrC1-YAP^{S127A} cells grew significantly faster than

those derived from HGrC1-YAP cells (Fig. 3-1 F & G). Surprisingly, histological analysis showed that tumors derived from HGrC1-YAP and HGrC1-YAP^{S127A} cells were not like typical granulosa cell tumors. H & E staining showed that tumor cells in xenograft tissues have pleomorphic nuclei, but not typical coffee bean-like nuclei (Fig. 3-1 H). These tumor tissues have no typical histological structures of GCT such as Call-Exner bodies, trabecular pattern, or macrofollicular structures (Fig. 3-1 H). These tumor cells were very proliferative, indicated by high mitotic index in the H & E staining, and the high expression of Ki-67 (Fig. 3-1 H & I). Moreover, IHC studies showed that these tumor cells have undetectable expression of aromatase which is the biomarker of GCT (Fig. 3-1 I). YAP staining confirmed the overexpression of YAP in tumor cells (Fig. 3-1 I). In addition, tumor cells were malignant, with invasion into adjacent adipose and muscle tissues. Together, these tumors are more likely poorly differentiated ovarian cancers, rather than granulosa cells tumors.

3.3.2. YAP overactivation induces malignant ovarian cancers like high-grade serous ovarian cancer from granulosa cells

Because *TP53* mutations are identified in most of ovarian cancer patients, mutant *TP53* is considered as a driver mutation in the pathogenesis of ovarian cancer (127, 128). To mimic the genetic alternations of ovarian cancer, we introduced the mutant p53^{R175H} into HGrC1 cells. *In vitro* studies showed that mutant p53 (HGrC1-p53^{R175H}) alone cannot transform HGrC1 cells, as indicated by the colony formation assays (Fig. 3-2 A). Introduction of p53^{R175H} into HGrC1-YAP^{S127A} cells (HGrC1-YAP^{S127A}p53^{R175H}) slightly increased colony formation (Fig. 3-2 A). As an ovarian cancer susceptibility gene, *BRCA1* gene mutations predispose women to ovarian cancer and more than 20% of ovarian cancer patients have been found to have loss-of-function *BRCA1*, including inherited mutations, somatic mutations, and promoter methylation (128). With the introduction of

BRCA1 gene deletion by the CRISPR Cas9 system, HGrC1-YAP^{S127A}p53^{R175H}*BRCA1*^{-/-} cells formed more colonies compared with HGrC1-YAP^{S127A}p53^{R175H} group, suggesting the significant role of *BRCA1* in ovarian cancer development.

Most patients diagnosed with ovarian cancer present at later stages, at which ovarian cancer cells have spread in the peritoneal cavity. To mimic the environment of ovarian cancer development, we intraperitoneally injected HGrC1-CTL, HGrC1-p53^{R175H}, HGrC1-YAP^{S127A}, HGrC1-YAP^{S127A}p53^{R175H}, and HGrC1-YAP^{S127A}p53^{R175H}*BRCA1*^{-/-} cells into NSG mice (NOD.Cg-*Prkdc*^{scid} *Il2rg*^{tm1Wjl}/SzJ, The Jackson Laboratory # 005557) to monitor cancer development. Consistent with *in vitro* studies, all mice implanted with HGrC1 cells with overactive YAP (HGrC1-YAP^{S127A}, HGrC1-YAP^{S127A}p53^{R175H}, and HGrC1-YAP^{S127A}p53^{R175H}*BRCA1*^{-/-} 3 groups) developed malignant cancers, accompanied by abdomen distension and weight loss (Fig. 3-2 B). Late stage cancers were associated with large amount of ascitic fluid in the peritoneal cavity (Fig. 3-2 B). After open the abdomen, we found that tumors were widespread in the peritoneal cavity and metastasized to multiple organs/tissues including diaphragm, mesentery, peritoneum, pancreas, and liver (Fig. 3-2 B), which is reminiscent of the typical presentation of malignant human ovarian cancer. Histological analyses further support the metastasis of tumors to multiple organs/tissues in the peritoneal cavity and also metastasis to outside muscle tissues, indicating the malignance of these tumors (Fig. 3-2 C). Moreover, the Kaplan-Meier survival analysis of these host mice showed that all tumor-burden mice died in 6 months (Fig. 3-2 D). HGrC1-YAP^{S127A}p53^{R175H}*BRCA1*^{-/-} hosted mice start to die at 2 months after injection, while HGrC1-YAP^{S127A} and HGrC1-YAP^{S127A}p53^{R175H} injected mice had similar survival time and started to die after injection for 3 months (Fig. 3-2 D). The median survival times are 99 days for HGrC1-YAP^{S127A}p53^{R175H}*BRCA1*^{-/-} mice, 130 days for HGrC1-YAP^{S127A}p53^{R175H} mice, and 127.5 days for HGrC1-YAP^{S127A} mice, respectively

(Fig. 3-2 D). Log-rank test suggested that mutation of *TP53* (p53^{R175H}) had no significant effect on the mouse survival rate. However, deficiency of *BRCA1* gene in the YAP^{S127A}p53^{R175H} mice significantly hastened the onset of death and reduced survival time ($P < 0.001$) (Fig. 3-2 C), indicating BRCA1 loss promotes ovarian cancer development.

Hematoxylin and eosin staining showed the histology of tumors resembled HGSOE (129, 130). Tumor cells are distinct pleomorphism and marked nuclear atypia, with prominent nucleoli (Fig. 3-2 C). These tumor tissues have a very high mitotic index, including many abnormal mitotic figures (Fig. 3-2 C). Tumor cells isolated from the ascitic fluid were very proliferative in culture and nuclear atypia is a common feature of these cells. Consistently, immunohistochemistry analysis showed that proliferation marker Ki67 is highly expressed in tumor tissues (Fig. 3-3 A). Moreover, WT1, PAX8, MYC, and keratin 7 proteins were detected in the tumor cells with immunohistochemistry (Fig. 3-3 A), which are characteristics of ovarian HGSOE (129, 131). YAP and p53 expression in the tumor cells were confirmed (Fig. 3-3 A & D). In addition, tumor tissues were stained negative for aromatase and inhibin, which are two markers for granulosa cell tumors (Fig. 3-3 B). PAX2, a marker for low grade serous carcinoma, and mucinous ovarian cancer marker cytokeratin 20 were also negative in the immunohistochemistry examination (Fig. 3-3 B) (132, 133). We further determined that tumor tissues were negative for Alcian blue (pH 2.5)-periodic acid–Schiff (PAS) staining, confirming that these tumors are not mucinous ovarian cancers (Fig. 3-3 C) (134). These findings support pathological diagnoses that these tumors are like HGSOE, but not other ovarian tumors.

Western blot results further confirmed the expression of WT1, PAX8, MYC and keratin 7 in tumor cells (Fig. 3-4). Interestingly, we found overactive YAP induced increasing protein expression of WT1, PAX8, and MYC in poorly differentiated granulosa cell HGrC1

(Fig. 3-4). The expression of YAP, p53, and BRCA1 were also confirmed by Western blots (Fig. 3-4).

One of the most important features of HGSOC is genome instability (128, 135), we performed array comparative genomic hybridization (aCGH) to examine whether tumors developed in our mouse models resemble human HGSOC at the genomic level. YAP overactivation induced considerable genome instability in tumor cells (Fig. 3-5). Combined with YAP overactivation, p53 mutation, and BRCA1 deletion, tumors cells presented multiple regions of DNA gain and loss, indicating severe genome instability, which is the genomic feature of human HGSOC (Fig. 3-5).

3.3.3. YAP induces high-grade ovarian cancers with mesenchymal features from granulosa cells

Interestingly, these tumor cells retain some mesenchymal features of ovarian granulosa cells. We detected an elevated level of mesenchymal markers like N-Cadherin and vimentin but a low level of CA125 and E-Cadherin expression in these tumors with immunohistochemistry and western blot analyses (Fig. 3-3 A & B and Fig. 3-4). Recently, TCGA and AOCs studies identified a novel molecular subtype of high-grade serous carcinoma in patients which reflect a mesenchymal cell type, with overexpression of mesenchymal markers including N-cadherin and vimentin but with low CA125 and E-cadherin expression (117, 118). This mesenchymal type HGSOC predicts a reduced overall survival (117, 118). With similar aggressive mesenchymal features, the tumors derived from our mouse models resemble this novel mesenchymal subtype of HGSOC in human.

3.4. DISCUSSION

3.4.1. YAP induces high-grade ovarian cancers from poorly differentiated granulosa cells

In the present study, we show that overactive YAP induced HGSOE with mesenchymal features from poorly differentiated granulosa cells. Tumor cells in subcutaneous xenograft tissues have pleomorphic nuclei in high-grade ovarian cancer (129, 136), but not coffee bean-like nuclei in GCT (137). These tumors also do not have typical histological characteristics of GCT like Call-Exner bodies, trabecular pattern, or macrofollicular structures (137). Moreover, these tumor tissues have very high mitotic index, which is indicated by the presence of many cells with mitotic figures and the high expression of Ki-67. Furthermore, IHC studies showed that these tumor cells have undetectable aromatase and inhibin, which are biomarkers of GCT. Based on the histology and molecular features, these tumors are more like poorly differentiated ovarian carcinoma but not like GCT.

After intraperitoneal implantation of YAP^{S127A} overexpressing granulosa cells (HGrC1-YAP^{S127A}, HGrC1-YAP^{S127A}p53^{R175H}, and HGrC1-YAP^{S127A}p53^{R175H}BRCA1^{-/-} cells), large amounts of ascites in the peritoneal cavity were induced in the later stage of tumor progression. These tumor cells were very invasive and metastasized to the omentum, mesentery, visceral fat tissue, diaphragm membrane, liver, pancreas, and muscle tissues. Histological studies showed that the nuclei of these tumor cells are highly pleomorphic and larger with coarsely clumped chromatin. Moreover, these tumor tissues have very high mitotic index, including many abnormal mitotic figures. Furthermore, cultured tumor cells derived from the ascitic fluid were very proliferative and the nuclear atypia was very common. In addition, the known biomarkers for HGSOE, such as high Ki-67, PAX8, WT1,

Keratin 7 are expressed in the cancer cells derived from all three YAP^{S127A} expressing cells (129, 132, 138). The morphological features and negative expression of PAX-2 in these tumor cells suggest that these tumors are not low-grade serous carcinomas (129). The negative keratin 20 and PAS staining suggests that these tumors are not mucinous ovarian cancers (132). The molecular features of these tumors indicated that these tumors are high-grade ovarian carcinoma with serous features.

3.4.2. YAP elicits mesenchymal subtype of HGSOc from poorly differentiated granulosa cells

Both the TCGA and AOCS studies revealed multiple subtypes of human HGSOc, including “differentiated”, “immunoreactive”, “proliferative”, and “mesenchymal” 4 subtypes (117, 118). Of importance herein, both groups identified a mesenchymal type of HGSOc with poor prognosis (117, 118). Due to its mesenchymal molecular features, the cell-of-origin for the newly identified mesenchymal type of HGSOc remains unknown. However, it is known that this type of HGSOc has very high level of mesenchymal markers including N-cadherin and vimentin, but it has very low expression of epithelial proteins like E-cadherin and CA125 (MUC16) (117, 118). In the present study, we found that overactivation of YAP in the poorly differentiated ovarian granulosa cells induced HGSOc-like tumors. Importantly, these tumors express high levels of N-cadherin and vimentin but have low expression of E-cadherin and CA125. Granulosa cells are mesenchymal type of ovarian cells, which can be induced to differentiate into osteoblast, muscle cells and neurons (120, 122). The tumor cells derived from poorly differentiated granulosa cells in our mouse models kept their mesenchymal cell markers such as N-cadherin and vimentin. Based on these novel findings, we speculate that poorly differentiated granulosa cell could be a potential cell-of-origin of the lethal mesenchymal type of HGSOc.

The mechanism by which YAP induces the mesenchymal type of HGSOC from granulosa cells is unclear. Granulosa cells are very special cells in human body. Previous studies have shown that a subpopulation of granulosa cells in early-stage follicles (poorly differentiated granulosa cells) possess properties of stem or tumor cells, including loss of cellular contact inhibition and anchorage-free growth (119, 121, 139, 140). Isolated granulosa cells express stem cell markers with high telomerase activity, and can differentiate into other cell types (120, 141, 142). This evidence suggests that poorly differentiated granulosa cells are mesenchymal cells with high plasticity. As an oncoprotein, YAP has also been implicated in stem cell function of embryonic stem cells, adult stem cells, and cancer stem cells (125). Importantly, YAP has been shown to be overexpressed in cancer stem cells and high-grade carcinomas (68, 143, 144). Very recent studies show that YAP was able to induce terminally differentiated luminal breast epithelial cells, neurons, and the pancreatic acinar cells into tissue specific pluripotent cells (145). Therefore, it is possible that disruption of the Hippo pathway in granulosa cells leads to overactivation of YAP, which may induce dedifferentiation of granulosa cells and uncontrolled proliferation. Further loss function of p53 and BRCA1 can induce malignant transformation, eliciting poorly differentiated ovarian cancers. The observation that mesenchymal type of HGSOC is characterized with poorly differentiated phenotype supports our idea (118). The detailed mechanism underlying YAP regulation of granulosa cell reprogramming and transformation warrants further investigations. Currently, we are also using several mouse strains to study the tumorigenesis of granulosa cells.

3.4.3. The genomic instability of HGSOC

Cell reprogramming factors have potential to induce DNA damage (146). DNA damage response pathways might be a potential link between somatic cell dedifferentiation and tumorigenesis. p53 plays critical role in the cellular DNA damage response process to

protect cells from potential inherited chromosomal aberrations during the process of dedifferentiation. Abrogation of p53 leads to persistent DNA damage and chromosomal aberrations during cell reprogramming (146, 147). Importantly, recent studies showed that mutated p53 could promote tumor progression via gain-of-function, further supporting the importance of p53 in the development of HGSOC (148-150). Similarly, BRCA1/2 are also critical for maintaining genome stability (151, 152). Unfortunately, *TP53* is mutated in the majority of patients with HGSOC (128). Abnormal inactivation of *BRCA1/2* genes is considered to contribute to the development of more than half of HGSOC (110). Genome instability is one of the most important genetic features of HGSOC (128, 135). In the present study, we found that YAP overactivation was able to induce malignant ovarian tumors from poorly differentiated granulosa cells with genome instability, which is supported by recently studies showing genome instability induced by YAP (153, 154). Combined YAP overactivation with alternations of *TP53* and *BRCA1* genes, two notorious susceptibility genes in HGSOC, tumor progression was significantly promoted. More importantly, tumor cells shown severe genome instability, mimicking the genetic feature of human HGSOC. Therefore, with the combination of overactive YAP oncoprotein and inactivation of tumor suppressors p53 and/or BRCA1, poorly differentiated granulosa cells can be vulnerable for malignant transformation, leading to the development of mesenchymal type of HGSOC.

3.4.4. Clinical significance

Our findings have significant clinical relevance. Tumor heterogeneity in histology and genome has been blamed, in part, for the poor prognosis of the HGSOC. Understanding on the cell-of-origin of different subtype of HGSOC and the molecular events underlying the initiation and progression of HGSOC should provide clues for the effective prevention, early diagnosis, and personalized treatment of HGSOC. In the present study, we showed

that disruption of the Hippo-YAP pathway may result in malignant transformation of ovarian poorly differentiated granulosa cells, leading to the development of HGSOC with mesenchymal features. Targeting the Hippo-YAP pathway may represent a novel strategy for the improved treatment of HGSOC.

Figure 3-1. YAP induces non-granulosa cell tumors from poorly differentiated granulosa cells.

A) Western blot showing overexpression of wild type YAP and constitutively active YAP^{S127A} protein in HGrC1 cells. β -Actin as control.

B) Overexpression of YAP promotes HGrC1 cell proliferation; each point on the growth curves represents the mean \pm SEM ($n \geq 4$); when compared with control at 10 d, **: $P < 0.01$, ***: $P < 0.001$.

C) Representative pictures and quantitative data showing the size of spheroids formed by HGrC1-MX, HGrC1-YAP, and HGrC1-YAPS127A cells in the 3D culture system after loading for 5 d; scale bar: 200 μ m; each bar represents the mean \pm SEM ($n \geq 4$); bars with different letters are significantly different from each other ($P < 0.05$).

D) Representative images and quantitative data showing colony formation by HGrC1-MX, HGrC1-YAP, and HGrC1-YAPS127A cells; scale bar: 500 μ m; each bar represents the mean \pm SEM ($n \geq 4$); bars with different letters are significantly different from each other ($P < 0.05$).

E) Representative pictures show tumor formation by HGrC1-YAP and HGrC1-YAPS127A but not HGrC1-MX cells using xenograft mouse models.

F) Tumor growth indicated by increasing volume of tumors; each point on the growth curves represents the mean \pm SEM ($n = 10$); when compared with control at the end point, ***: $P < 0.001$.

G) Bar graph showing tumor weight; each bar represents the mean \pm SEM ($n = 10$); bars with different letters are significantly different from each other ($P < 0.05$).

H) Representative picture showing hematoxylin and Eosin stain (H & E) of tumor tissues; scale bar: 50 μ m.

I) Representative images showing the expression of Ki67, aromatase, and YAP in tumor cells by immunohistochemistry; scale bar: 50 μ m.

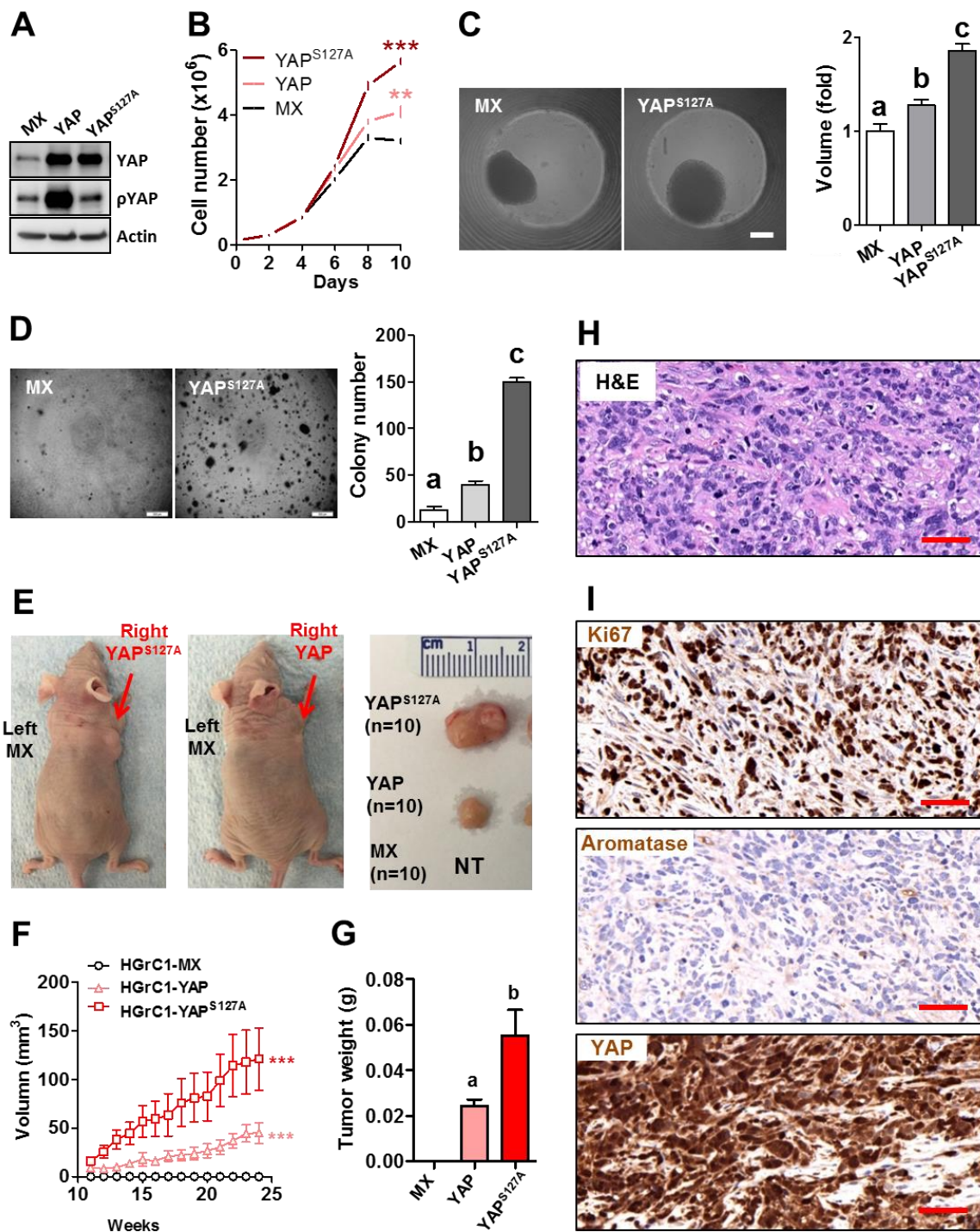


Figure 3-2. YAP induces malignant ovarian cancers from poorly differentiated granulosa cells.

A) Representative images showing colonies formed by HGrC1-CTL, HGrC1-p53^{R175H}, HGrC1-YAP^{S127A}, HGrC1-YAP^{S127A}p53^{R175H}, and HGrC1-YAP^{S127A}p53^{R175H}BRCA1^{-/-} cells; scale bar: 500 μ m; right graph showing quantitative data of colony numbers; each bar represents the mean \pm SEM ($n \geq 6$); ns: no significance, **: $P < 0.01$, ***: $P < 0.001$.

B) Representative images show that ascites presents and malignant ovarian cancer spreads in the mouse abdomen, including peritoneum, mesentery, diaphragm, pancreas, and liver, in the host mice intraperitoneally injected with HGrC1-YAP^{S127A}, HGrC1-YAP^{S127A}p53^{R175H}, and HGrC1-YAP^{S127A}p53^{R175H}BRCA1^{-/-} cells; the same color of arrows and organ/tissue names are matched.

C) Representative images showing the histology of the malignant ovarian cancers metastasized to multiple organs/tissues; scale bar: 50 μ m.

D) Survival data of host mice injected with HGrC1-CTL, HGrC1-p53^{R175H}, HGrC1-YAP^{S127A}, HGrC1-YAP^{S127A}p53^{R175H}, and HGrC1-YAP^{S127A}p53^{R175H}BRCA1^{-/-} cells.

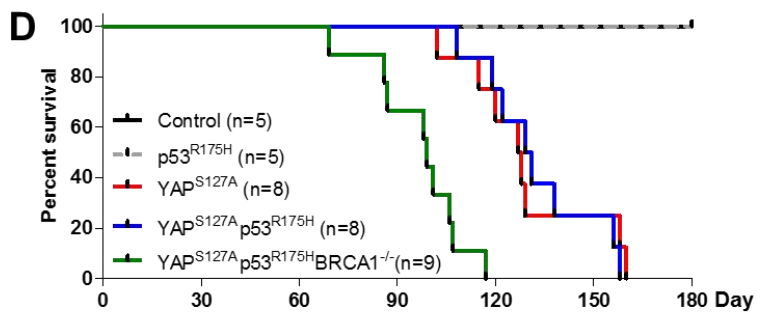
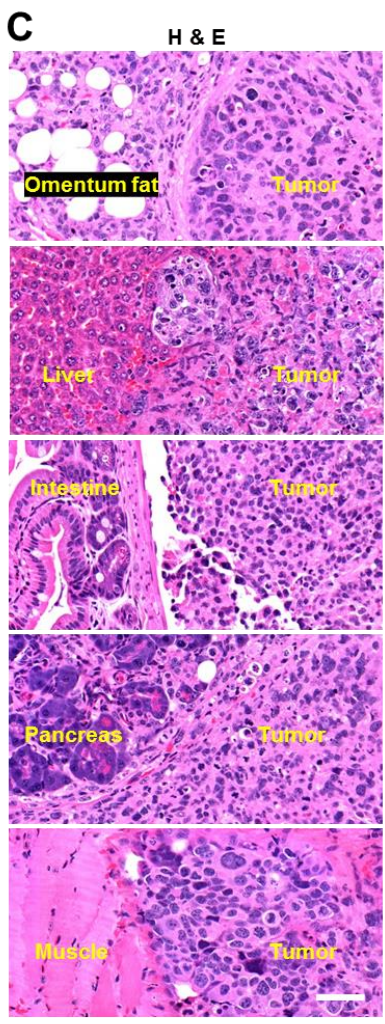
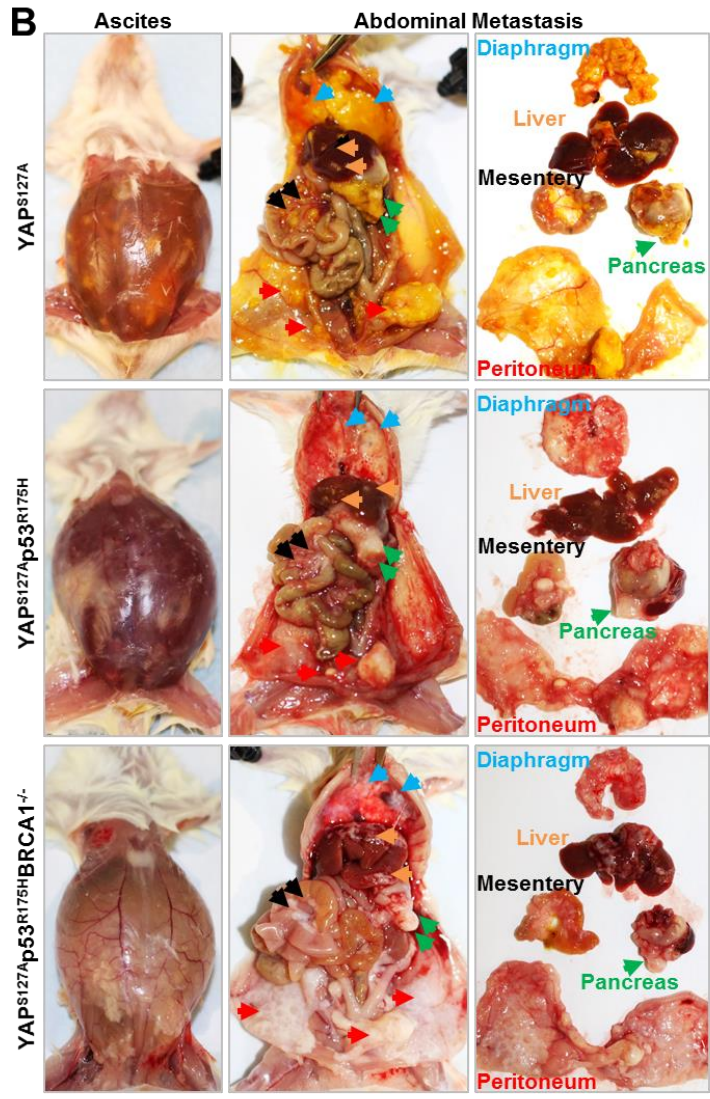
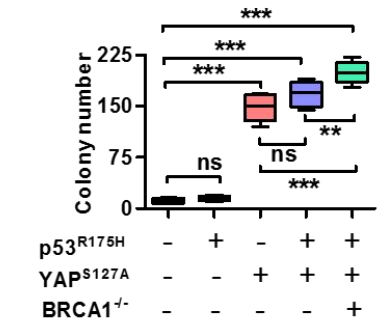
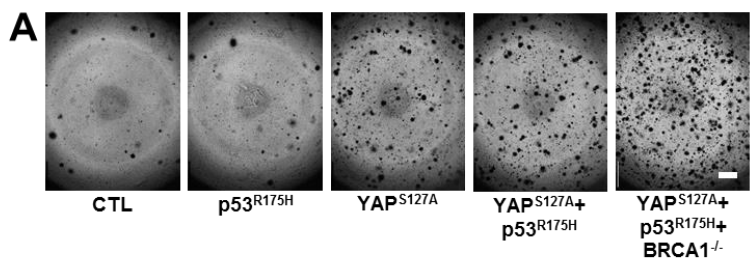


Figure 3-3. YAP elicits HGSOc-like tumors from poorly differentiated granulosa cells.

A) Representative images showing expression of Ki-67, WT-1, PAX8, Myc, Keratin 7 (KRT7), YAP, and N-Cadherin protein in tumor tissues analyzed by immunohistochemistry; scale bar: 50 μ m.

B) Representative images showing that tumor tissues are negative for the expression of aromatase, inhibin, Keratin 20 (KRT20), PAX2, E-Cadherin, and CA125; scale bar: 50 μ m.

C) Representative picture showing tumor tissues are negative for PAS stain; scale bar: 50 μ m.

D) Representative images showing nuclear p53 expression in tumors derived from HGrC1-YAP^{S127A}p53^{R175H} and HGrC1-YAP^{S127A}p53^{R175H}BRCA1^{-/-} cells, but not in tumors from HGrC1-YAP^{S127A}; scale bar: 50 μ m.

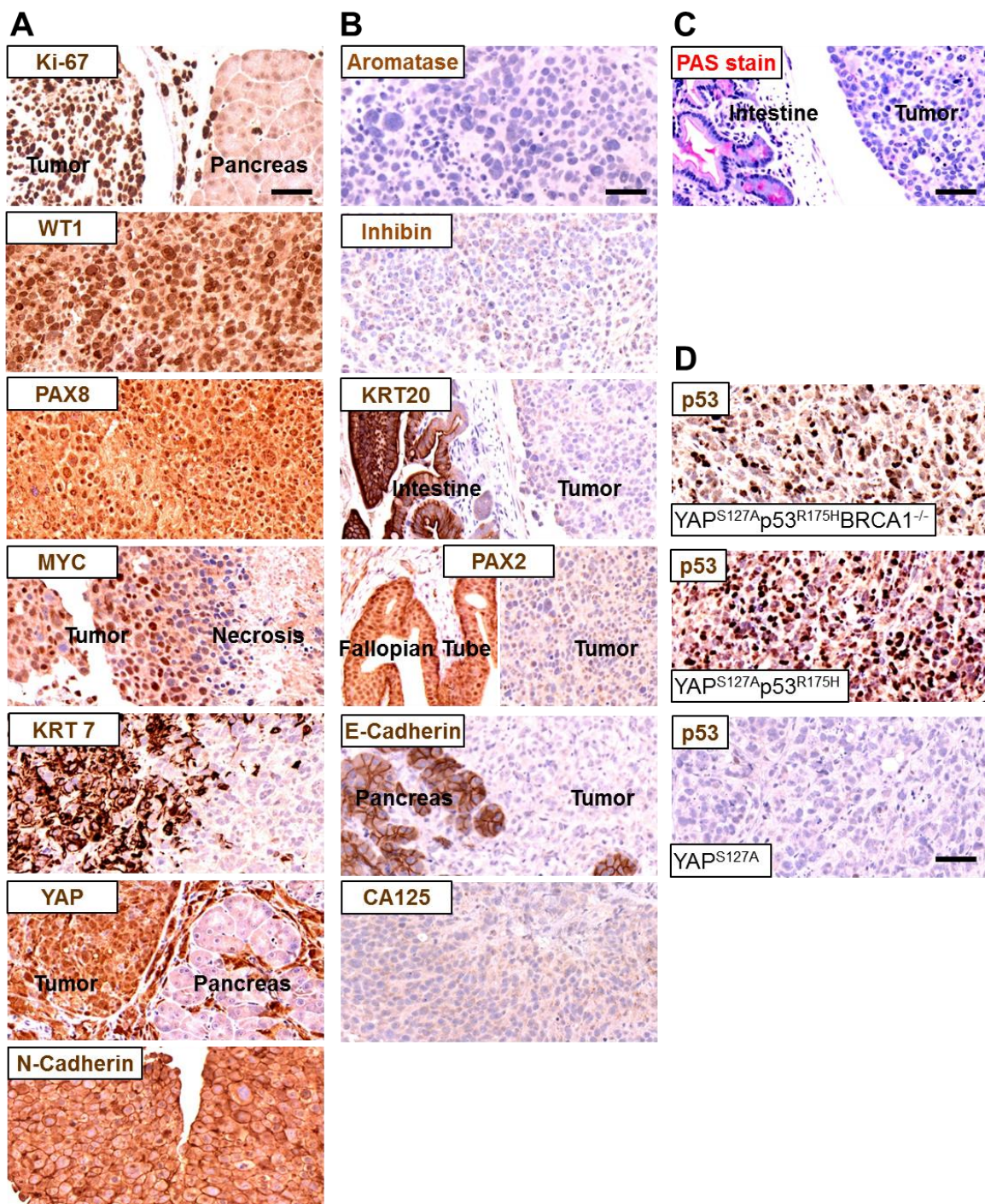


Figure 3-4. YAP induces HGSOc-like tumors with mesenchymal feature from poorly differentiated granulosa cells.

Western blot analyses showing the expression of WT1, PAX8, Myc, Keratin 7 (KRT7), N-Cadherin, E-Cadherin, vimentin, p53, YAP, and BRCA1 in cell lines and tumor cells. Ovsaho cells was used as positive control for HGSOc.

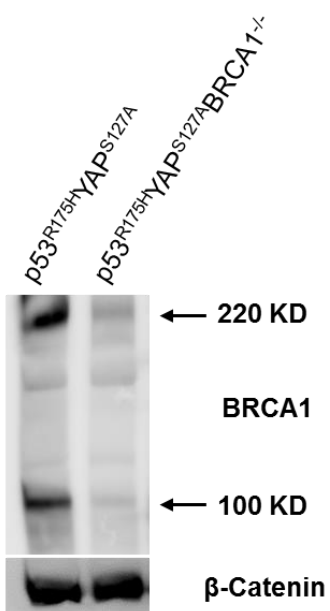
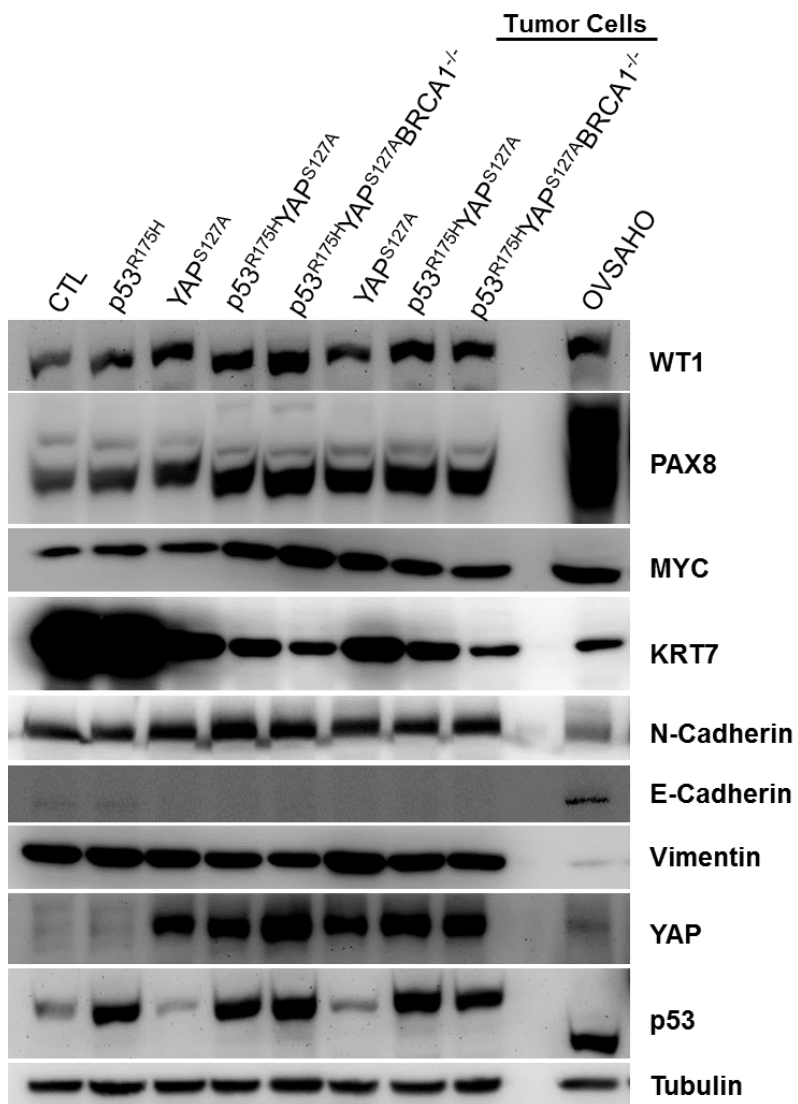


Figure 3-5. Tumors derived from poorly differentiated granulosa cells genetically resemble HGSOC.

Tumors derived from granulosa cells exhibits genomic instability as women's HGSOC. aCGH analysis results showing DNA copy number changes of tumors formed by HGrC1-YAP^{S127A}, HGrC1-YAP^{S127A}p53^{R175H}, and HGrC1-YAP^{S127A}p53^{R175H}BRCA1^{-/-} cells, as well as control cells (HGrC1-CTL). The y axis represents gain (positive, blue) or loss (negative, red) of copy number, while the x axis represents each chromosome. Tumors from HGrC1-YAP^{S127A}p53^{R175H}BRCA1^{-/-} cells showing the most severe genomic instability.

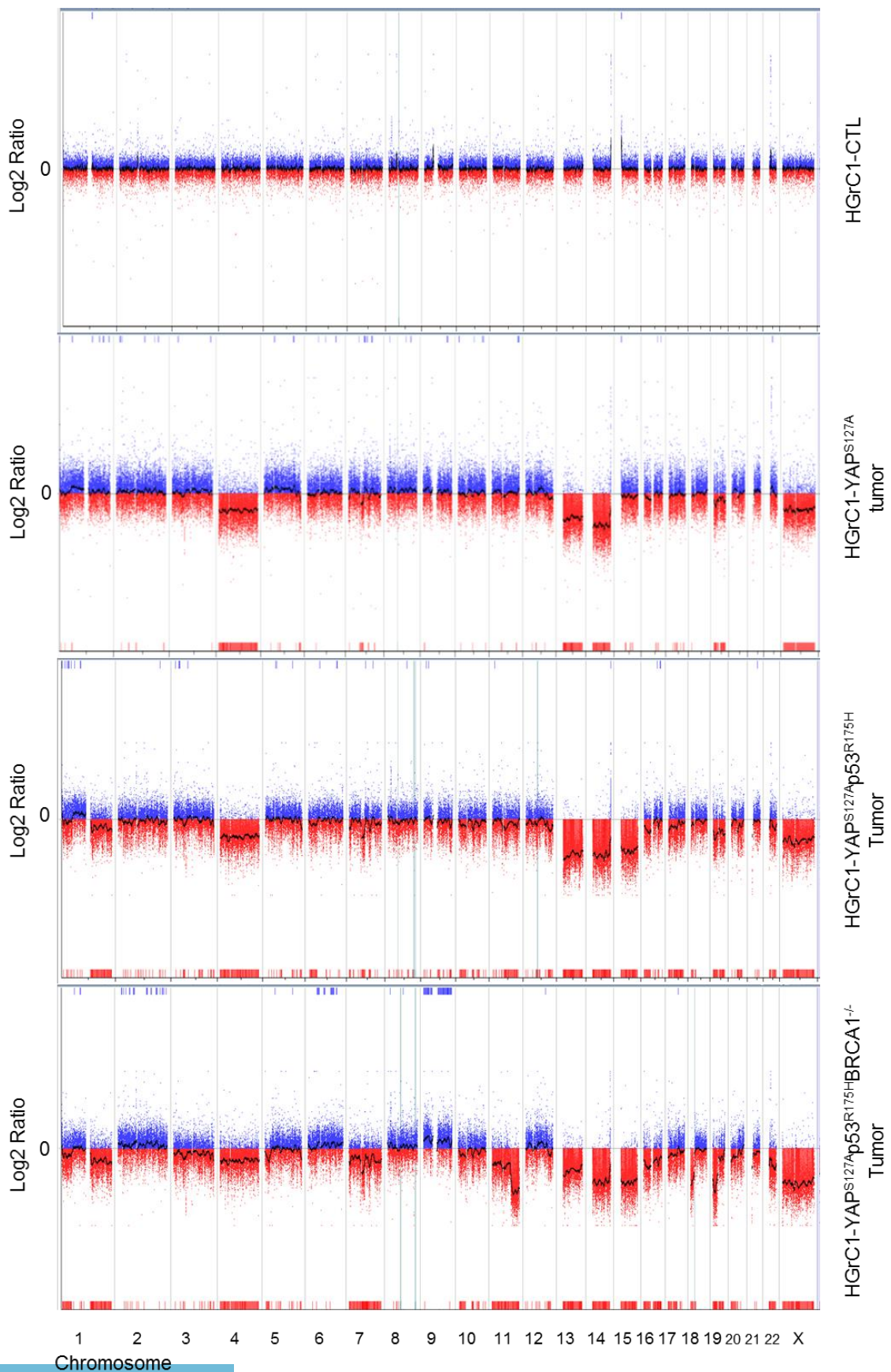


Table 1. Primers for PCR.

Gene Name	Primers
Human	
HBEGF	F: GCTCCCTCCTGCATCTGCCA R: GAGGCTCAGCCCATGACACCTCT
CYP19A1	F: TGAATATTGGAAGGATGCACAGAC R: TGAATCGTCTCAGAAGTGTAACGAG
CYP11A1	F: TGGGTGCGCCTATCACCAGTAT R: CCACCCGGTCTTTCTTCCA
FSHR	F: TTCAAGAACAAGGATCCATTCC R: CCTGGCCCTCAGCTTCTTAA
LHCGR	F: TCAATGTGGTGGCCTTCTTCATA R: TTGGCACAAGAATTGATGGGATA
INHA	F: GTCTCCAAGCCATCCTTTT R: TGGCAGCTGACTTGTCCCTC
INHBB	F: ATCAGCTTCGCCGAGACA R: GCCTTCGTTGGAGATGAAGA
INHBA	F: CTCGGAGATCATCACCGTTTG R: CCTTGGAATCTCGAAGTGC
PLIN2	F: TCAGCTCCATTCTACTGTTCCACC R: CCTGAATTTTCTGATTGGCACT
MYC	F: CCTACCCTCTCAACGAC R: ATCTTCTTGTTCCCTCCTCAG
TERT	F: GCCTGAGCTGTACTTTGTCAA R: CGCAAACAGCTTGTTCTCCATGTC
YAP	F: GCAACTCCAACCAGCAGCAACA R: CGCAGCCTCTCCTTCTCCATCTG
CTGF	F: ACCTGTGGGATGGGCATCT R: CAGGCGGCTCTGCTTCTCTA
AREG	F: TGGAAGCAGTAACATGCAAATGTC

GAPDH R: GGCTGCTAATGCAATTTTGGATAA
 F: CAGCCTCAAGATCATCAGCA
 R: GTCTTCTGGGTGGCAGTGAT

Mouse

Hsd3b1 F: ACTGCAGGAGGTCAGAGCT
 R: GCCAGTAACACACAGAATACC

Hbegf F: ATGAAGCTGCTGCCGTCGGT
 R: TCAGTGGGAGCTAGCCACGC

Ctgf F: CCCGCCAACC GCAAGATT
 R: AGGCGGCTCTGCTTCTCCA

Areg F: AATGAGAACTCCGCTGCTAC
 R: CCCCTGTGGAGAGTTCACTG

Yap F: CCCGACTCCTTCTTCAAGC
 R: CTCGAACATGCTGTGGAGTC

Gapdh F: CCCTTCATTGACCTCAACTA
 R: CCAAAGTTGTCATGGATGAC

Table 2. Antibodies

Antibody	Vendor
YAP	<i>Cell Signaling (Danvers, MA, USA)</i>
Phospho YAP	<i>Cell Signaling (Danvers, MA, USA)</i>
LATS1	<i>Cell Signaling (Danvers, MA, USA)</i>
Phospho LATS1	<i>Cell Signaling (Danvers, MA, USA)</i>
LATS2	<i>Cell Signaling (Danvers, MA, USA)</i>
Phospho ERK1/2	<i>Cell Signaling (Danvers, MA, USA)</i>
Phospho CREB	<i>Cell Signaling (Danvers, MA, USA)</i>
Phospho AKT	<i>Cell Signaling (Danvers, MA, USA)</i>
Cleaved Caspase 3	<i>Cell Signaling (Danvers, MA, USA)</i>
Vimentin	<i>Cell Signaling (Danvers, MA, USA)</i>
Snail	<i>Cell Signaling (Danvers, MA, USA)</i>
Slug	<i>Cell Signaling (Danvers, MA, USA)</i>
ZO-1	<i>Cell Signaling (Danvers, MA, USA)</i>
ErbB3	<i>Cell Signaling (Danvers, MA, USA)</i>
E-cadherin	<i>Cell Signaling (Danvers, MA, USA)</i>
N-cadherin (WB)	<i>Cell Signaling (Danvers, MA, USA)</i>
N-cadherin (IHC)	<i>Abcam (Cambridge, MA, USA)</i>
Myc (WB)	<i>Cell Signaling (Danvers, MA, USA)</i>
Myc (IHC)	<i>Abcam (Cambridge, MA, USA)</i>
Aromatase (rabbit, IHC)	<i>Cell Signaling (Danvers, MA, USA)</i>
Aromatase (mouse, WB)	<i>Bio-Rad (Hercules, CA, USA)</i>
3 β -HSD	<i>Ian Mason, Ph.D. (Dallas, TX, USA)</i>
P450scc	<i>Millipore (Danvers, MA, USA)</i>
p53 (rabbit, IHC)	<i>Santa Cruz (Dallas, TX, USA)</i>
p53 (mouse, IF, WB)	<i>Agilent Technologies (Santa Clara, CA, USA)</i>
BRCA1	<i>Santa Cruz (Dallas, TX, USA)</i>

Keratin 20	<i>Cell Signaling (Danvers, MA, USA)</i>
PAX8	<i>Proteintech (Rosemont, IL, USA)</i>
PAX2	<i>Proteintech (Rosemont, IL, USA)</i>
WT1	<i>Cell Signaling (Danvers, MA, USA)</i>
Inhibin beta A	<i>Abcam (Cambridge, MA, USA)</i>
CA125	<i>Abcam (Cambridge, MA, USA)</i>
KI67	<i>Abcam (Cambridge, MA, USA)</i>
β -Actin	<i>Sigma-Aldrich (St. Louis, MO, USA)</i>
β -Tubulin	<i>Sigma-Aldrich (St. Louis, MO, USA)</i>

BIBLIOGRAPHY

1. Hsueh AJ, Kawamura K, Cheng Y, & Fauser BC (2015) Intraovarian control of early folliculogenesis. *Endocrine reviews* 36(1):1-24.
2. Kumar TR, Wang Y, Lu N, & Matzuk MM (1997) Follicle stimulating hormone is required for ovarian follicle maturation but not male fertility. *Nature genetics* 15(2):201-204.
3. Stocco C, Telleria C, & Gibori G (2007) The molecular control of corpus luteum formation, function, and regression. *Endocrine reviews* 28(1):117-149.
4. Pan D (2010) The hippo signaling pathway in development and cancer. *Developmental cell* 19(4):491-505.
5. Zhao B, Li L, Lei Q, & Guan KL (2010) The Hippo-YAP pathway in organ size control and tumorigenesis: an updated version. *Genes & development* 24(9):862-874.
6. Halder G & Johnson RL (2011) Hippo signaling: growth control and beyond. *Development* 138(1):9-22.
7. Barry ER & Camargo FD (2013) The Hippo superhighway: signaling crossroads converging on the Hippo/Yap pathway in stem cells and development. *Current opinion in cell biology* 25(2):247-253.
8. Yu FX & Guan KL (2013) The Hippo pathway: regulators and regulations. *Genes & development* 27(4):355-371.
9. Dong J, *et al.* (2007) Elucidation of a universal size-control mechanism in *Drosophila* and mammals. *Cell* 130(6):1120-1133.

10. Zhao B, *et al.* (2007) Inactivation of YAP oncoprotein by the Hippo pathway is involved in cell contact inhibition and tissue growth control. *Genes & development* 21(21):2747-2761.
11. Camargo FD, *et al.* (2007) YAP1 increases organ size and expands undifferentiated progenitor cells. *Current biology : CB* 17(23):2054-2060.
12. Hansen CG, Moroishi T, & Guan KL (2015) YAP and TAZ: a nexus for Hippo signaling and beyond. *Trends in cell biology* 25(9):499-513.
13. Lian I, *et al.* (2010) The role of YAP transcription coactivator in regulating stem cell self-renewal and differentiation. *Genes & development* 24(11):1106-1118.
14. Beverdam A, *et al.* (2013) Yap controls stem/progenitor cell proliferation in the mouse postnatal epidermis. *The Journal of investigative dermatology* 133(6):1497-1505.
15. Zhao R, *et al.* (2014) Yap tunes airway epithelial size and architecture by regulating the identity, maintenance, and self-renewal of stem cells. *Developmental cell* 30(2):151-165.
16. Mahoney JE, Mori M, Szymaniak AD, Varelas X, & Cardoso WV (2014) The hippo pathway effector Yap controls patterning and differentiation of airway epithelial progenitors. *Developmental cell* 30(2):137-150.
17. Zhang H, Pasolli HA, & Fuchs E (2011) Yes-associated protein (YAP) transcriptional coactivator functions in balancing growth and differentiation in skin. *Proceedings of the National Academy of Sciences of the United States of America* 108(6):2270-2275.
18. Yu FX, *et al.* (2013) Protein kinase A activates the Hippo pathway to modulate cell proliferation and differentiation. *Genes & development* 27(11):1223-1232.

19. Musah S, *et al.* (2014) Substratum-induced differentiation of human pluripotent stem cells reveals the coactivator YAP is a potent regulator of neuronal specification. *Proceedings of the National Academy of Sciences of the United States of America* 111(38):13805-13810.
20. Schlegelmilch K, *et al.* (2011) Yap1 acts downstream of alpha-catenin to control epidermal proliferation. *Cell* 144(5):782-795.
21. Seo E, *et al.* (2013) SOX2 regulates YAP1 to maintain stemness and determine cell fate in the osteo-adipo lineage. *Cell reports* 3(6):2075-2087.
22. Yimlamai D, *et al.* (2014) Hippo pathway activity influences liver cell fate. *Cell* 157(6):1324-1338.
23. Fu D, *et al.* (2014) YAP regulates cell proliferation, migration, and steroidogenesis in adult granulosa cell tumors. *Endocrine-related cancer* 21(2):297-310.
24. Kawamura K, *et al.* (2013) Hippo signaling disruption and Akt stimulation of ovarian follicles for infertility treatment. *Proceedings of the National Academy of Sciences of the United States of America* 110(43):17474-17479.
25. Cheng Y, *et al.* (2015) Actin polymerization-enhancing drugs promote ovarian follicle growth mediated by the Hippo signaling effector YAP. *FASEB journal : official publication of the Federation of American Societies for Experimental Biology* 29(6):2423-2430.
26. Yu C, *et al.* (2016) Oocyte-expressed yes-associated protein is a key activator of the early zygotic genome in mouse. *Cell research* 26(3):275-287.
27. Wigglesworth K, Lee KB, Emori C, Sugiura K, & Eppig JJ (2015) Transcriptomic diversification of developing cumulus and mural granulosa cells in mouse ovarian follicles. *Biology of reproduction* 92(1):23.

28. Shamir ER & Ewald AJ (2014) Three-dimensional organotypic culture: experimental models of mammalian biology and disease. *Nature reviews. Molecular cell biology* 15(10):647-664.
29. Liu-Chittenden Y, *et al.* (2012) Genetic and pharmacological disruption of the TEAD-YAP complex suppresses the oncogenic activity of YAP. *Genes & development* 26(12):1300-1305.
30. Salvador LM, *et al.* (2001) Follicle-stimulating hormone stimulates protein kinase A-mediated histone H3 phosphorylation and acetylation leading to select gene activation in ovarian granulosa cells. *The Journal of biological chemistry* 276(43):40146-40155.
31. Escamilla-Hernandez R, *et al.* (2008) Constitutively active protein kinase A qualitatively mimics the effects of follicle-stimulating hormone on granulosa cell differentiation. *Mol Endocrinol* 22(8):1842-1852.
32. Seamon KB & Daly JW (1986) Forskolin: its biological and chemical properties. *Advances in cyclic nucleotide and protein phosphorylation research* 20:1-150.
33. Amsterdam A & Aharoni D (1994) Plasticity of cell organization during differentiation of normal and oncogene transformed granulosa cells. *Microscopy research and technique* 27(2):108-124.
34. Blanchette EJ (1966) Ovarian steroid cells. I. Differentiation of the lutein cell from the granulosa follicle cell during the preovulatory stage and under the influence of exogenous gonadotrophins. *The Journal of cell biology* 31(3):501-516.
35. Li S, Maruo T, Ladines-Llave CA, Kondo H, & Mochizuki M (1994) Stage-limited expression of myc oncoprotein in the human ovary during follicular growth, regression and atresia. *Endocrine journal* 41(1):83-92.

36. Liu JP & Li H (2010) Telomerase in the ovary. *Reproduction* 140(2):215-222.
37. Overholtzer M, *et al.* (2006) Transforming properties of YAP, a candidate oncogene on the chromosome 11q22 amplicon. *Proceedings of the National Academy of Sciences of the United States of America* 103(33):12405-12410.
38. Shao DD, *et al.* (2014) KRAS and YAP1 converge to regulate EMT and tumor survival. *Cell* 158(1):171-184.
39. Zhao B, Tumaneng K, & Guan KL (2011) The Hippo pathway in organ size control, tissue regeneration and stem cell self-renewal. *Nature cell biology* 13(8):877-883.
40. Li R, *et al.* (2010) A mesenchymal-to-epithelial transition initiates and is required for the nuclear reprogramming of mouse fibroblasts. *Cell stem cell* 7(1):51-63.
41. Samavarchi-Tehrani P, *et al.* (2010) Functional genomics reveals a BMP-driven mesenchymal-to-epithelial transition in the initiation of somatic cell reprogramming. *Cell stem cell* 7(1):64-77.
42. Giudice LC, Cataldo NA, van Dessel HJ, Yap OW, & Chandrasekher YA (1996) Growth factors in normal ovarian follicle development. *Seminars in reproductive endocrinology* 14(3):179-196.
43. Pan B, *et al.* (2004) Differential expression of heparin-binding epidermal growth factor-like growth factor in the rat ovary. *Molecular and cellular endocrinology* 214(1-2):1-8.
44. Fuller PJ & Chu S (2004) Signalling pathways in the molecular pathogenesis of ovarian granulosa cell tumours. *Trends in endocrinology and metabolism: TEM* 15(3):122-128.

45. Edson MA, Nagaraja AK, & Matzuk MM (2009) The mammalian ovary from genesis to revelation. *Endocrine reviews* 30(6):624-712.
46. Wang C, *et al.* (2012) Transforming growth factor alpha (TGFalpha) regulates granulosa cell tumor (GCT) cell proliferation and migration through activation of multiple pathways. *PloS one* 7(11):e48299.
47. Reddy BV & Irvine KD (2013) Regulation of Hippo signaling by EGFR-MAPK signaling through Ajuba family proteins. *Developmental cell* 24(5):459-471.
48. Zhang J, *et al.* (2009) YAP-dependent induction of amphiregulin identifies a non-cell-autonomous component of the Hippo pathway. *Nature cell biology* 11(12):1444-1450.
49. Song S, *et al.* (2015) The Hippo Coactivator YAP1 Mediates EGFR Overexpression and Confers Chemoresistance in Esophageal Cancer. *Clinical cancer research : an official journal of the American Association for Cancer Research* 21(11):2580-2590.
50. Hua G, *et al.* (2016) YAP induces high-grade serous carcinoma in fallopian tube secretory epithelial cells. *Oncogene* 35(17):2247-2265.
51. He C, *et al.* (2015) YAP forms autocrine loops with the ERBB pathway to regulate ovarian cancer initiation and progression. *Oncogene*.
52. Garor R, *et al.* (2009) Effects of basic fibroblast growth factor on in vitro development of human ovarian primordial follicles. *Fertility and sterility* 91(5 Suppl):1967-1975.
53. Nilsson E, Parrott JA, & Skinner MK (2001) Basic fibroblast growth factor induces primordial follicle development and initiates folliculogenesis. *Molecular and cellular endocrinology* 175(1-2):123-130.

54. Boland NI & Gosden RG (1994) Effects of epidermal growth factor on the growth and differentiation of cultured mouse ovarian follicles. *Journal of reproduction and fertility* 101(2):369-374.
55. Park JY, *et al.* (2004) EGF-like growth factors as mediators of LH action in the ovulatory follicle. *Science* 303(5658):682-684.
56. Kranc W, *et al.* (2017) Molecular basis of growth, proliferation, and differentiation of mammalian follicular granulosa cells. *Journal of biological regulators and homeostatic agents* 31(1):1-8.
57. Puri P, *et al.* (2016) Protein Kinase A: A Master Kinase of Granulosa Cell Differentiation. *Scientific reports* 6:28132.
58. Reinholz MM, Zschunke MA, & Roche PC (2000) Loss of alternately spliced messenger RNA of the luteinizing hormone receptor and stability of the follicle-stimulating hormone receptor messenger RNA in granulosa cell tumors of the human ovary. *Gynecologic oncology* 79(2):264-271.
59. St John MA, *et al.* (1999) Mice deficient of Lats1 develop soft-tissue sarcomas, ovarian tumours and pituitary dysfunction. *Nature genetics* 21(2):182-186.
60. Sun T, Pepling ME, & Diaz FJ (2015) Lats1 Deletion Causes Increased Germ Cell Apoptosis and Follicular Cysts in Mouse Ovaries. *Biology of reproduction* 93(1):22.
61. Pisarska MD, Kuo FT, Bentsi-Barnes IK, Khan S, & Barlow GM (2010) LATS1 phosphorylates forkhead L2 and regulates its transcriptional activity. *American journal of physiology. Endocrinology and metabolism* 299(1):E101-109.
62. Li T, *et al.* (2012) Identification of YAP1 as a novel susceptibility gene for polycystic ovary syndrome. *Journal of medical genetics* 49(4):254-257.

63. Huang J, Wu S, Barrera J, Matthews K, & Pan D (2005) The Hippo signaling pathway coordinately regulates cell proliferation and apoptosis by inactivating Yorkie, the *Drosophila* Homolog of YAP. *Cell* 122(3):421-434.
64. Harvey KF, Zhang X, & Thomas DM (2013) The Hippo pathway and human cancer. *Nature reviews. Cancer* 13(4):246-257.
65. Strano S, *et al.* (2005) The transcriptional coactivator Yes-associated protein drives p73 gene-target specificity in response to DNA Damage. *Molecular cell* 18(4):447-459.
66. Snijders AM, *et al.* (2005) Rare amplicons implicate frequent deregulation of cell fate specification pathways in oral squamous cell carcinoma. *Oncogene* 24(26):4232-4242.
67. Zender L, *et al.* (2006) Identification and validation of oncogenes in liver cancer using an integrative oncogenomic approach. *Cell* 125(7):1253-1267.
68. Fernandez LA, *et al.* (2009) YAP1 is amplified and up-regulated in hedgehog-associated medulloblastomas and mediates Sonic hedgehog-driven neural precursor proliferation. *Genes & development* 23(23):2729-2741.
69. Muramatsu T, *et al.* (2011) YAP is a candidate oncogene for esophageal squamous cell carcinoma. *Carcinogenesis* 32(3):389-398.
70. Steinhardt AA, *et al.* (2008) Expression of Yes-associated protein in common solid tumors. *Human pathology* 39(11):1582-1589.
71. Strano S, Fausti F, Di Agostino S, Sudol M, & Blandino G (2013) PML Surfs into HIPPO Tumor Suppressor Pathway. *Frontiers in oncology* 3:36.

72. Yuan M, *et al.* (2008) Yes-associated protein (YAP) functions as a tumor suppressor in breast. *Cell death and differentiation* 15(11):1752-1759.
73. Jamieson S & Fuller PJ (2012) Molecular pathogenesis of granulosa cell tumors of the ovary. *Endocrine reviews* 33(1):109-144.
74. Sehouli J, *et al.* (2004) Granulosa cell tumor of the ovary: 10 years follow-up data of 65 patients. *Anticancer research* 24(2C):1223-1229.
75. Crew KD, *et al.* (2005) Long natural history of recurrent granulosa cell tumor of the ovary 23 years after initial diagnosis: a case report and review of the literature. *Gynecologic oncology* 96(1):235-240.
76. Vilella J, *et al.* (2007) Clinical and pathological predictive factors in women with adult-type granulosa cell tumor of the ovary. *International journal of gynecological pathology : official journal of the International Society of Gynecological Pathologists* 26(2):154-159.
77. Amsterdam A & Selvaraj N (1997) Control of differentiation, transformation, and apoptosis in granulosa cells by oncogenes, oncoviruses, and tumor suppressor genes. *Endocrine reviews* 18(4):435-461.
78. Yamagami W, *et al.* (2012) Effective multidisciplinary treatment for ovarian granulosa cell tumor with multiple metastases--a case report. *European journal of gynaecological oncology* 33(4):370-375.
79. Shah SP, *et al.* (2009) Mutation of FOXL2 in granulosa-cell tumors of the ovary. *The New England journal of medicine* 360(26):2719-2729.
80. Jamieson S, *et al.* (2010) The FOXL2 C134W mutation is characteristic of adult granulosa cell tumors of the ovary. *Modern pathology : an official journal of the United States and Canadian Academy of Pathology, Inc* 23(11):1477-1485.

81. Al-Agha OM, *et al.* (2011) FOXL2 is a sensitive and specific marker for sex cord-stromal tumors of the ovary. *The American journal of surgical pathology* 35(4):484-494.
82. Rosario R, Araki H, Print CG, & Shelling AN (2012) The transcriptional targets of mutant FOXL2 in granulosa cell tumours. *PLoS one* 7(9):e46270.
83. Benayoun BA, *et al.* (2013) Adult ovarian granulosa cell tumor transcriptomics: prevalence of FOXL2 target genes misregulation gives insights into the pathogenic mechanism of the p.Cys134Trp somatic mutation. *Oncogene* 32(22):2739-2746.
84. Georges A, *et al.* (2014) FOXL2: a central transcription factor of the ovary. *Journal of molecular endocrinology* 52(1):R17-33.
85. Young RH, Dickersin GR, & Scully RE (1984) Juvenile granulosa cell tumor of the ovary. A clinicopathological analysis of 125 cases. *The American journal of surgical pathology* 8(8):575-596.
86. Aboud E (1997) A review of granulosa cell tumours and thecomas of the ovary. *Archives of gynecology and obstetrics* 259(4):161-165.
87. Ko SF, *et al.* (1999) Adult ovarian granulosa cell tumors: spectrum of sonographic and CT findings with pathologic correlation. *AJR. American journal of roentgenology* 172(5):1227-1233.
88. Stenwig JT, Hazekamp JT, & Beecham JB (1979) Granulosa cell tumors of the ovary. A clinicopathological study of 118 cases with long-term follow-up. *Gynecologic oncology* 7(2):136-152.
89. Ohel G, Kaneti H, & Schenker JG (1983) Granulosa cell tumors in Israel: a study of 172 cases. *Gynecologic oncology* 15(2):278-286.

90. Cronje HS, Niemand I, Bam RH, & Woodruff JD (1999) Review of the granulosa-theca cell tumors from the emil Novak ovarian tumor registry. *American journal of obstetrics and gynecology* 180(2 Pt 1):323-327.
91. Nishi Y, *et al.* (2001) Establishment and characterization of a steroidogenic human granulosa-like tumor cell line, KGN, that expresses functional follicle-stimulating hormone receptor. *Endocrinology* 142(1):437-445.
92. Imai M, *et al.* (2008) Spontaneous transformation of human granulosa cell tumours into an aggressive phenotype: a metastasis model cell line. *BMC cancer* 8:319.
93. Malmstrom H, Hogberg T, Risberg B, & Simonsen E (1994) Granulosa cell tumors of the ovary: prognostic factors and outcome. *Gynecologic oncology* 52(1):50-55.
94. Craig J, *et al.* (2007) Gonadotropin and intra-ovarian signals regulating follicle development and atresia: the delicate balance between life and death. *Frontiers in bioscience : a journal and virtual library* 12:3628-3639.
95. Smith ER & Xu XX (2008) Ovarian ageing, follicle depletion, and cancer: a hypothesis for the aetiology of epithelial ovarian cancer involving follicle depletion. *The Lancet. Oncology* 9(11):1108-1111.
96. Matzuk MM, Finegold MJ, Su JG, Hsueh AJ, & Bradley A (1992) Alpha-inhibin is a tumour-suppressor gene with gonadal specificity in mice. *Nature* 360(6402):313-319.
97. Watson RH, Roy WJ, Jr., Davis M, Hitchcock A, & Campbell IG (1997) Loss of heterozygosity at the alpha-inhibin locus on chromosome 2q is not a feature of human granulosa cell tumors. *Gynecologic oncology* 65(3):387-390.
98. Boerboom D, *et al.* (2005) Misregulated Wnt/beta-catenin signaling leads to ovarian granulosa cell tumor development. *Cancer research* 65(20):9206-9215.

99. Rosario R, *et al.* (2013) Adult granulosa cell tumours (GCT): clinicopathological outcomes including FOXL2 mutational status and expression. *Gynecologic oncology* 131(2):325-329.
100. Xu MZ, *et al.* (2009) Yes-associated protein is an independent prognostic marker in hepatocellular carcinoma. *Cancer* 115(19):4576-4585.
101. Hall CA, *et al.* (2010) Hippo pathway effector Yap is an ovarian cancer oncogene. *Cancer research* 70(21):8517-8525.
102. Zhang X, *et al.* (2011) The Hippo pathway transcriptional co-activator, YAP, is an ovarian cancer oncogene. *Oncogene* 30(25):2810-2822.
103. Richards JS, *et al.* (2012) Either Kras activation or Pten loss similarly enhance the dominant-stable CTNNB1-induced genetic program to promote granulosa cell tumor development in the ovary and testis. *Oncogene* 31(12):1504-1520.
104. Fujii M, *et al.* (2012) TGF-beta synergizes with defects in the Hippo pathway to stimulate human malignant mesothelioma growth. *The Journal of experimental medicine* 209(3):479-494.
105. Skinner MK, Keski-Oja J, Osteen KG, & Moses HL (1987) Ovarian thecal cells produce transforming growth factor-beta which can regulate granulosa cell growth. *Endocrinology* 121(2):786-792.
106. Komuro A, Nagai M, Navin NE, & Sudol M (2003) WW domain-containing protein YAP associates with ErbB-4 and acts as a co-transcriptional activator for the carboxyl-terminal fragment of ErbB-4 that translocates to the nucleus. *The Journal of biological chemistry* 278(35):33334-33341.

107. Huang JM, *et al.* (2013) YAP modifies cancer cell sensitivity to EGFR and survivin inhibitors and is negatively regulated by the non-receptor type protein tyrosine phosphatase 14. *Oncogene* 32(17):2220-2229.
108. Torre LA, *et al.* (2015) Global cancer statistics, 2012. *CA: a cancer journal for clinicians* 65(2):87-108.
109. Vaughan S, *et al.* (2011) Rethinking ovarian cancer: recommendations for improving outcomes. *Nature reviews. Cancer* 11(10):719-725.
110. Bowtell DD, *et al.* (2015) Rethinking ovarian cancer II: reducing mortality from high-grade serous ovarian cancer. *Nature reviews. Cancer* 15(11):668-679.
111. Karnezis AN, Cho KR, Gilks CB, Pearce CL, & Huntsman DG (2017) The disparate origins of ovarian cancers: pathogenesis and prevention strategies. *Nature reviews. Cancer* 17(1):65-74.
112. Howitt BE, *et al.* (2015) Evidence for a dualistic model of high-grade serous carcinoma: BRCA mutation status, histology, and tubal intraepithelial carcinoma. *The American journal of surgical pathology* 39(3):287-293.
113. Przybycin CG, Kurman RJ, Ronnett BM, Shih Ie M, & Vang R (2010) Are all pelvic (nonuterine) serous carcinomas of tubal origin? *The American journal of surgical pathology* 34(10):1407-1416.
114. Scully RE (1995) Pathology of ovarian cancer precursors. *Journal of cellular biochemistry. Supplement* 23:208-218.
115. Auersperg N, Wong AS, Choi KC, Kang SK, & Leung PC (2001) Ovarian surface epithelium: biology, endocrinology, and pathology. *Endocrine reviews* 22(2):255-288.

116. Auersperg N (2013) Ovarian surface epithelium as a source of ovarian cancers: unwarranted speculation or evidence-based hypothesis? *Gynecologic oncology* 130(1):246-251.
117. Verhaak RG, *et al.* (2013) Prognostically relevant gene signatures of high-grade serous ovarian carcinoma. *The Journal of clinical investigation* 123(1):517-525.
118. Tothill RW, *et al.* (2008) Novel molecular subtypes of serous and endometrioid ovarian cancer linked to clinical outcome. *Clinical cancer research : an official journal of the American Association for Cancer Research* 14(16):5198-5208.
119. Chronowska E (2012) Regulation of telomerase activity in ovarian granulosa cells. *Indian journal of experimental biology* 50(9):595-601.
120. Dzafic E, Stimpfel M, & Virant-Klun I (2013) Plasticity of granulosa cells: on the crossroad of stemness and transdifferentiation potential. *Journal of assisted reproduction and genetics* 30(10):1255-1261.
121. Rodgers RJ, Lavranos TC, van Wezel IL, & Irving-Rodgers HF (1999) Development of the ovarian follicular epithelium. *Molecular and cellular endocrinology* 151(1-2):171-179.
122. Kossowska-Tomaszczuk K, *et al.* (2009) The multipotency of luteinizing granulosa cells collected from mature ovarian follicles. *Stem Cells* 27(1):210-219.
123. Yu FX, Zhao B, & Guan KL (2015) Hippo Pathway in Organ Size Control, Tissue Homeostasis, and Cancer. *Cell* 163(4):811-828.
124. Ramos A & Camargo FD (2012) The Hippo signaling pathway and stem cell biology. *Trends in cell biology* 22(7):339-346.

125. Mo JS, Park HW, & Guan KL (2014) The Hippo signaling pathway in stem cell biology and cancer. *EMBO reports* 15(6):642-656.
126. Bayasula, *et al.* (2012) Establishment of a human nonluteinized granulosa cell line that transitions from the gonadotropin-independent to the gonadotropin-dependent status. *Endocrinology* 153(6):2851-2860.
127. Ahmed AA, *et al.* (2010) Driver mutations in TP53 are ubiquitous in high grade serous carcinoma of the ovary. *The Journal of pathology* 221(1):49-56.
128. Cancer Genome Atlas Research N (2011) Integrated genomic analyses of ovarian carcinoma. *Nature* 474(7353):609-615.
129. Vang R, Shih le M, & Kurman RJ (2009) Ovarian low-grade and high-grade serous carcinoma: pathogenesis, clinicopathologic and molecular biologic features, and diagnostic problems. *Advances in anatomic pathology* 16(5):267-282.
130. Kuhn E, *et al.* (2010) Shortened telomeres in serous tubal intraepithelial carcinoma: an early event in ovarian high-grade serous carcinogenesis. *The American journal of surgical pathology* 34(6):829-836.
131. Madore J, *et al.* (2010) Characterization of the molecular differences between ovarian endometrioid carcinoma and ovarian serous carcinoma. *The Journal of pathology* 220(3):392-400.
132. Cathro HP & Stoler MH (2002) Expression of cytokeratins 7 and 20 in ovarian neoplasia. *American journal of clinical pathology* 117(6):944-951.
133. Tung CS, *et al.* (2009) PAX2 expression in low malignant potential ovarian tumors and low-grade ovarian serous carcinomas. *Modern pathology : an official journal of the United States and Canadian Academy of Pathology, Inc* 22(9):1243-1250.

134. Fenoglio CM, Cottral GA, Ferenczy A, & Richart RM (1976) Mucinous tumors of the ovary. III. Histochemical studies. *Gynecologic oncology* 4(2):151-157.
135. Domcke S, Sinha R, Levine DA, Sander C, & Schultz N (2013) Evaluating cell lines as tumour models by comparison of genomic profiles. *Nature communications* 4:2126.
136. Kurman RJ (2013) Origin and molecular pathogenesis of ovarian high-grade serous carcinoma. *Annals of oncology : official journal of the European Society for Medical Oncology* 24 Suppl 10:x16-21.
137. Schumer ST & Cannistra SA (2003) Granulosa cell tumor of the ovary. *Journal of clinical oncology : official journal of the American Society of Clinical Oncology* 21(6):1180-1189.
138. Berns EM & Bowtell DD (2012) The changing view of high-grade serous ovarian cancer. *Cancer research* 72(11):2701-2704.
139. Rodgers HF, Lavranos TC, Vella CA, & Rodgers RJ (1995) Basal lamina and other extracellular matrix produced by bovine granulosa cells in anchorage-independent culture. *Cell and tissue research* 282(3):463-471.
140. Lavranos TC, Rodgers HF, Bertoncello I, & Rodgers RJ (1994) Anchorage-independent culture of bovine granulosa cells: the effects of basic fibroblast growth factor and dibutyryl cAMP on cell division and differentiation. *Experimental cell research* 211(2):245-251.
141. Varras M, Griva T, Kalles V, Akrivis C, & Papanisteidis N (2012) Markers of stem cells in human ovarian granulosa cells: is there a clinical significance in ART? *Journal of ovarian research* 5(1):36.

142. Kossowska-Tomaszczuk K & De Geyter C (2013) Cells with stem cell characteristics in somatic compartments of the ovary. *BioMed research international* 2013:310859.
143. Pece S, *et al.* (2010) Biological and molecular heterogeneity of breast cancers correlates with their cancer stem cell content. *Cell* 140(1):62-73.
144. Xia Y, Zhang YL, Yu C, Chang T, & Fan HY (2014) YAP/TEAD co-activator regulated pluripotency and chemoresistance in ovarian cancer initiated cells. *PLoS one* 9(11):e109575.
145. Panciera T, *et al.* (2016) Induction of Expandable Tissue-Specific Stem/Progenitor Cells through Transient Expression of YAP/TAZ. *Cell stem cell* 19(6):725-737.
146. Zhao T & Xu Y (2010) p53 and stem cells: new developments and new concerns. *Trends in cell biology* 20(3):170-175.
147. Bonizzi G, Cicalese A, Insinga A, & Pelicci PG (2012) The emerging role of p53 in stem cells. *Trends in molecular medicine* 18(1):6-12.
148. Oren M & Rotter V (2010) Mutant p53 gain-of-function in cancer. *Cold Spring Harbor perspectives in biology* 2(2):a001107.
149. Shetzer Y, Molchadsky A, & Rotter V (2016) Oncogenic Mutant p53 Gain of Function Nourishes the Vicious Cycle of Tumor Development and Cancer Stem-Cell Formation. *Cold Spring Harbor perspectives in medicine* 6(10).
150. Zhou G, *et al.* (2014) Gain-of-function mutant p53 promotes cell growth and cancer cell metabolism via inhibition of AMPK activation. *Molecular cell* 54(6):960-974.
151. O'Connor MJ (2015) Targeting the DNA Damage Response in Cancer. *Molecular cell* 60(4):547-560.

152. Deng CX (2006) BRCA1: cell cycle checkpoint, genetic instability, DNA damage response and cancer evolution. *Nucleic acids research* 34(5):1416-1426.
153. Yang S, *et al.* (2013) CDK1 phosphorylation of YAP promotes mitotic defects and cell motility and is essential for neoplastic transformation. *Cancer research* 73(22):6722-6733.
154. Zhang S, *et al.* (2017) Hippo Signaling Suppresses Cell Ploidy and Tumorigenesis through Skp2. *Cancer cell* 31(5):669-684 e667.